MULTIDISCIPLINARY STUDY OF EARTHQUAKE PRECURSORS AT THE EASTERN PART OF CENTRAL GREECE (THESSALIA)

FINAL REPORT
ON THE "E.C.P.F.E" PROJECT (No 122/1.11.1991)

ATHENS, APRIL 1994

FINAL REPORT OF THE GEOPHYSICAL LABORATORY, ARISTOTLE UNIVERSITY OF THESSALONIKI ON THE "E. C. P. F. E." PROJECT (No 122/1.11.91)

MULTIDISCIPLINARY STUDY OF EARTHQUAKE PRECURSORS AT THE EASTERN PART OF CENTRAL GREECE (THESSALIA)

E. E. PAPADIMITRIOU, Scientific Responsible.

1. INTRODUCTION

This final report covers the 1-year period from February 1993 to February 1994. According to the objectives of the work programme, which concern the scientific team of Aristotle University of Thessaloniki, the project has two main tasks:

1. Seismicity Characteristics
2. Geophysical Precursory Phenomena

In the present report, the results of the investigations during the time period mentioned above, which have been conducted by the scientists of the Aristotle University of Thessaloniki who participate in the programme, are presented. It includes the following subreports:

2.1. Seismicity and long term earthquake prediction in Thessalia area.

2.2. Temporal variations of seismicity in Thessalia (central Greece).

2.3. Relative site amplification factors using the coda waves from local earthquakes for the seismological network of the Geophysical Laboratory of the University of Thessaloniki.

2.4. Electric and magnetic field measurements for earthquake prediction in Thessalia.

2.1. SEISMICITY AND LONG TERM EARTHQUAKE PREDICTION IN THESSALIA AREA

B. C. Papazachos and E. E. Papadimitriou

Laboratory of Geophysics, University of Thessaloniki, GR-54006 Thessaloniki, Greece

ABSTRACT

Seismicity parameters have been determined for two seismogenic sources in which Thessalia (central Greece) area has been divided. Instrumental data concerning events which occurred during the present century have been used for this determination. The repeat times of the stronger ($M_s \geq 5.5$) earthquakes have been estimated and used for the long term prediction in this area, on the basis of the validity of the time-predictable model. Adopting the lognormal distribution as provided better fit to the T/T_t data, where T is the actual and T_t the theoretical repeat time, the probabilities P_{10}, for the occurrence of strong ($M \geq 6.0$) mainshocks during the next decade have been calculated for each seismogenic source. The magnitude, M_t, of the expected mainshock is also given.

INTRODUCTION

The area of Thessalia is one of the most seismically active regions in the broader Aegean area. The area has been repeatedly struck by large ($M_s \geq 6.0$) earthquakes, as it is known both from historical (Papazachos and Papazachou, 1989) and instrumental data (Comninakis and Papazachos, 1986). Seismological and geological evidence suggest that the tectonics is dominated by extensional features (Papazachos et al., 1983; 1992; Mountrakis et al., 1993). The high level of seismicity and the occurrence of strong ($M \geq 6.5$) earthquakes causing considerable damage in urban areas, increase the scientific and public interest for seismicity and earthquake prediction studies. This is the reason for which this area was selected as a pilot study area for a joint multidisciplinary experiment of European countries for identification of short term earthquake precursors.

Papazachos et al. (1993) studied extensively this area using several geophysical information (surface breakages, macroseismic fields, aftershock distribution, hot springs, gravimetric data) to accurately define the rupture zones of the three strongest earthquakes which occurred there during the present century (1954 M=7.0, 1957 M=6.8, 1980 M=6.5). They found that the rupture zones of these three large ($M \geq 6.5$) successive earthquakes trend in an about east-west direction, tend to abut without significant overlap, cover the whole

southernmost part of the Thessalia plain and are due to normal type of faulting. Furthermore, they used reliable fault plane solutions and seismic moment release rate and found that the upper crust is seismically extending at a rate of 7 mm/yr in a N6°W and is vertically thinning at a rate of 3 mm/y, which is in full agreement with a normal faulting striking in a N80°E direction.

It is the aim of the present study to more accurately define seismogenic sources in this area, that is, parts of the area that exhibit different behaviour as far as the seismic activity concerns. Furthermore, after an estimation of the basic seismicity parameters, to attempt a long term earthquake forecasting for the occurrence of the next strong ($M_s \geq 6.0$) mainshocks.

SEISMICITY OF THE AREA

For the area under study there are abundant instrumental data and historical records. The data available are sufficient for studying the seismicity characteristics. Information on the surface wave magnitudes and on the epicenters of the earthquakes plotted in figure 1 (after Papazachos et al., 1993) were received from the catalogue of Comninakis and Papazachos (1986) for the time period 1901-1985 and from the monthly bulletins of the National Observatory of Athens and of the Geophysical Laboratory of the University of Thessaloniki for the period 1986-1992. Table 1 gives information on the strong ($M_s \geq 5.5$) earthquakes which are known to have occurred in this area by historical reports (Papazachos and Papazachou, 1989) or instrumental information. Looking at this table, one can mention the absence of strong earthquake occurrence during the last (19th) century, while this is not the case for the 18th century, when four events with magnitudes larger or equal to 6.0 are known to have occurred.

Table 1. Information on historical and instrumental data concerning strong ($M_s \geq 5.5$) earthquakes which occurred in Thessalia.

Date	Origin Time	φ°N	λ°E	Depth (Km)	M_s
510 B.C.		39.4	22.3	0.0	7.0
1621, Feb. 24		39.4	22.0	0.0	6.2
1661, Mar. 31		39.4	22.1	0.0	6.1
1668, Aug.		39.6	22.4	0.0.	6.2
1674, Jan. 26	07:	39.4	21.9	0.0	6.2

1731		39.6	22.5	0.0	6.0
1735, Sep. 1	06:	39.5	21.8	0.0	6.5
1743, Feb. 12		39.3	22.8	0.0	6.8
1766, Nov. 9		39.7	22.2	0.0	6.3
1773, Mar. 16	08:	39.3	22.7	0.0	6.6
1781, Aug. 28		39.6	22.5	0.0	6.3
1787, June 19	03:	39.5	21.9	0.0	6.0
1905, Jan. 20	02:32:30	39.6	23.0	0.0	6.3
1909, June 15	23:30:30	39.1	22.2	0.0	5.7
1911, Oct. 22	22:31:45	39.5	23.0	0.0	6.0
1930, Feb. 23	18:19:12	39.5	23.0	0.0	6.0
1930, Mar. 31	12:33:48	39.5	23.0	0.0	6.1
1941, Mar. 1	03:52:47	39.6	22.5	0.0	6.3
1941, May 14	08:36:21	39.5	22.6	0.0	5.5
1942, June 1	09:17:40	39.3	22.4	0.0	5.6
1954, Apr. 30	13:02:36	39.3	22.2	7.0	7.0
1954, May 4	16:43:20	39.3	22.2	0.0	5.6
1954, May 4	16:45:27	39.3	22.2	0.0	5.7
1954, May 25	22:03:32	39.3	22.2	0.0	5.6
1955, Oct. 3	01:07:03	39.2	22.1	0.0	5.6
1955, Apr. 19	16:47:19	39.3	23.0	0.0	6.3
1955, Apr. 21	07:18:19	39.3	23.1	0.0	5.8
1956, Nov. 2	16:04:33	39.3	23.1	0.0	5.6
1957, Mar. 8	12:14:14	39.3	22.7	0.0	6.5
1957, Mar. 8	12:21:13	39.3	22.6	6.0	6.8
1957, Mar. 8	23:35:09	39.2	22.8	9.0	6.0
1957, Mar. 28	22:26:01	39.3	22.7	0.0	5.5
1957, May 21	13:24:18	39.4	22.8	0.0	5.6
1957, Nov. 27	03:08:04	39.2	22.6	0.0	5.6
1980, July 9	02:10:16	39.2	22.9	0.0	5.7
1980, July 9	02:11:53	39.2	23.1	14.0	6.5
1980, July 9	02:35:50	39.3	22.6	18.0	6.1
1985, Apr. 30	18:14:13	39.3	22.8	27.0	5.8

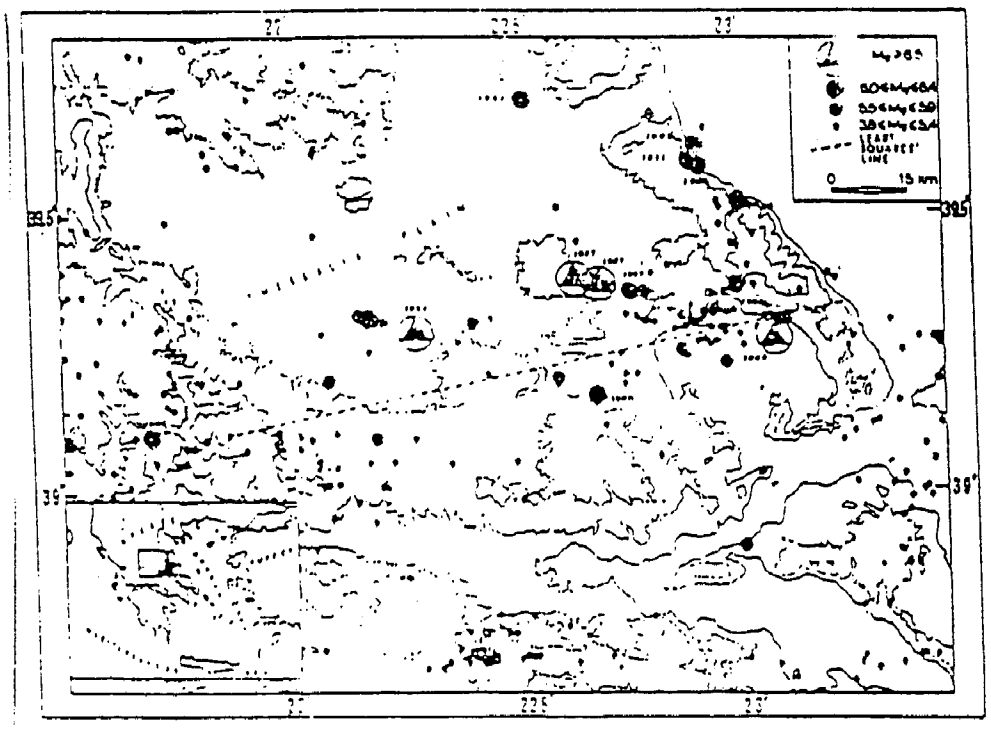

Fig. 1. Distribution of epicenters of earthquakes which occurred in Thessalia and surrounding area during the present century with the seismic belt in southern Thessalia well defined (after Papazachos et al., 1993).

The southern part of the area exhibits higher level of seismicity compared to the northern one. Although during the last century as well as during the first half of the present century this part was seismically quiescent in strong ($M \geq 6.0$) earthquakes occurrence, a series of catastrophic events took place there during the last four decades, the first and larger one beeing the 1954 ($M = 7.0$) event. The seismicity rate in the northern part is moderate, with the largest events having magnitudes equal to 6.3 (1781 and 1941). Based on this observation and on seismological, geological and geomorphological criteria, such as spatial clustering of the epicenters of strong earthquakes, seismicity level, maximum earthquake observed, according to Papazachos (1992), two seismogenic sources have been defined. The first one in the southern part of the area (South Thessalia), and the second one in the northeastern part of the area (Northeastern Thessalia).

The constants of the well-known Gutenberg-Richter (1944) relation:

$$logN=a_t-bM \quad (1)$$

have been calculated for each seismogenic source. Accurate determination of the parameters a_t and b of the relation (1) is of primary importance for seismicity studies since almost all currently used seismicity measures depend on these two parameters. The data used for this calculation are complete for the following time intervals and magnitude ranges (Papazachos et al., 1993):

Time	M_{min}
1901 - 1990	*6.0*
1911 - 1990	*5.6*
1970 - 1990	*4.5*

Figure 2 shows a plot of the logarithm of the number, N, of the earthquakes with magnitude equal or larger than M as a function of the magnitude. The relations:

$$logN=5.71-0.80M \quad (2)$$

$$logN=5.23-0.80M \quad (3)$$

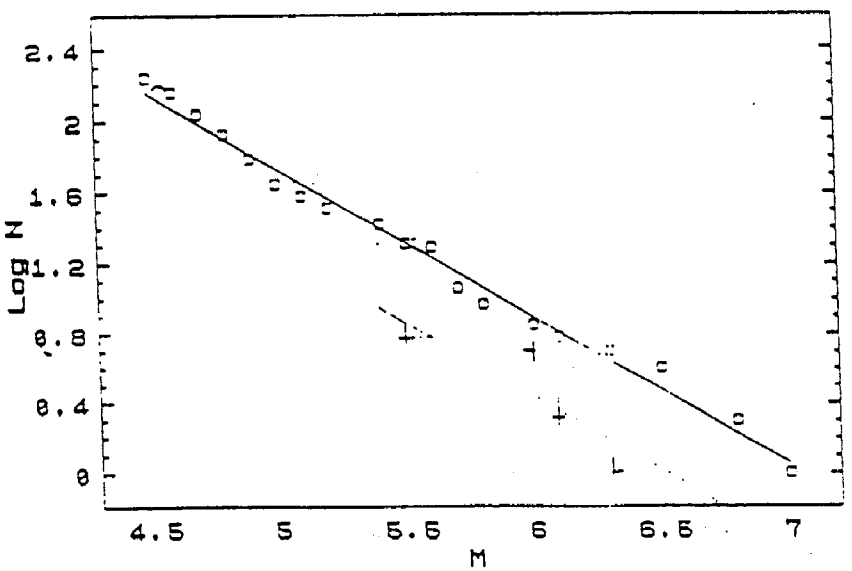

Fig. 2. Logarithm of the cumulative frequency, N, of earthquakes in the two seismogenic sources as a function of the surface wave magnitude, M.

for the southern and northern part, respectively, fit the data in the least squares' sense. The constants a and b for one year period, accordingly, are:

$$a=3.77 \quad b=0.80$$

$$a=3.28 \quad b=0.80$$

These values are in good agreement with the values a=3.83 and b=0.80 found by Papazachos (1990) for the whole examined area.

The most frequently observed magnitude in t years is given by the relation:

$$M_t=\frac{a}{b}+\frac{\log t}{b} \tag{4}$$

By applying this relation for time period of t=10 years, it is derived

$M_t=6.0$ for the southern Thessalia

$M_t=5.4$ for the northeastern Thessalia

It is now well established that the seismic moment, M_o, is a proper quantity for measuring the size of an earthquake (Aki, 1966; Hanks and Kanamori, 1979). For this reason, the rate of moment accumulation in a seismic source can be considered as a good measure of seismicity in that source. For the determination of the moment rate in the present study, the procedure suggested by Papazachos and Kiratzi (1993) is followed, which is based on a methodology proposed by Molnar (1979). Starting from the Gutenberg-Richter empirical expression, and using another empirical relation between magnitude and seismic moment, the relative number of events with seismic moment greater or equal to M_o is given by the relation:

$$N(M_o)=G\cdot M_o^{-E} \tag{5}$$

where

$$G=10^{\left(a-\frac{bk}{r}\right)} \qquad \text{and} \qquad E=\frac{b}{r} \tag{6}$$

where a,b are the constants of the Gutenberg-Richter relation (normalized for one year and for each seismogenic source) and r,k the constants of the following empirical moment-magnitude relation:

$$\log M_o=rM+k \tag{7}$$

having values r=1.5 and k=15.89 for shallow earthquakes, in the broader Aegean area (Papazachos and Kiratzi, 1993). The rate of occurrence of the seismic moment, M_o, is then

given by the relation:

$$\dot{M}_o = \frac{G}{1-E} \cdot M_{o,max}^{1-E} \qquad (8)$$

where $M_{o,max}$ is the seismic moment released by the maximum earthquake in the source, with magnitude M_{max}.

The values of the parameters b, a, M_{max} and $\log M_o$ for each seismogenic source are given on Table (2). The name of each seismogenic source, corresponding to that of figure 1 is written in the first column of this table. The M_{max} was estimated by considering all the available (historical and instrumental) data for each seismogenic source.

Table 2. Information on the basic parameters used for the two sources. The first column gives the name of the source. The constants for the Gutenberg-Richter relation are given in the next two columns. In the last two columns, the maximum magnitude and the logarithm of the moment rate are given.

Source Name	a	b	M_{max}	$\log M_o$
South Thessalia	3.77	0.80	7.0	24.89
Northeastern Thessalia	3.28	0.80	6.3	23.91

LONG TERM EARTHQUAKE PREDICTION OF STRONG MAINSHOCKS

Papazachos and Papaioannou (1993) found that the time-predictable model holds for the seismogenic sources in which the Aegean and the surrounding area has been divided. They used the interevent times of the strong mainshocks occurred in these sources to determine the following relations:

$$\log T_t = 0.24 M_{min} + 0.25 M_p - 0.36 \log \dot{M}_o + 7.36 \qquad (9)$$

$$M_f = 1.04 M_{min} - 0.31 M_p + 0.28 \log \dot{M}_o - 4.85 \qquad (10)$$

where T_t is the interevent time, measured in years, M_{min} the surface wave magnitude of the smallest mainshock considered, M_p the magnitude of the preceding mainshock, M_f the magnitude of the following mainshock, M_o the moment rate in each source per year. On the basis of the first of these relations and taking into consideration the time of occurrence and

the magnitude of the last mainshock, they determined the probabilities for the occurrence of strong mainshocks in each seismogenic source during the decade 1993-2002. They estimated the magnitude of the expected mainshock by using the second of these relations.

Following the methodology suggested by the above mentioned authors, the interevent times of strong ($M_s \geq 5.5$) earthquakes have been estimated. The two sources are shown in figure (3) along with the epicenters of the complete data used. Black circles represent epicenters of mainshocks, while open circles epicenters of foreshocks and aftershocks, that is, earthquakes which precede or follow mainshocks with magnitudes 5.5-5.7, 5.8-6.0, 6.1-7.0, and larger than 7.0 up to 6, 7, 9 and 12.5 years, respectively (Papazachos, 1992).

Papazachos (1991, 1993) and Papazachos and Papaioannou (1993) found that the ratio T/T_t follows a lognormal distribution with a mean equal to zero and a standard deviation $\sigma=0.18$. Based on these results and given the date of the last event in each seismogenic source and considering the time of occurrence of the preceding mainshock, the probabilities, P_{10}, for the occurrence of the next strong mainshocks ($M_s \geq 6.0$) during the next ten years (1993-2002) were calculated.

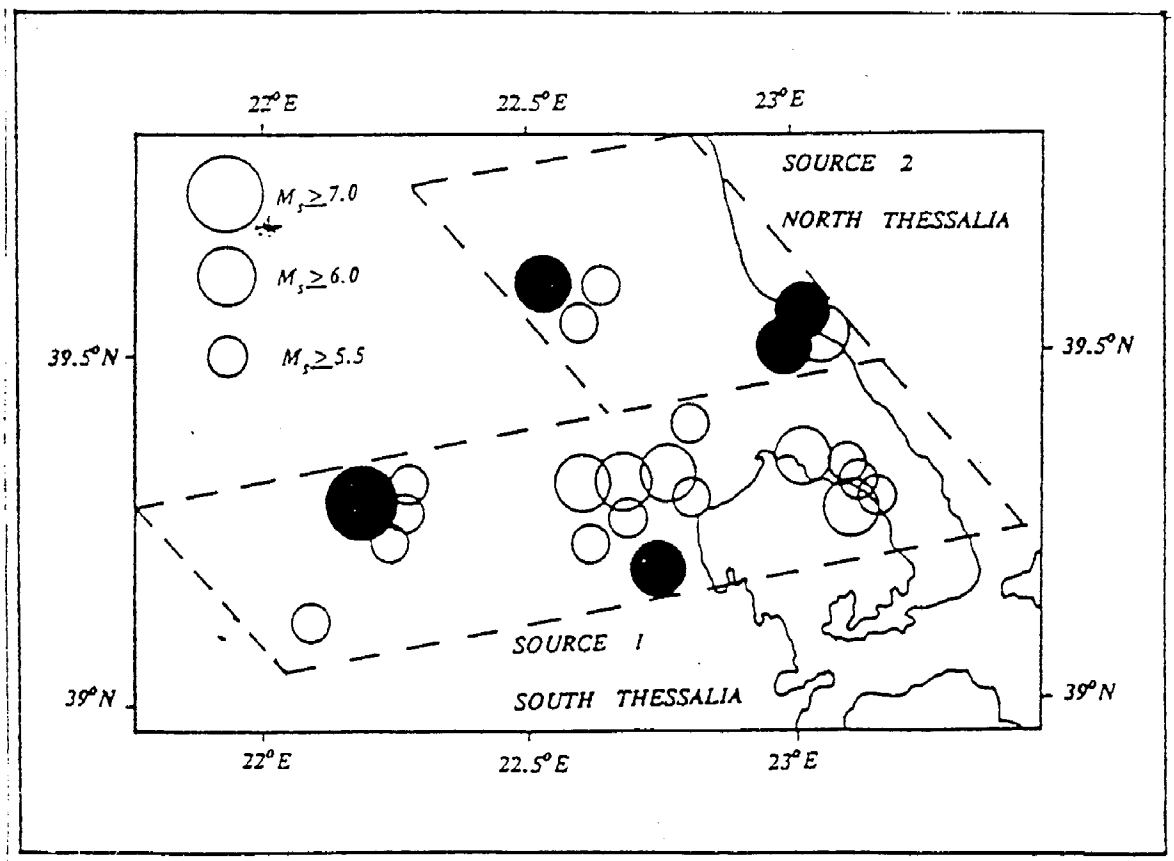

Fig. 3. The two seismogenic sources in which the area of Thessalia has been divided along with the epicenters of the mainshocks (black circles) and large ($M_s \geq 6.0$) fore- and aftershocks in the broad sense.

Table 3 gives information on the expected strong ($M_s \geq 6.0$) mainshocks in the area under study. The first column gives the name of the seismogenic source. The other two columns give the probability, P_{10}, for the occurrence of strong ($M_s \geq 6.0$) mainshocks during the next decade (1993-2002) and the corresponding magnitudes, M_f, of the expected events, as these magnitudes were calculated by the relation (10).

Table 3. Information on the expected magnitudes, M_f, and the corresponding probabilities, P_{10}, for the occurrence of strong ($M_s \geq 6.0$) shallow mainshocks during the period 1993-2002 in the area of Thessalia (central Greece).

Seismogenic Source	M_f	P_{10}
South Thessalia	6.3	0.22
Northeastern Thessalia	6.1	0.27

Acknowledgements. A computer program for the determination of the parameters of the relations (5), (6), written by C. Papazachos, another one for distiguishing foreshocks and aftershocks, written by E. Scordilis and a third one for the estimation of probabilities, written by C. Papaioannou, were used. The authors express their sincere appreciation for their help. This work was financially supported by the European Centre on Prevention and Forecasting of Earthquakes under the contract 122/1.11.91.

REFERENCES

Aki, K. (1966). Generation and propagation of G waves from the Niigata earthquake of June, 1964. "Bull. Earthquake Res. Inst., Univ. Tokyo", 44, 23-88.

Comninakis, P.E. and Papazachos, B.C. (1986). A catalogue of earthquakes in Greece and surrounding area for the period 1901-1985. "Publ. Geophys. Lab., Univ. Thessaloniki", 1, pp. 167.

Gutenberg, B. and Richter, C.F. (1944). Frequency of earthquakes in California. "Bull. Seism. Soc. Am.", 34, 185-188.

Hanks, T.C. and Kanamori, H. (1979). A moment magnitude scale. "J. Geophys. Res.", 84, 2348-2350.

Molnar, P. (1979). Earthquake recurrence intervals and plate tectonics. "Bull. Seism. Soc.

Am.", 69, 115-133.

Mountrakis, D., Kilias, A., Pavlides, S., Zouros, N., Spyropoulos, N., Tranos, M. and Soulakelis, N. (1993). Field study of the highly active fault zone southern Thessalia. "2nd Cong. Hellenic Geophys. Union, 5-7 May 1993, Florina, Greece", (in press).

Papazachos, B. C. (1990). Seismicity of the Aegean and the surrounding area. "Tectonophysics", 178, 287-308.

Papazachos, B.C. (1991). Long term earthquake prediction in south Balkan region based on a time dependent seismicity model. "1st General Conference of the B. P. U., Thessaloniki, September 26-28, 1991", 1-7.

Papazachos, B.C. (1993). Long term earthquake prediction of intermediate depth earthquakes in southern Aegean region based on a time predictable model. "Natural Hazards", 7, 211-218.

Papazachos, B.C., Kiratzi, A.A., Hatzidimitriou, P.M. and Rocca, A.Ch. (1984). Seismic faults in the Aegean area. "Tectonophysics", 106, 71-85.

Papazachos, B.C., Kiratzi, A.A. and Papadimitriou, E.E. (1991). Regional focal mechanisms for earthquakes in the Aegean area. "Pure Appl. Geophys.", 136, 405-420.

Papazachos, B.C., Hatzidimitriou, P.M., Karakaisis, G.F., Papazachos, C.B. and Tsokas, G.N. (1993). Rupture zones and active crustal deformation in southern Thessalia, central Greece. "Boll. Geof. Teor. Appl.", (in press).

Papazachos, B.C. and Papaioannou, Ch. A. (1993). Long term earthquake prediction in the Aegean area based on a time and magnitude predictable model. "Pure Appl. Geophys.", (in press).

Papazachos, B.C. and Papazachou, C.B. (1989). The earthquakes of Greece. "Ziti publ. Co, Thessaloniki-Greece", pp. 365 (in Greek).

Papazachos, C.B. and Kiratzi, A.A. (1993). A formulation for reliable estimation of active crustal deformation and its application in Greece. "Geophys. J. Intern.", 111, 424-432.

2.2. TEMPORAL VARIATIONS OF SEISMICITY IN THESSALIA (CENTRAL GREECE)

By

G. F. Karakaisis

GLaboratory of Geophysics, University of Thessaloniki, 54006 Thessaloniki, Greece

ABSTRACT

An attempt is made to reveal any precursory seismicity changes before strong earthquakes in Thessalia, central Greece. For this reason, all earthquakes which occurred since 1901 in this area and were larger than certain cut-off magnitudes were considered. It was found that the 1980 Magnesia earthquake (M_s=6.5) had been preceded by an increased seismic activity which started about four years before. On the other hand, trying to identify the current phase of the seismic cycle in Thessalia by using small magnitude seismicity data for the period 1981-1991, it was found that the seismicity rate shows no significant precursory variation while no earthquake with magnitude $M_L \geq 3.6$ occurred there since 1988.

INTRODUCTION

Precursory temporal seismicity variations have played an important role in most of the successful earthquake predictions that have been made to date. All of the successful predictions that have been made relied to a great extent on analysis of seismicity data (Habermann, 1988). A number of seismologists have examined seismicity prior to past earthquakes and proposed various patterns as precursors. Kanamori (1981), McNally (1982) and Habermann (1988) reviewed many of these studies and outlined the basic types of seismicity precursors (foreshocks, quiescence, swarms, accelerated activity and doughnuts). These precursors reflect time variations of earthquake occurrence frequency during the last phase of the seismic cycle. Recent work on the nature of the seismic cycle resulted in the refinement of the different phases of the cycle and it is presented in Figure 1 (Karakaisis et al., 1991). The post shock activity follows the first main shock of the seismic cycle and lasts up to several years, with its duration being dependent on the magnitude of the main shock. Then, the seismicity drops to the background level. During the last one-fourth of this phase, the seismicity exhibits a tendency to increase gradually. This phase, with duration dependent on the magnitude of the first main shock, is followed by a period of increased activity with an average duration of about 2.7 years which culminates before the second main shock, while its duration does not depend neither on the first nor on the second main shock magnitudes.

of seismicity before strong main shocks which occurred in Thessalia (central Greece) in the past and to identify, if possible, the current phase of the seismic cycle in this area.

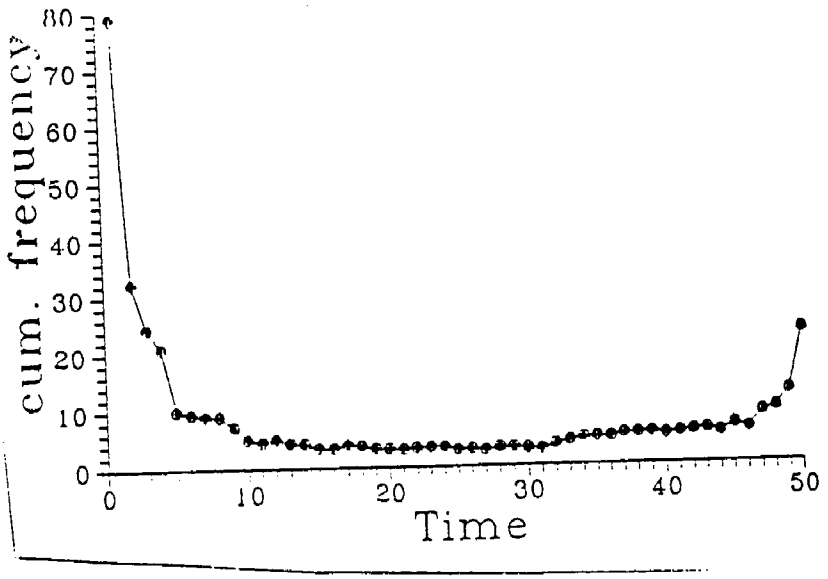

Fig. 1. Temporal variation of seismicity during a single seismic cycle (Karakaisis et al., 1991).

TEMPORAL VARIATIONS OF SEISMICITY BEFORE MAIN SHOCKS IN THESSALIA

During the present century, five strong main shocks occurred in Thessalia: i) 1905, 6.0; ii) 1930, 6.0; iii) 1941, 6.3; iv) 1954, 7.0; v) 1980, 6.5. Figure 2 shows a geomorphological map (contour lines of 300 m and 900 m are drawn) of the broader area of Thessalia along with the epicentres of the earthquakes, as it has been compiled by Papazachos et al. (1993). It is observed that most of the seismic activity is concentrated along a seismic belt which follows the southern boundary of the plain.

Figure 3 is a simple plot of the number and the magnitudes of earthquakes that occurred in Thessalia as a function of time. The data used come from the catalogue of Comninakis and Papazachos (1986) for the period 1901-1985 and from the monthly bulletins of the National Observatory of Athens and of the Geophysical Laboratory of the University of Thessaloniki for the period 1986-1991. It is observed that the seismic activity had started to increase a few years before the 1980 earthquake.

CURRENT SEISMICITY IN THESSALIA

It has been found that small magnitude seismicity variations, which may reflect

changes in tectonic processes, can contribute greatly to the identification of the phase of the seismic cycle in certain seismogenic source (Aki, 1986; Habermann, 1988; Karakaisis, 1993).

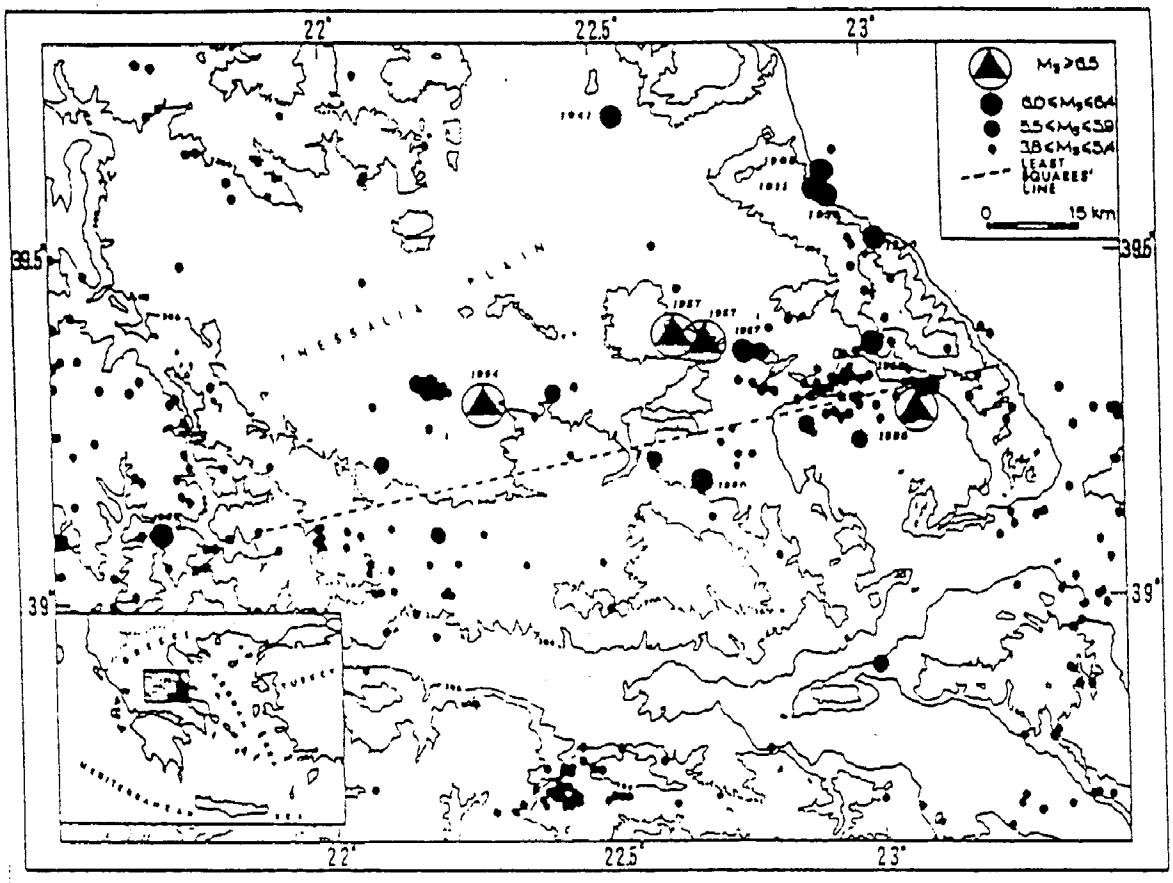

Fig. 2. Distribution of epicenters of earthquakes in the broader area of Thessalia (Papazachos et., 1993).

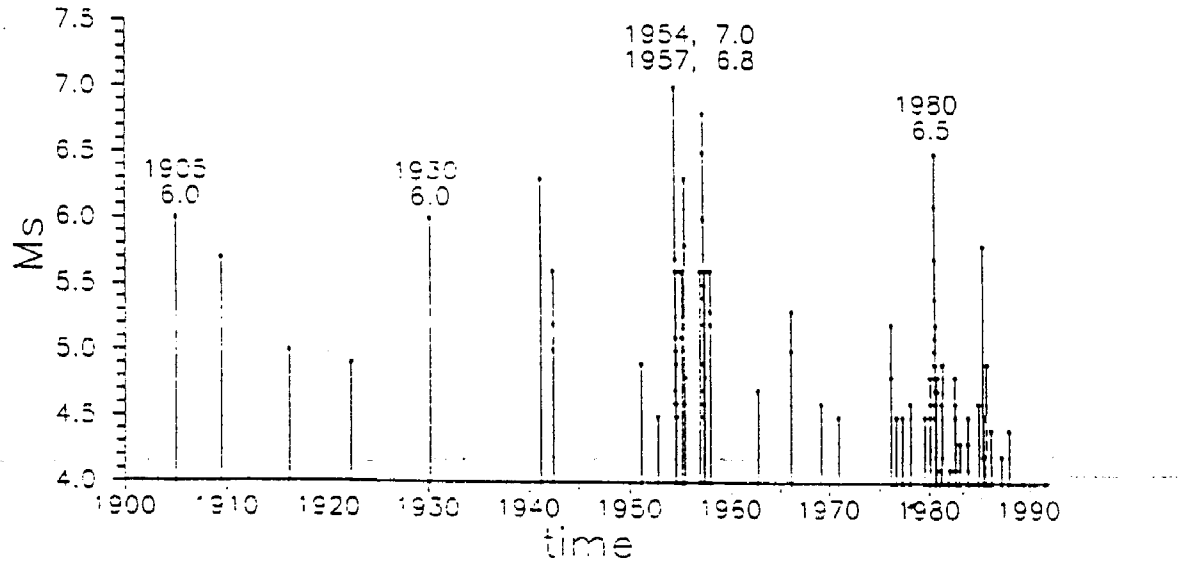

Fig. 3. Plot of the number and magnitudes of earthquakes which occurred in the area studied, as a function of time.

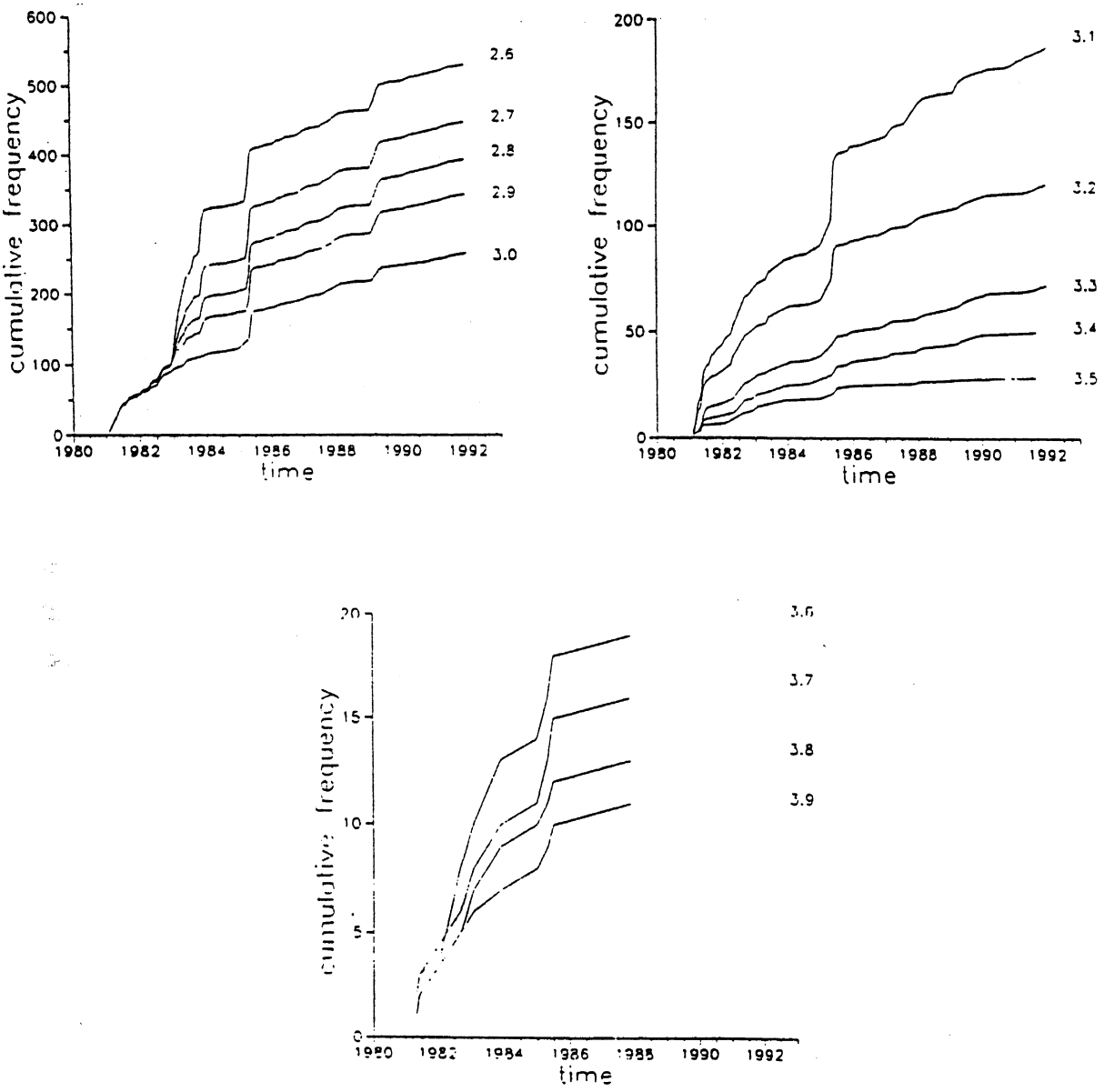

Fig. 4. Cumulative earthquake occurrence frequency for different cut-off magnitudes of the area studied.

In the present case, the data were found to be complete since 1981 onwards for earthquakes with magnitudes $M_L \geq 2.6$. Figure 4 shows the cumulative earthquake occurrence frequency during 1981-1991 for different cut-off magnitudes. It is observed that the seismicity rate had been high until 1985. The abrupt increase of seismicity in the beginning of 1985 corresponds to the 1985 (M_s=5.8) earthquake, which is considered to be a late aftershock of the 1980 (M_s=6.5) main shock. After 1985 the seismicity was continuously decreasing

while no earthquake with $M_L \geq 3.6$ occurred in the area since 1988.

CONCLUSION

An attempt was made in the present study to search for temporal seismicity precursors before strong earthquakes in the area of Thessalia and to identify the current phase of the seismic cycle. It was found that the 1980 Magnesia earthquake (M_s=6.5) had been preceded by an increased seismic activity which started about four years before. On the other hand, cumulative small magnitude seismicity plots till 1991 show that the seismicity has entered a low period, which probably corresponds to the background seismicity phase of the seismic cycle.

ACKNOWLEDGMENTS

The author is very grateful to Prof. Papazachos for stimulating discussions and for critically reading the manuscript. This work was financially supported by the European Center on Prevention and Forecasting of Earthquakes under the contract 122/1.11.91.

REFERENCES

Aki, K., (1986). Analysis of USGS local seismic network data for earthquake prediction. USGS Open-File Report 87-63, 183-185.

Comninakis, P. E. and Papazachos, B. C., (1986). A catalogue of earthquakes in Greece and surrounding area for the period 1901-1985. Publication of Geophys. Lab., Univ. of Thessaloniki, pp. 167.

Habermann, R. E., (1988). Precursory seismic quiescence: past, present and future. Pure and Appl. Geophys., 126, 279-318.

Kanamori, H., (1981). The nature of seismicity patterns before large earthquakes, in: Earthquake Prediction: an International Review, Maurice Ewing Series, vol. 4, D. Simpson and P. Richards, (eds.), AGU, 1-19.

Karakaisis, G. F., (1993). A microseismicity precursor before December 21, 1990 earthquake (M_s=5.9, northern Greece). 2nd Congress of Hellenic Geophys. Union, Florina, Greece, 5-7 May 1993, 147-153.

Karakaisis, G. F., Kourouzidis, M. C. and Papazachos, B. C., (1991). Behaviour of the seismic activity during a single seismic cycle. International Conference on Earthquake Prediction: State-of-the-Art, Strasbourg, France, 15-18 October 1991, 47-54.

McNally, K. C., (1982). Variations in seismicity as a fundamental tool in earthquake prediction. Bull. Seism. Soc. Am., 72, S351-S366.

Papazachos, B. C., Hatzidimitriou, P. M., Karakaisis, G. F., Papazachos, C. B. and Tsokas, G. N., (1993). Rupture zones and active crustal deformation in southern Thessalia, central Greece. Boll. Geofis. Teor. ed Appl., pp. 25, (in press).

2.3. RELATIVE SITE AMPLIFICATION FACTORS USING THE CODA WAVES FROM LOCAL EARTHQUAKES FOR THE SEISMOLOGICAL NETWORK OF THE GEOPHYSICAL LABORATORY

By

Hatzidimitriou, P.M.

Geophysical Laboratory, University of Thessaloniki, GR-54006 Thessaloniki, Greece.

ABSTRACT

The goal of the present paper is to determine the relative site amplification factors at the recording stations of the telemetric seismological network, operated by the Geophysical Laboratory of the University of Thessaloniki at northern Greece. For this purpose the properties of coda waves were used by applying the single S to S back-scattering model. We used data of local earthquakes occurred during the period 1983-1989 and recorded by the eight stations of the network. Spectral ratios of coda amplitudes have been calculated for lapse times between 30 sec and 60 sec and for frequencies of 1.5, 3.0, 6.0 and 12.0 Hz. The average site amplification relative to the mean of all stations is calculated. All of the stations show no or very low amplification and a stability over all frequencies.

INTRODUCTION

The geological characteristics of the upper layers beneath the seismological station affect the spectral shape of the recorded seismic waves. This effect, particularly known in the strong motion seismology, is called "site effect", (Aki, 1988; 1991). Traditionally, direct waves were used for the estimation of the site effects (eg. Borcherdt, 1970; Tucker et al., 1984). By comparing the results from direct S waves and coda waves Tsujura (1978) and Tucker and King (1984) showed that the site effects computed by using S and coda waves were very close and also that using coda waves more stable estimates of site amplification can be obtained. Since coda waves are considered to be composed of backscattered waves coming from many heterogeneities surrounding the source and receiver, the result is an average over all directions and furthermore, the separation of source, path and site effects is much simpler for coda waves than for S waves. Since then, site specific amplification factors using weak motion data from S wave coda have been successfully determined at sites of complex geology (Phillips and Aki, 1986; Mayeda et al., 1991; Su et al., 1992; Koyanagi et al., 1992).

However, the question of whether weak motion amplification scales linearly with strong

motion is still under investigation. Recently, Chin and Aki (1991) using strong motion records obtained from the 1989 Loma Prieta earthquake found that a non linear effect of sediment sites existed above a threshold acceleration of 0.1 to 0.3 g.

The purpose of the present paper is to estimate the site amplification factors by means of coda waves, for the eight stations of the telemetered seismologic network operated by the Geophysical Laboratory of the Universtity of Thessaloniki (Fig.1). These stations, which are Sohos (SOH), Serres (SRS), Ouranoupolis (OUR), Litochoron (LIT), Griva (GRG), Paliourion (PAIG), Kentriko (KNT), and Thessaloniki (THE), started their operation in 1981 while in 1989 four more stations have been installed but which are not studied in the present work.

METHOD APPLIED

Assuming that the local earthquake coda is composed of single backscattered S waves Aki and Chouet (1975) have shown that the amplitude spectrum, $A_c(\omega,t)$, of the coda at times greater than twice the S wave travel time can be expressed as

$$A_c=(\omega,t)=S_o(\omega)\cdot R(\omega)\cdot t^{-1}\cdot\exp(-\frac{bt}{2}) \qquad (1)$$

where t is the lapse time after twice the S wave travel time measured from the origin. So(ω) is a term that describes the source as a function of angular frequency , ω, and R(ω) is the site term. $b=2\pi f/Q$ is the coda attenuation coefficient and Q is the coda Q , which is independent of the location of source or the recording site. This equation shows that the effects of source, site and path can be isolated by taking spectral ratios of coda amplitude (Philips and Aki, 1986; Mayeda et al., 1991; Su et al., 1992). To determine relative site amplification between two stations, the same event must be recorded at both sites at the same lapse time. By taking the ratio of coda spectra, according to relation (1), both source and path effects are eliminated and thus the ratio depends only on the local site amplification of the two stations.

Implicit in the elimination of the path effect is the assumption that the shape of the coda decay curve $t^{-1}\exp(-\frac{bt}{2})$ is common to all stations. However, recent studies (Steck et al., 1989; Mayeda et al., 1991) have shown cases where the coda Q determined from the early coda was strongly dependent on the geology of the site. In these cases, in order to overcome this violation of the single scattering model data from larger lapse times must be used. For the area which is studied in the present study Hatzidimitriou (1993) has estimated

mean coda Q values for different lapse times. It was found that these coda Q values are very much dependent on the lapse time used for lapse times less than about 30 sec. Therefore in the present study in order to avoid the influence of the lapse time on the early coda we restricted to times greater than 30 sec.

DATA AND ANALYSIS

The data used in the present study come from local earthquakes recorded by the telemetric network, located at northern Greece, which is operated by the Geophysical Laboratory of the University of Thessaloniki. The network started its operation in 1981 and the data we used cover the period 1983-1989. During that time the network had eight stations each one equipped with one vertical and two horizontal of 1Hz natural frequency (S-13 Teledyne Geotech) seismometers. The signals from all stations are transmitted via telephone lines to the central station of Thessaloniki, digitized at 50 samples/second and the detected events are stored on magnetic tapes by a PDP 11/34 (Skordilis, 1985). Off-line P and S wave phase picking is made for each event on a daily basis and the earthquake parameters are determined using the HYPO71 computer program (Lee and Lahr, 1975), while the magnitudes of the earthquakes are determined from the signal duration. All the stations are calibrated every year and therefore their frequency responce is accurately known.

The seismograms of all the well located events (more than one thousand earthquakes) were visually examined to check whether there were any recording problems such as noise, saturation, missed recordings, overlapping (a second earthquake at the coda of the first one) or early cut off (the seismogram recording was terminated too early to have well developed coda waves). In this way 317 events were finally selected for further analysis. In Figure (1) we show the epicenters of these earthquakes (circles) and the seismological stations (black triangles). The local magnitudes of these events are between 1.0 to 4.5, while the focal depths are all less than 20 km.

For the present study only the vertical components of the seismograms have been used.The Fourier amplitude spectrum, $F(\omega)$, was computed at lapse times 30, 40, 50 and 60 sec all of which are after twice the S wave travel time.The window lengths were 512 points for frequency 1.5 Hz, 256 points for 3.0 Hz and 128 points for frequencies 6.0 and 12 Hz. $F(\omega)$ was corrected for instrument gain and averaged over octave frequency bands centered at 1.5 , 3.0, 6.0 and 12.0 Hz. The Fourier amplitude spectrum of the noise before the P-wave arrival for the same time windows was calculated, corrected for the instrument gain, averaged over the same frequency band and then subtracted from the corrected coda amplitude.

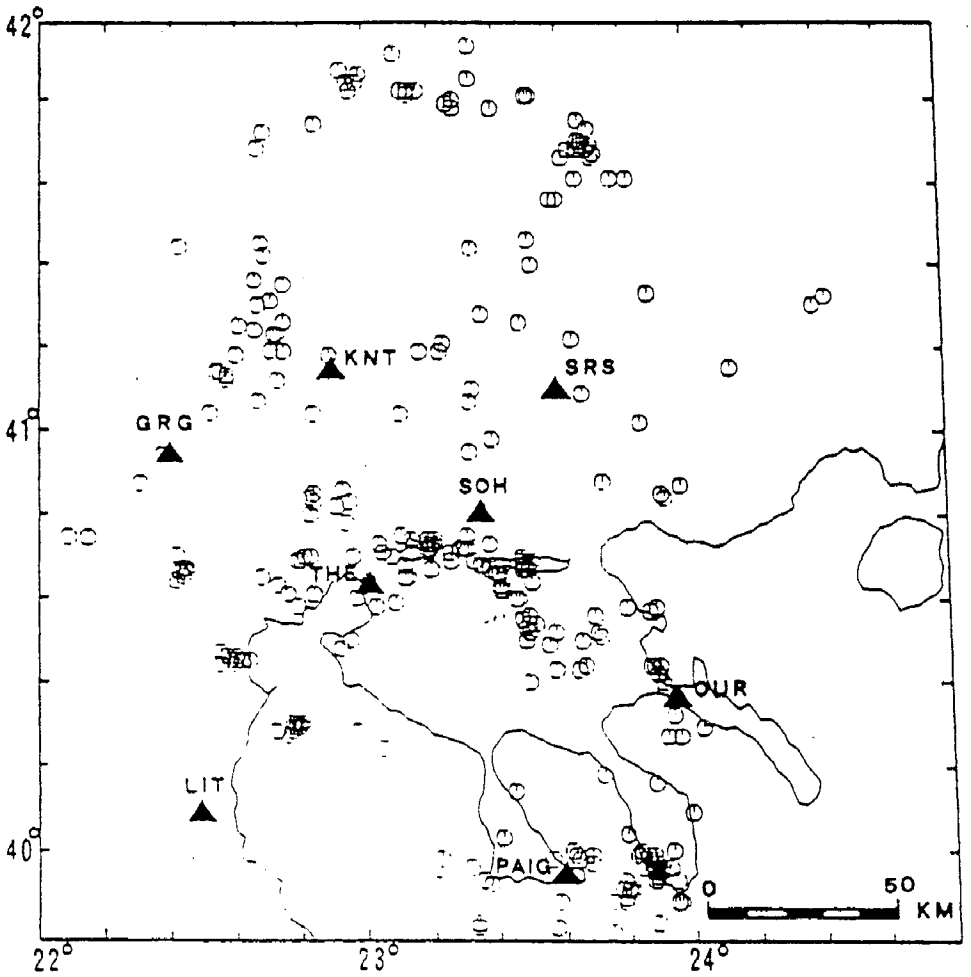

Fig.1. Map showing the stations (black triangles) and the events (open circles) used for the estimation of the relative site amplification.

RESULTS AND DISCUSSION

From the first processing of the data it was found that there were not many earthquakes which were recorded by all stations of the network so it was not possible to define one station as a "reference station". For this reason, for each earthquake and frequency we calculated the mean coda amplitude of all the stations for each of the four lapse times and then the coda amplitude ratio for each station was calculated relative to this mean value. Then the logarithm of the average of the ratios of all four times was calculated for each station and this is the logarithmic average relative site amplification for each station.

Table 1. Logarithmic average relative site amplification values and their standard deviation for eight stations of the seismologic network operated by the Geophysical Laboratory, for frequencies of 1.5 Hz, 3.0 Hz, 6.0 Hz and 12.0 Hz. The numbers in parentheses are the number of data used for the calculation of the mean.

Station	***Frequency***			
	1.5 Hz	***3.0 Hz***	***6.0 Hz***	***12.0 Hz***
SOH	0.01 ± 0.14	0.06 ± 0.14	0.00 ± 0.12	-0.02 ± 0.11
	(134)	(217)	(135)	(158)
LIT	0.20 ± 0.22	0.17 ± 0.15	0.17 ± 0.11	0.14 ± 0.14
	(21)	(43)	(27)	(7)
GRG	-0.04 ± 0.15	-0.05 ± 0.13	-0.13 ± 0.13	-0.29 ± 0.18
	(101)	(150)	(116)	(60)
PAIG	0.06 ± 0.13	-0.06 ± 0.16	-0.20 ± 0.10	-0.25 ± 0.09
	(41)	(92)	(76)	(51)
KNT	-0.16 ± 0.15	-0.14 ± 0.18	-0.11 ± 0.13	-0.06 ± 0.13
	(91)	(221)	(198)	(192)
OUR	-0.04 ± 0.16	0.02 ± 0.15	0.14 ± 0.11	0.10 ± 0.10
	(53)	(112)	(154)	(133)
SRS	0.04 ± 0.12	0.03 ± 0.11	0.04 ± 0.10	0.09 ± 0.10
	(108)	(111)	(187)	(163)
THE	-0.14 ± 0.15	-0.17 ± 0.18	-0.13 ± 0.16	-0.22 ± 0.20
	(55)	(92)	(73)	(46)

The values of the logarithmic average relative site amplification for four frequencies, calculated for the eight stations are given in Table 1, with their standard deviations of the mean and the number of observations used for their estimation.

In Figure 2 we show the plots of the logarithm of the average relative site amplification for each station versus frequency. Vertical bars are the standard deviations of the mean.

Two main characteristics can be obtained from Figure 2. The first is that the stations show very small or not at all site amplifications with very small standard deviations. The second is that the relative site amplification for each station is stable for all frequencies, with the exception of stations GRG and PAIG who show no amplification at 1.5 and 3.0 Hz and negative amplification at 6.0 and 12.0 Hz. Stations SOH and SRS show no amplification over

all frequencies. OUR and LIT show systematically small amplifications over all frequencies while THE and KNT show small negative amplifications over all frequencies. During the installation of the network the sites of the stations have been carefully chosen in order to be on hard crystalline rocks. For that reason the small and stable site amplifications found in the present study were expected.

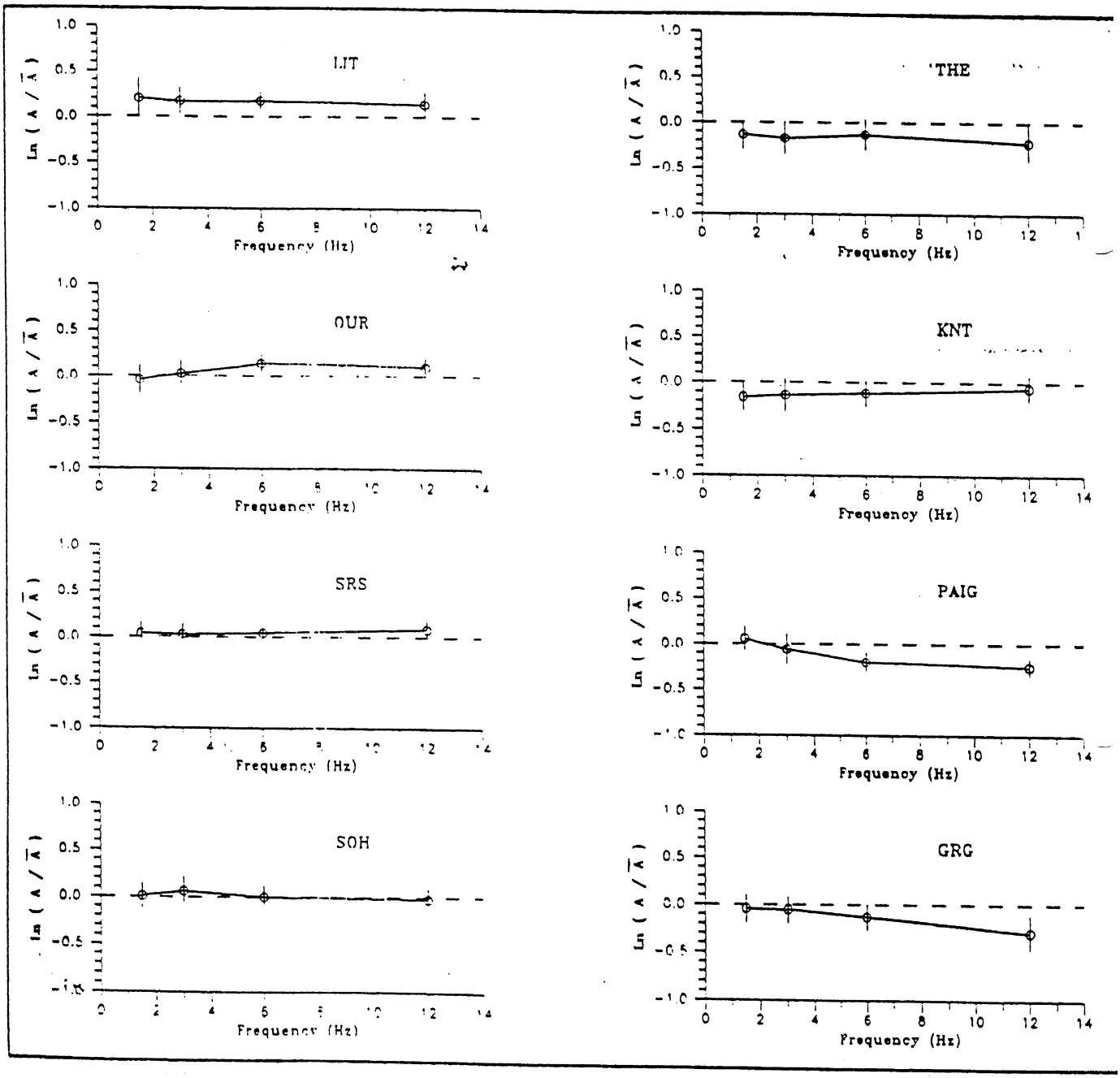

Fig.2. Frequency dependence of the logarithm of the S-wave coda average site amplification calculated relative to the mean of all eight stations. Vertical lines represent one standard deviation.

The results of the present study are in very good agreement with the results of Chavez-Garcia et al. (1990) who studied the site effects using five digital portable stations around the city of Thessaloniki, one of which was very close to the central station of Thessaloniki. They also found no significant site amplifications at the stations located on crystaline rocks.

ACKNOWLEDGMENTS

A part of this work has been done when the author was a visiting scholar at the University of Southern California. From that position he would like to express his sincere gratitude to Prof. Keiti Aki for his great help and encouragment during his stay at USC. Special thanks are due to F.Su and K.Mayeda for their help in the computing and their useful comments and discussions. The author is grateful to Prof. B.C.Papazachos for his encouragment and his critical comments. This work has been supported by the European Centre on Prevention and Forecasting of Earthquakes under the contract 122/1.11.91 and by the Earthquake Planning and Protection Organization project No. 2904/93.

REFERENCES

Aki,K., (1988). Local site effects on strong ground motion. Proc. Earthquake Eng. Soil. Dyn. II, GT Div/ASCE, Park City, Utah, 27-30 June, 1988, 103-155.

Aki,K., (1991). Local site effects on weak and strong ground motion. Proc. New Horizons in Strong Motion: Seismic Studies and Engineering Practice, Santiago, Chile,4-7 June 1991, 35 pp.

Aki,K. and Chouet,B., (1975). Origin of coda waves: source, attenuation and scattering effects. J.Geophys.Res. 80, 3322-3342.

Borcherdt, R.D., (1970). Effects of local geology on ground motion near San Francisco Bay. Bull. Seism. Soc. Am., 60, 29-61.

Chavez-Garcia,F.J., Pedotti, G., Hatzfeld, D. and Bard, P-Y.,(1990). An experimental study of site effects near Thessaloniki (northern Greece). Bull. Seism. Soc. Am., 80, 784-806.

Chin,B-H. Aki,K., (1991). Simultaneous study of the source path and site effects on strong ground motion during the 1989 Loma Prieta earthquake: a preliminary result on pervasive nonlinear site effects. Bull. Seism. Soc. Am., 81, 1859 1884.

Hatzidimitriou,P.M., (1993). Attenuation of coda waves in northern Greece. Pure Appl. Geoph., (in press).

Koyanagi,S., Mayeda,K. and Aki,K., (1992). Frequency dependent site amplification factors using the S-wave coda for the island of Hawaii. Bull. Seism. Soc. Am., 82, 1151-1185.

Lee,W.H.K. and Lahr,J.C., (1975), HYPO71: A computer program for determining hypocenter, magnitude and first motion pattern of local earthquakes. U.S. Geol. Surv. Open File Report, 114p.

Mayeda,K., Koyanagi,S. and Aki,K., (1991), Site amplification from S-wave coda in the long Valley Caldera region, California. Bull. Seism. Soc. Am. 81, 2194-2213.

Phillips,W.S. and Aki,K., (1986). Site amplification of coda waves from local earthquakes in central California. Bull. Seism. Soc. Am. 76, 627-648.

Scordilis,E.M., (1985). Microseismic study of the Serbomacedonian zone and the surrounding area. Ph.D Thesis, University of Thessaloniki, Thessaloniki. (in Greek)

Steck,L.K., Prothero,W.A. and Scheimer,J., (1989). Site dependent coda Q at Mono Craters, California. Bull. Seism. Soc. Am. 79, 1559-1574.

Su,F., Aki,K., Teng,T., Zeng,Y., Koyanagi,S. and Mayeda,K., (1992). The relation between site amplification factor and surficial geology in central California. Bull. Seism. Soc. Am., 82, 580-602.

Tucker,B.E. and King,J.L., (1984). Dependence of sediment filled valey response on the input amplitude and the valey properties. Bull. Earthq. Res. Inst., 74, 153-165.

Tucker,B.E., King,J.L., Hatzfeld,D. and Nersesov,I.L., (1984). Observations of hard-rock site effects. Bull. Seism. Soc. Am., 74, 121-136.

Tsujura,M., (1978). Spectral analysis of the coda waves from local earthquakes. Bull. Earthq. Res. Inst., 53, 1-48.

2.4. ELECTRIC AND MAGNETIC FIELD MEASUREMENTS FOR EARTHQUAKE PREDICTION IN SOUTHERN THESSALIA

G. N. VARGEMEZIS and G. N. TSOKAS

Laboratory of Geophysics, University of Thessaloniki, GR-54006 Thessaloniki, Greece

INTRODUCTION

Monitoring of a few geophysical fields which show an abnormal behavior associated with earthquakes was attempted. Electromagnetic methods were employed for the time being and therefore quantities like the magnetic induction and the natural potential are recorded. It is well known that the referred to fields show time and space dependent variations of precursory nature. However, it is also well known that these signals do not appear in a regular pattern. Furthermore they strongly differ in magnitude, duration and occurrence time.

The activities reported below concern a repeated magnetic survey and the monitoring of the electric and magnetic field in a permanent base station.

MAGNETIC NETWORK

A total number of 10 locations were selected along the fracture zone forming the southern boundary of the Thessalia plane (Fig. 1). That fracture zone was traced by Papazachos et al. (1993) using seismological, gravimetric and geomorphological data. As shown in Figure 1, the magnetic stations are laid on both sides of the fracture zone.

Each station consists of a concrete base where an alluminium frame had been implanted. An alluminium tower of 2m hight was placed in the frame, and thus stabilized, each time a measurement had to be taken (Fig. 2).

The measurements were carried out in a differential fashion using the station of EUX near Euxinoupolis as base one. The reasoning is that this station is located relatively far away from the fracture zone. Thus, it is considered to be in an "unaffected" environment with respect to the particular fracturing zone.

The difference of the earth's magnetic field intensity was recorded overnight between the base station and each one of the others, one at a time. Therefore, each time the survey has to be repeated, 9 days of field work are needed if two instruments are used.

Proton precession magnetometers were used for this study. The difference between two stations was measured every 30 seconds for a total of 12 hours. Finally, the survey has been carried out two times for the time being. The whole procedure commenced at the interval 10-20 March 1993.

The installation needed and the initial repeated surveys were carried out by means of other sources. The network measurement was scheduled to be repeated every 3 months. The survey has been repeated 5 times since the beginning of the project.

The value, assigned to a particular station at each survey, was considered as the mean of the difference recorded overnight between that station and the base. The standard deviation of the readings was relatively low. Its maximum value of the order of 5nT was observed at the station of PETROTO during June 1993.

It must be considered that the time interval of the operation is rather too small to observe precursory phenomena in copmarison with other studies all around the globe. Therefore, the continuation of this work is necessary in order to reach some results.

ELECTRIC AND MAGNETIC FIELD MONITOR

It has been suggested long ago that the difference between observed earth potentials and those predicted by the theory of electromagnetic induction should be used to record any anomalous change in earth currents related to earthquakes.

The area of the village Neraida near Farsala was chosen for the installation of an electric and magnetic field monitor (Fig. 1). The particular area is relatively flat and fairly remote from irrigation pumps. On the other hand it is easily accessible and has been linked to the power supply and the communication networks.

A small room 3x4 m^2 houses the instrumentation, the local computer and the modem for telecommunication (Fig. 2).

The electric field is measured at two perpendicularly laid dipoles each of them having a length of 100m. The dipoles are orientated N-S and W-E and non polarizable electrodes of the Cu-$CuSO_4$ type are used.

The earth's magnetic field intensity is measured in the triaxial sense. The N-S, E-W and vertical components are recorded.

Each field is sampled at 30 second intervals and the readings are stored in a locally based computer.

The instrumentation is custom built. We built it in the Laboratories of the Dept. of Electrical Engineering of the Aristotle University of Thessaloniki. It includes input buffering, signal conditioning, communication and sampling software. Also, we developed software under MS-DOS Windows which is able to transmit data while sampling.

The whole system is supported by uninterruptable power supplies. Figure 3 shows a simplified diagram of the basic units of the instrumentation which was put in operation in March 1993.

A second unit is now built and planned to be installed in Northern Greece. This second unit will serve as reference to the first one. In other words, it will serve to disgard anomalies observed in a local bases.

As it is already refered, the parameter which is essentially monitored and whose variations are to be correlated to earthquake activity, is the difference between observed and calculated earth potential. Thus, the computation of this residual field is based upon the estimation of the induction caused to the electrical dipoles by variations of the earth's magnetic field.

The operation is done in the frequency domain. The elements of the tensor which represents the transfer function is obtained as a least squares solution in narrow bands of frequencies. The computer program used was developed by the research group participating in this project.

A sample of the raw data is shown in Figure 4. The uppermost diagram depicts the variation of the B_x (N-S) component of the Earth's magnetic field for the interval of one day, namely the 19th of April, 1993. The immediately following diagrams represent the variation of the B_y (E-W) and B_z components. The respective components of the Earth's potential (E_x, E_y) follow. The sixth channel at the lowermost part of the Figure, is a record of the potential difference which was produced by a small battery. It was set so in order to test the performance of our instrumentation.

Figure 5 shows the 5 components of the magnetotelluric field for the 8th of March 1993. Several variations are observed in the raw data which could be attributed to any cause. However, after the reduction of the data for the lectromagnetic effect both E_x and E_y components appear relatively flat (Figures 6 and 7).

REFERENCES

Papazachos, B.C., Hatzidimitriou, P.M., Karakaisis, G.F., Papazachos, C.B. and Tsokas, G.N. (1993). Rupture zones and active crustal deformation in southern Thessalia, central Greece. "Boll. Geofis. Teor. Appl.", (in press).

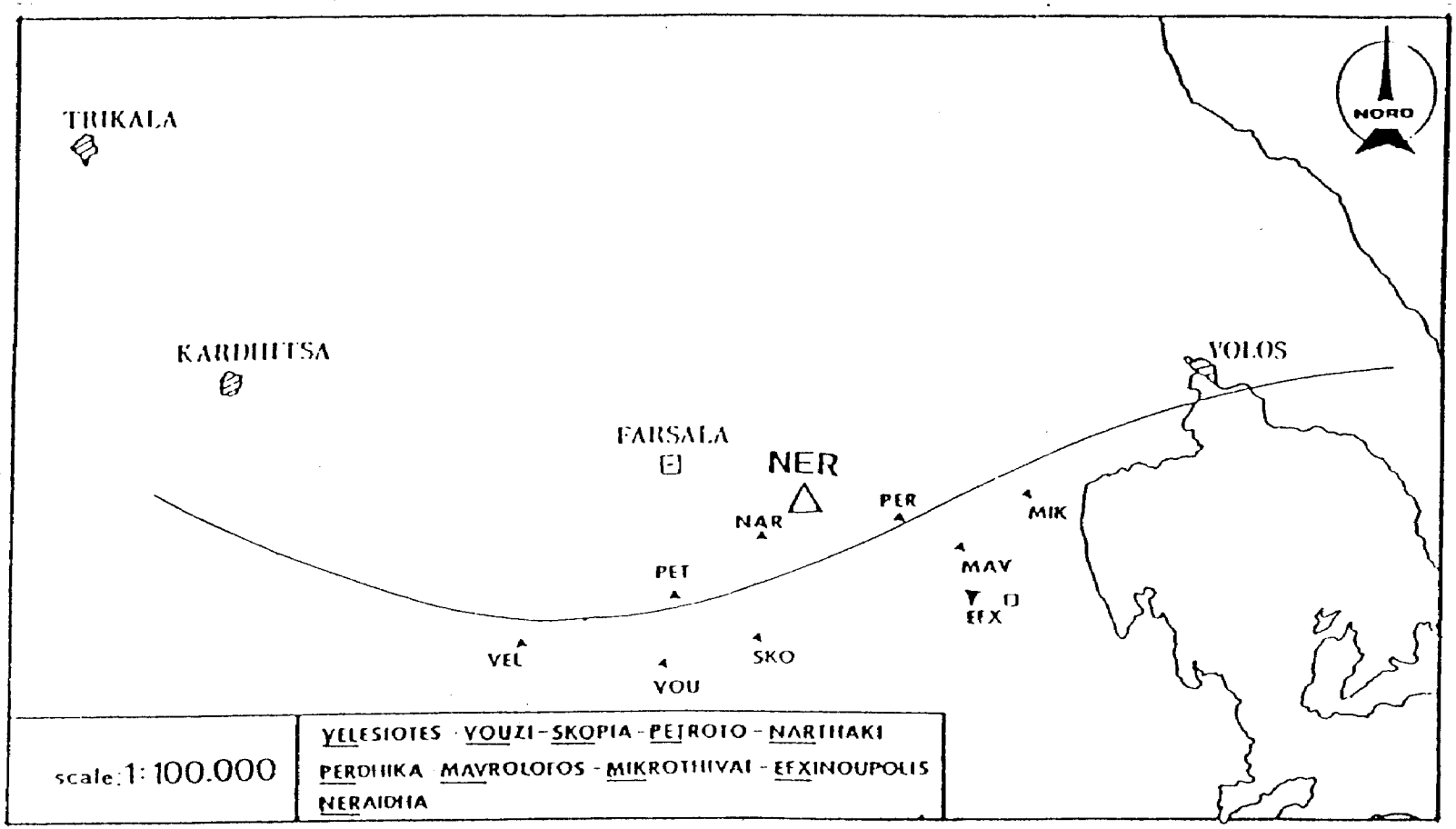

Figure 1. The solid line represents the approximate location of the fracture zone which forms the southern boundary of Thessalia plane. The locations of the stations forming the magnetic network are represented by small triangles annotated with the first 3 letters of the site name. The large blanc triangle marks the location of the permanent installation for the electromagnetic station. It is also a station of the magnetic network.

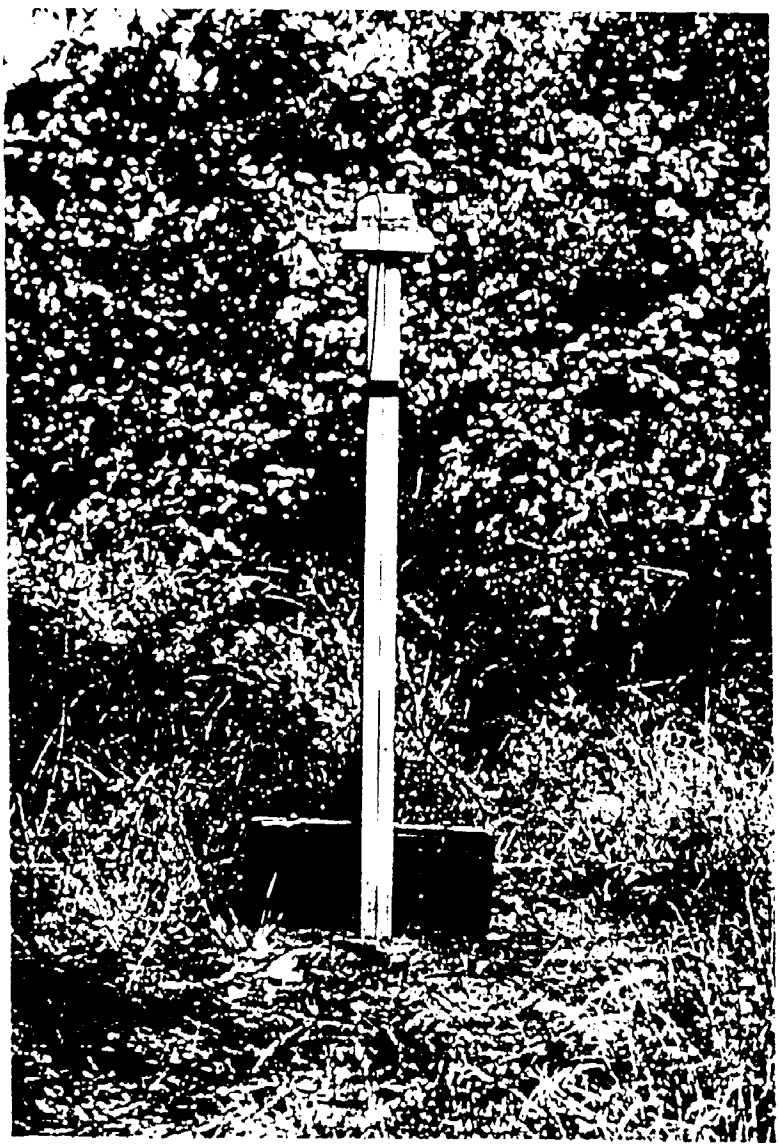

Fig. 2. The alluminium tower supporting the proton magnetometer's sensor at the station of Mavrolofos (MAV).

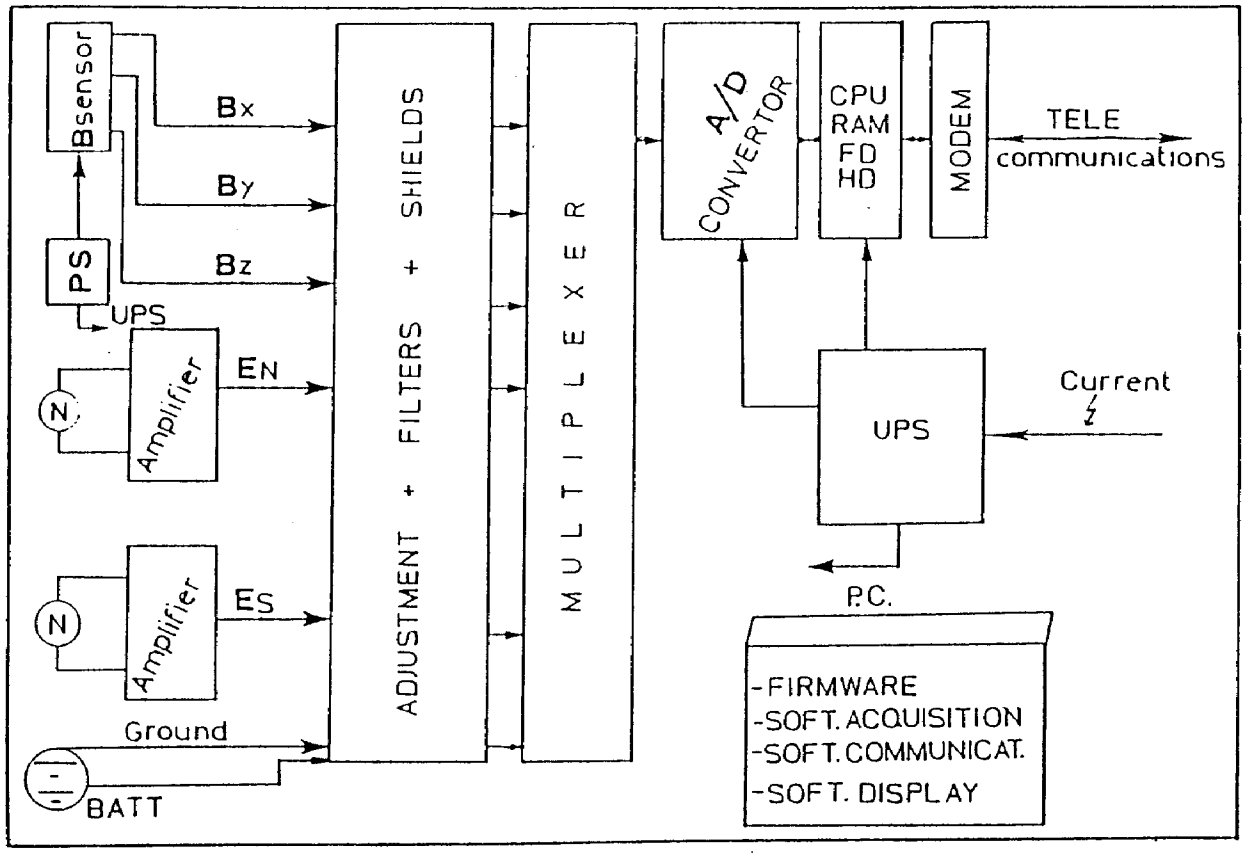

Fig. 3. Simplified diagram of the basic components of the custom built instrument which installed near the village Neraida.

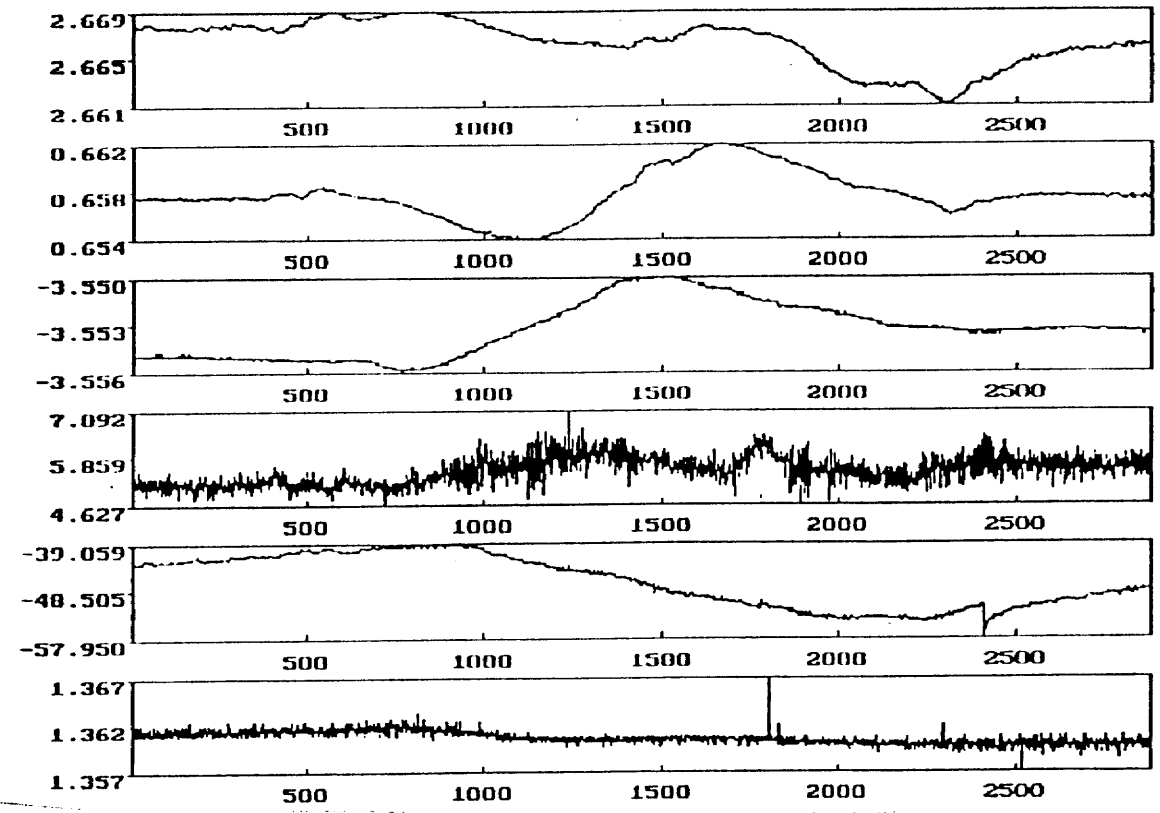

Fig. 4. Variation of the E_x, E_y, B_x, B_y, B_z components of the magnetotelluric field recorded during the 19th of April 1993. The lowermost diagram shows the time variation of the voltage of a small 1.5V battery which was set on the sixth channel for testing purposes.

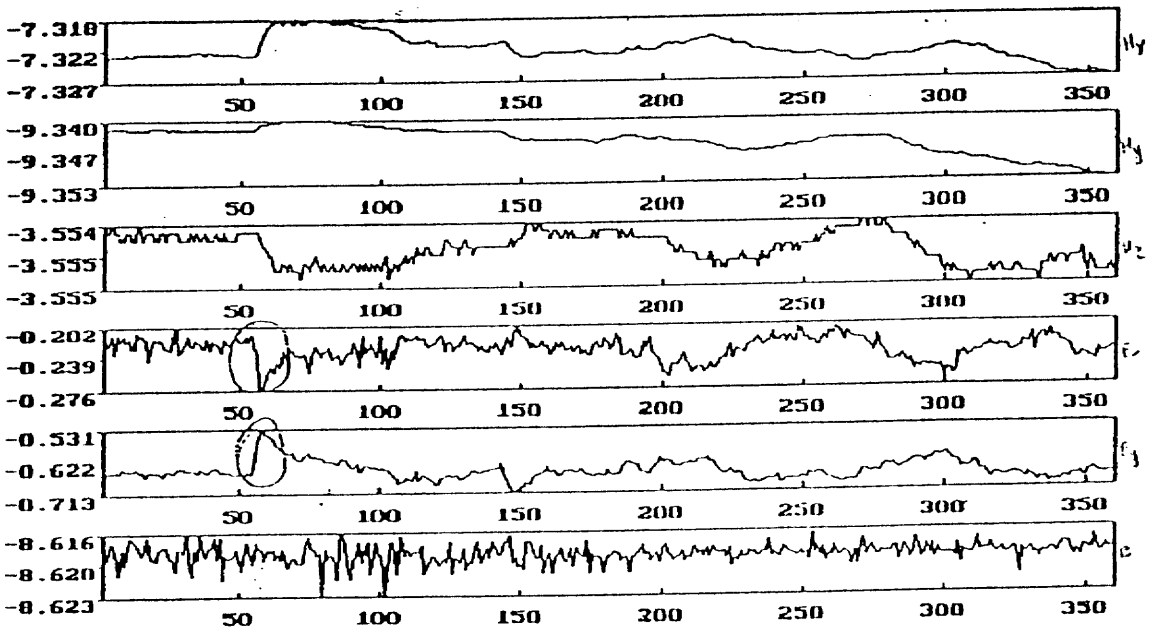

Fig. 5. Variation of the E_x, E_y, B_x, B_y, B_z components of the magnetotelluric field recorded during the 8th of March 1993. The lowermost diagram shows the time variation of the voltage of a small 1.5V battery which was set on the sixth channel for testing purposes.

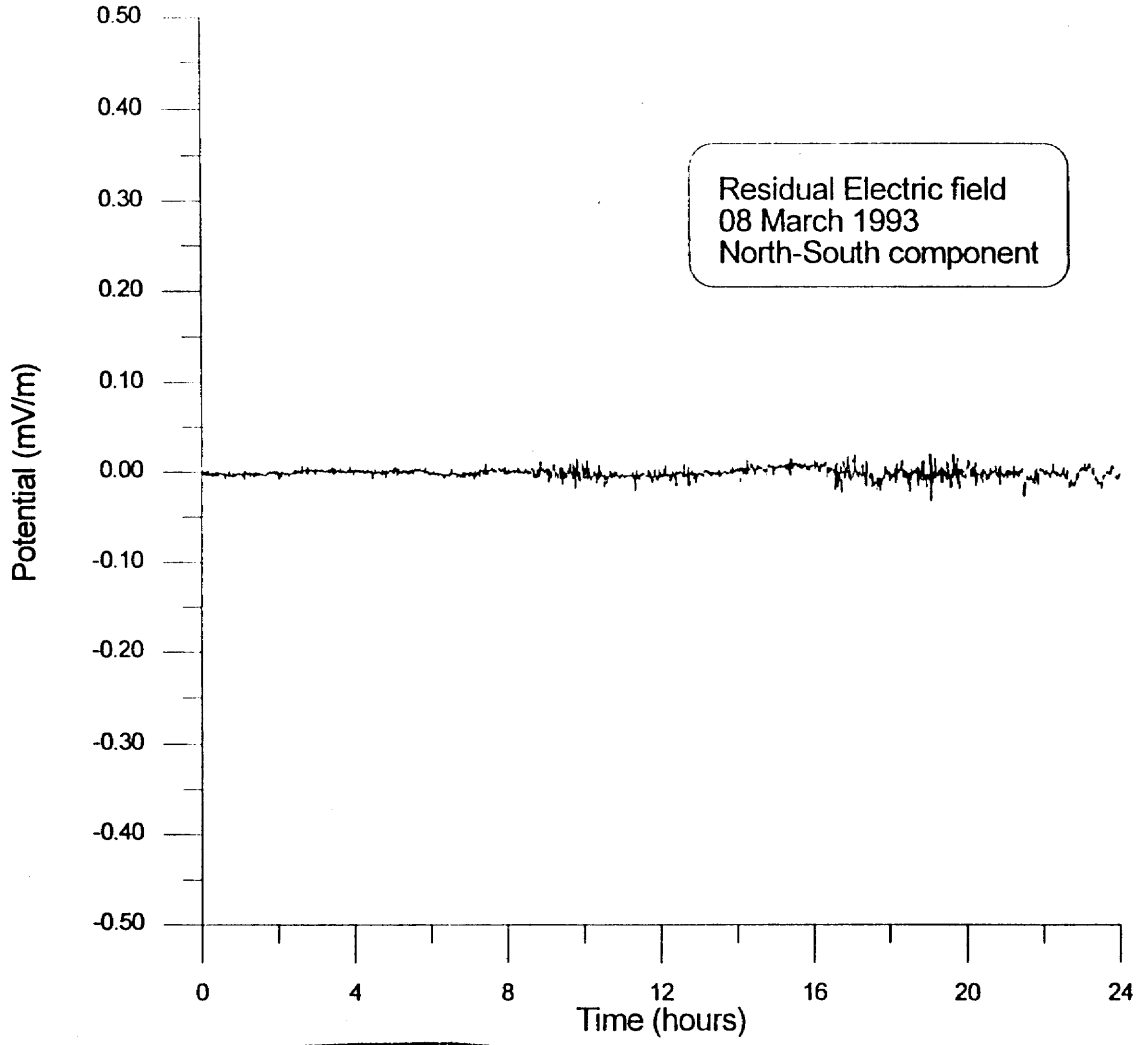

Fig. 6. Variation of the E_x component during the 8th of March

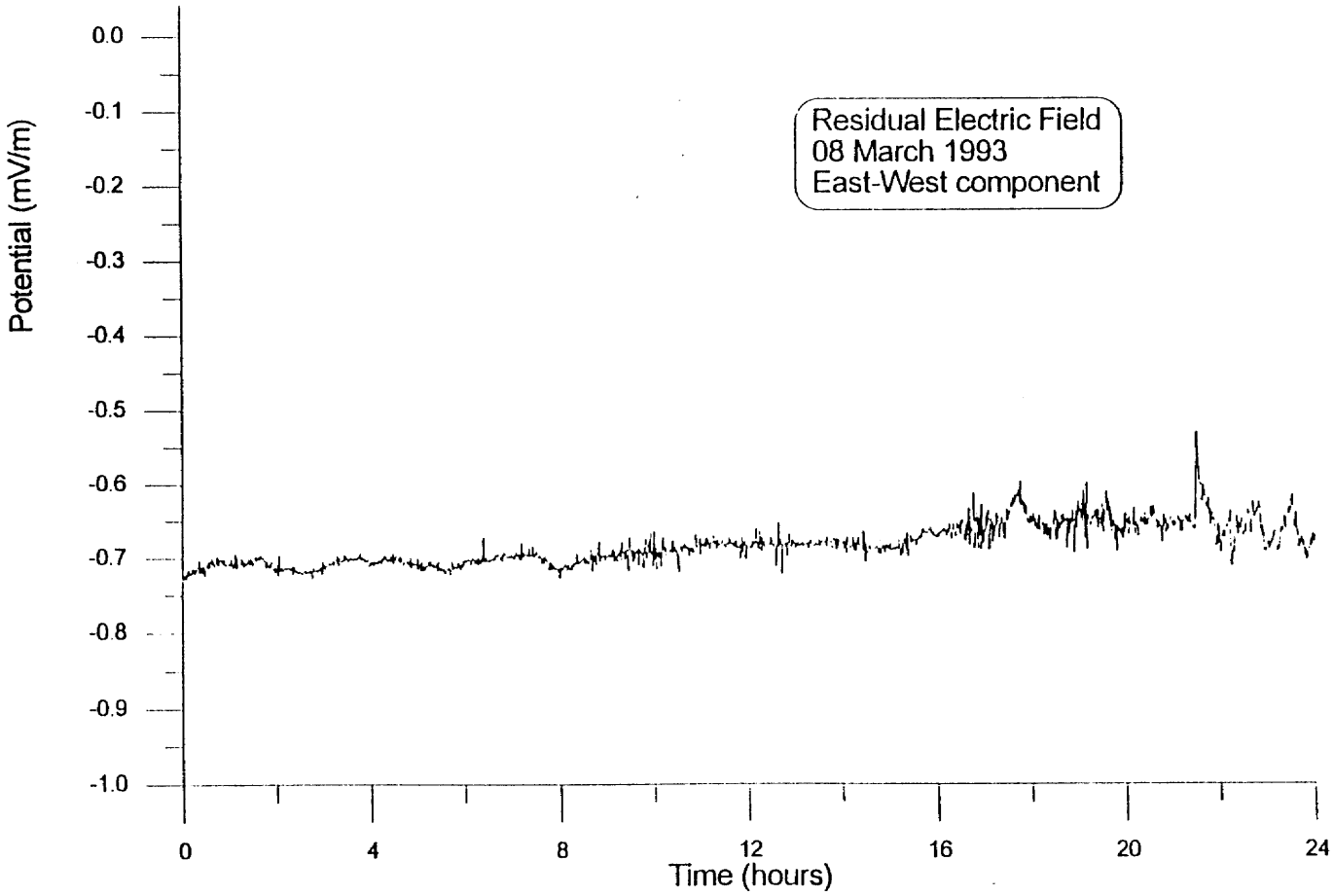

Fig. 7. Variation of the E_y component during the 8th of March

FINAL REPORT OF THE GEODYNAMIC INSTITUTE, NATIONAL OBSERVATORY OF ATHENS ON THE "E.C.P.F.E" PROJECT (No 122/1/11/91)

G.N. STAVRAKAKIS, *Scientific Responsible*

'ν-Value' Model for Earthquake Prediction. An Application to the Earthquakes Occurred in the Area of Magnesia (Central Greece)

PAPANASTASSIOU D. and G.N. STAVRAKAKIS

1. Introduction

Changes in the pattern of seismic activity, such as foreshocks and temporary changes in the *b* value prior to the occurrence of large earthquake, have been shown to be very useful for earthquake prediction. The identification, however, of foreshocks and their relation to the magnitude and time of the main shock is not so clear and discrimination cannot usually be made until the mainshock occurs. Several prediction algorithms essentially using the number of earthquakes occurring in a certain time window and the distribution of time intervals of earthquakes, have been proposed by *Keilis-Borok et al. (1978, 1980a, b)* and tested by *Sauber and Talwani (1980)* for identifying foreshocks.

Mogi (1967) concluded that the type of earthquake sequence depends mainly on the structural state of the Earth's crust and the space distribution of the applied stresses. Three kinds of sequence patterns, namely, successive, periodical, and random, can be found in most earthquake catalogs, and may reflect the relationship between the tectonic stresses and stress releases during earthquakes.

In view of earthquake prediction, *Matsumura (1982, 1984)* developed a new method for describing seismicity patterns in the space and time domain, and proposed a new parameter, the 'ν-value', which is closely related to the apparent interaction between two successive earthquakes. This parameter is derived on the basis of the Weibull distribution and the values characterize the earthquake sequence as being periodical ($\nu>0.5$), clustered ($\nu<0.5$), or random ($\nu=0.5$).

This method has been already applied to some earthquake sequences occurred in the area of Greece during the last 15 years in an attempt to discover temporal changes in seismicity *(Papanastassiou et al., 1989a, b)*. The analysis of these earthquake sequences

revealed that low 'ν-values' preceded the occurrence of large earthquakes.

In this study, the earthquakes which occurred in the area of Central Greece (near Volos), during the last 25 years, has been analyzed by using this method.

2. The 'ν-Value' Model - Theoretical Considerations

In the following analysis, it is assumed that the occurrence of earthquakes is treated as a probabilistic phenomenon. A crucial problem in reliability analysis is the determination of the probabilistic distribution of failure-occurrence time, which, in our case, corresponds to the earthquake occurrence. The Weibull distribution function, which is widely applied to quality-control research, has been used by *Hagiwara (1974)* to estimate the probability of earthquake occurrence on the basis of crustal strain data in the south Kanto District of Japan. Based on this model, *Matsumura (1982, 1984)* defined the ν-parameter to make an unbiased assessment of possible time-dependent changes in seismicity patterns. A bried description of the ω-value model is made here, following *Hagiwara (1974)* and *Matsumura (1984)*.

The conditional probability that the rupture (i.e. earthquake) will occur in a time interval between t and $t + \Delta t$, is defined by $\lambda(t)\Delta t$, where $\lambda(t)$ is the hazard rate and is given by:

$$\lambda(t) = \lambda_1 t^{p-1} \quad (\lambda_1 > 0, p > 0) \tag{1}$$

The reliability function $R(t)$ is:

$$R(t) = \exp\{ - \int_0^{\infty} \lambda(t)\, dt \} = \exp\{ -\lambda_1 t^p / p \} \tag{2}$$

and the corresponding density function $f(t)$ is:

$$f(t) = - dR(t)/dt = \lambda_1 t^{p-1} \exp\{ - \lambda_1 t^p/p \} \qquad (3)$$

The mean time interval $\bar{\tau}$ between $t=0$ and the time at which the earthquake occurs, is obtained as:

$$\bar{\tau} = \int_o^\infty tf(t)\,dt = (p/\lambda_1)^{1/p}\,\Gamma(1 + 1/p) \qquad (4)$$

where, é is a gamma function.

The mean-square time $\overline{\tau^2}$ is given by:

$$\overline{\tau^2} = \int_o^\infty t^2 f(t)\,dt = (p/\lambda_1)^{2/p}\,\Gamma(1 + 2/p) \qquad (5)$$

Dividing the square of **Equation (4)** by **Equation (5)**, we obtain the ν parameter:

$$\nu = \{\Gamma(1 + 1/p)\}^2 / \Gamma(1 + 2/p) = (\bar{\tau})^2 / \overline{\tau^2} \qquad (6)$$

Based on the ν-values, the earthquake occurrence patterns are classified into the following three categories: successive ($0<\nu<0.5$), random ($\nu=0.5$), and periodic ($0.5<\nu<1.0$).

The parameters λ_1 and p of the Weibull distribution {**Equation (1)**}, are related to the seismic activity and seismic pattern, respectively. From **Equation (6)**, it is evident that the ν-value is a function only of p.

3. Data Analysis

In this study, have been used 850 earthquakes which occurred in the "a-posteriori" defined area (39.15°N - 39.40°N, 22.70°E - 23.30°E) of Magnesia (Central Greece), during the time period from

1965 till the end of 1992.

Figures 1,2 show the spatial distribution of the epicenters.

The earthquake parameters (origin time, epicenter coordinates, local magnitude) are those listed into the Monthly Bulletins of the Seismological Institute of the NOA.

Till 1987 the lower threshold for the magnitude was 3.0. After the establishment of teh NEO Seismological Station, which located southeast of the city of Volos (in the area of Pilion mountain), the lower threshold for the magnitude reduced at the value of 2.5 *(Papanastassiou, 1989)*.

During the above mentioned time period in the examined area occurred two earthquake sequences. Those of July 9, 1980, and of April 30, 1985. The first sequence was strong enough and the main shock of July 9, 1980, caused intensive damages especially at the area of Almyros. The earthquakes of the sequences with local magnitude M_L greater than 5.0 are listed in **Table I**.

TABLE I

Date	Origin Time	Coordinates	ML
9 July 1980	02 : 10	39.20°N - 23.00°E	5.2
9 July 1980	02 : 11	39.20°N - 23.00°E	6.0 Ms
9 July 1980	02 : 35	39.20°N - 22.70°E	5.6
10 July 1980	19 : 39	39.30°N - 22.90°E	5.0
30 April 1989	18 : 14	39.29°N - 23.57°E	5.3 Ms

(*) Ms: Main Shock

4. Results

The 'ν-value' has been computed on the basis of a number of successive earthquakes comprising a certain group. This group is successively moved by a window of events until the end of the data.

Different number of earthquakes consisting the groups and the moving windows have been used and the obtained results are given in **Figures 3 - 8**.

A star was plotted at the time of the last event within the

window and the vertical arrows indicate the occurrence time of the two main shocks of the sequences of 1980 and 1985.

Different number of earthquakes consisting the groups and the moving windows have been used and the obtained results are given in **Figures 3 - 8**.

Although the 'ν-values' in almost all the figures have values smaller than 0.5, showing successive occurrence, it is very impressive the abrupt decreases at very low values before the occurrence of the sequences.

It should be emphasized that the 'ν-value' seems to depend strongly upon the number of successive earthquakes which are included in a certain group and upon the moving window of the events.

So the 'ν-values' which calculated for groups consisting of small number of earthquakes and moved by a small number of shocks (**Fig. 3 - 4**) show greater fluctuations than in **Fig. 5 - 8**, where the groups and the moving windows correspond to larger number of earthquakes.

The decrease of 'ν-value' at the beginning of 1989 is caused by the earthquake sequence of March 19, with sequence occurred outside the examined area and the main shock had coordinates 39.29°N - 23.57°E and a magnitude 5.3.

In order to examine the validity of these results, the method has been also applied to a adjacent area, those which is limited by the coordinates (39.40°N - 39.65°N, 22.70°E - 23.30°E). In this area 140 shocks occurred in the same time period.

The results from this area are quite different.

The 'ν-value' is stable or fluctuates slowly, in the range of 0.4 and 0.6, showing a nearby random occurrence (**Fig. 9 - 10**).

The big difference of the results between the two regions reflect the difference in their seismotectonic activity.

The obtained results show that the 'ν-value' model could be applied for monitoring the seismicity changes in the examined area and is worth to used as a tool in earthquake prediction studies.

References

Hagiwara, Y. (1974). A stochastic model of earthquake occurrence a the accompanying horizontal ground deformation. "Tectonophysi- 26, 91-101.

Keilis-Borok, V.I., Rotwain, I.M. and Sidorenko, T.S. (197 Increased stream of aftershocks as a forerunner of st earthquakes. *"Dokl. Akad. Nauk. USSR", 242, 567-569* (in Russia

Keilis-Borok, V.I., Knopoff, L., and Rotwain, I.M. (1980a). Bu of aftershocks, long-term precursors of strong earthqu *"Nature", 283, 259-263.*

Keilis-Borok, V.I., Knopoff, L., and Rotwain, I.M. and Sidore T.M. (1980b). Bursts of seismicity as long-term precursors strong earthquakes. *"J. Geophys. Res.", 85, 801-811.*

Matsumura, S. (1982). One-parameter expression of earthqua sequence and its application to earthquake prediction. *"Zisin-2 35, 65-75* (in Japanese with English Abstract).

Matsumura, S. (1984). One-parameter expression of seismici patterns in space and time. *"Bull. Seism. Soc. Amer.", 74, 25 2576.*

Mogi, K. (1967). Earthquake and fractures. *"Tectonophysics", 5,* 55.

Papanastassiou, D. (1989). Detectability and accuracy of the so parameters of the seismic networks of the National Observatory Athens. Ph.D. Thesis, University of Athens.

Papanastassiou, D., Drakopoulos, J., Drakatos, G., Latoussakis, Stavrakakis, G. (1989a). 'ν-Value' model for earthqua prediction: An application to some recent earthquakes sequences Greece. *"Bull. Geol. Soc. Greece", XXIII/3, 129-143.*

Papanastassiou, D., Latoussakis, J., Stavrakakis, G. and Drakopoul J. (1989b). The Aegean Sea (Greece) earthquake sequence of March, 1986: An application of the 'ν-Value' method for earthqua prediction. *"Natural Hazards", 2, 105-114.*

Sauber, J. and Talwani, P. (1980). Application of Keilis-Borok a McNally prediction algorithms to earthquakes in the Lake Joca area, South Carolina. *"Phys. Earth Planet. Inter." 21, 267-28*

Utsu, T. (1977). Probabilities in earthquake prediction. *"J. Seism. Soc. Japan II", 30, 179-185.*

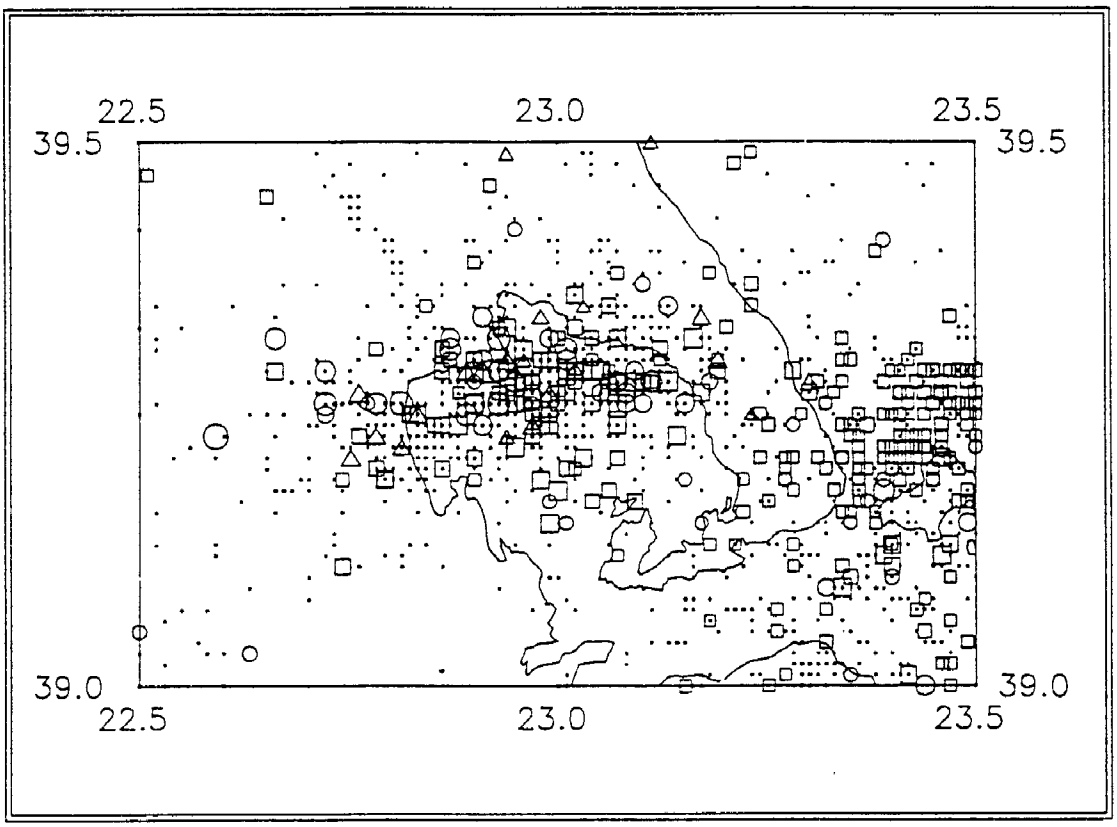

Depth(km)
□ < 20
○ 20 <and< 40
△ 40 <

□ M= 6.0
□ M= 5.0
□ M= 4.0
□ M= 3.0

0 30
km

1464 Events

Scale 1: 1000000

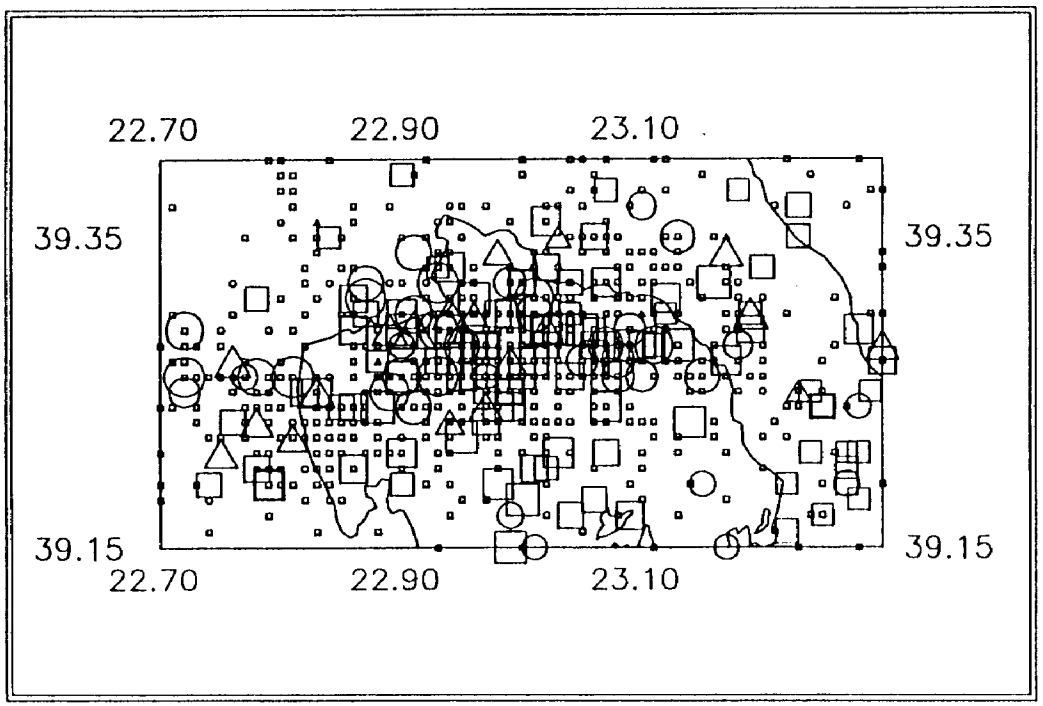

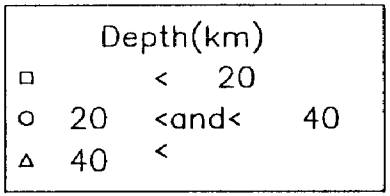

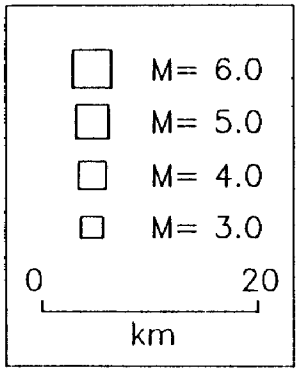

848 Events

Scale 1: 700000

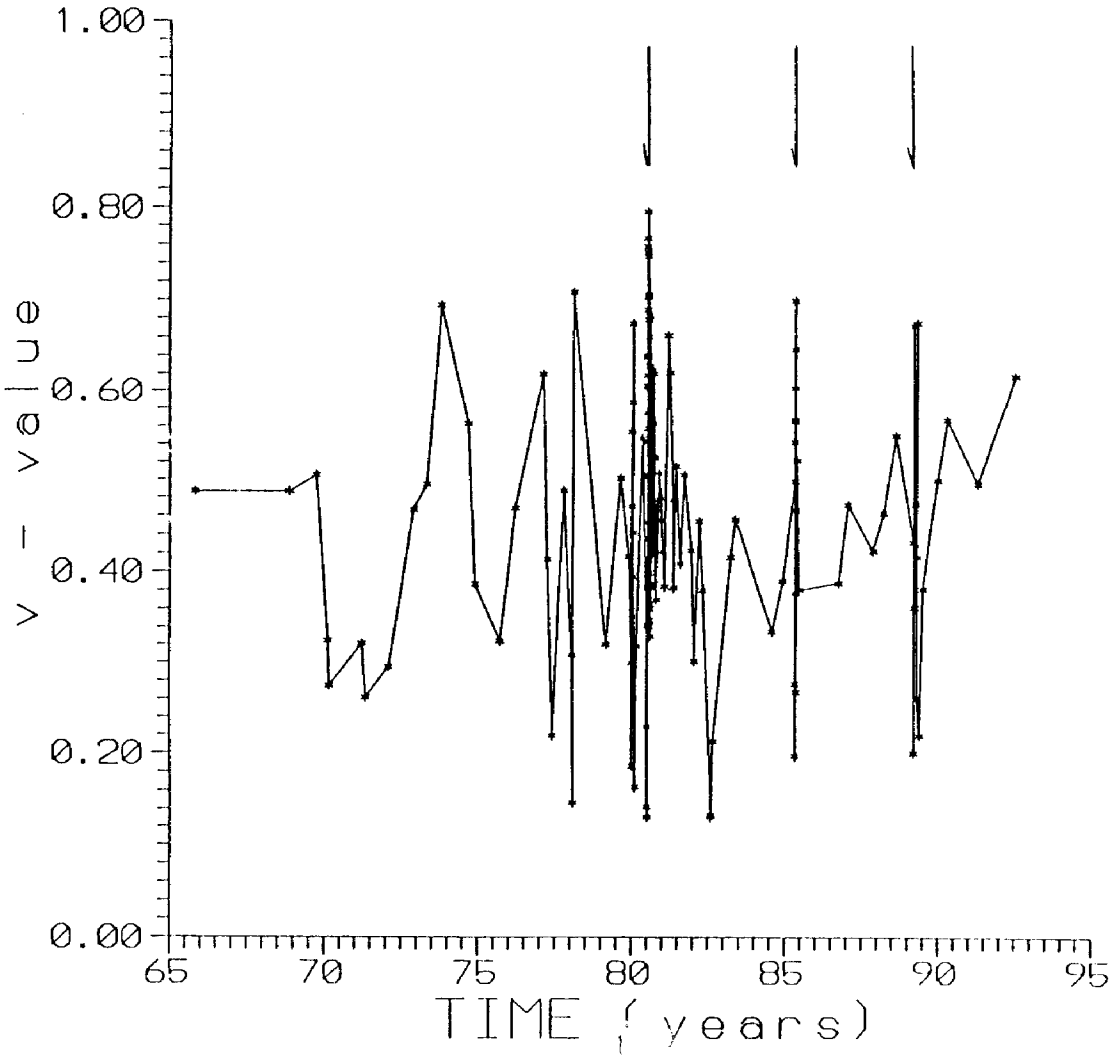
1.00
0.80
0.60
0.40
0.20
0.00
V - value
65
70
75
80
85
90
95
TIME (years)

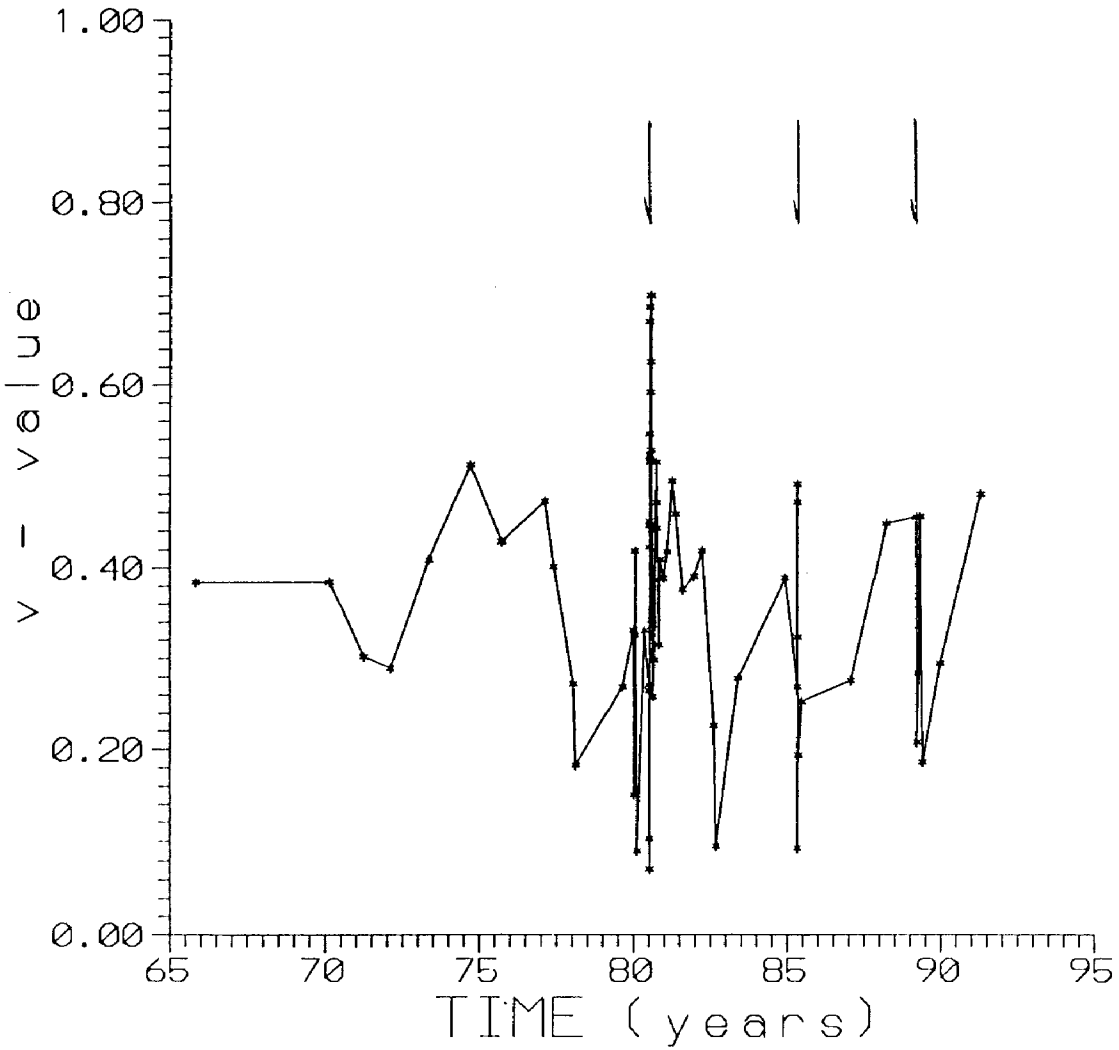
1.00
0.80
0.60
0.40
0.20
0.00
v - value
65
70
75
80
85
90
95
TIME (years)

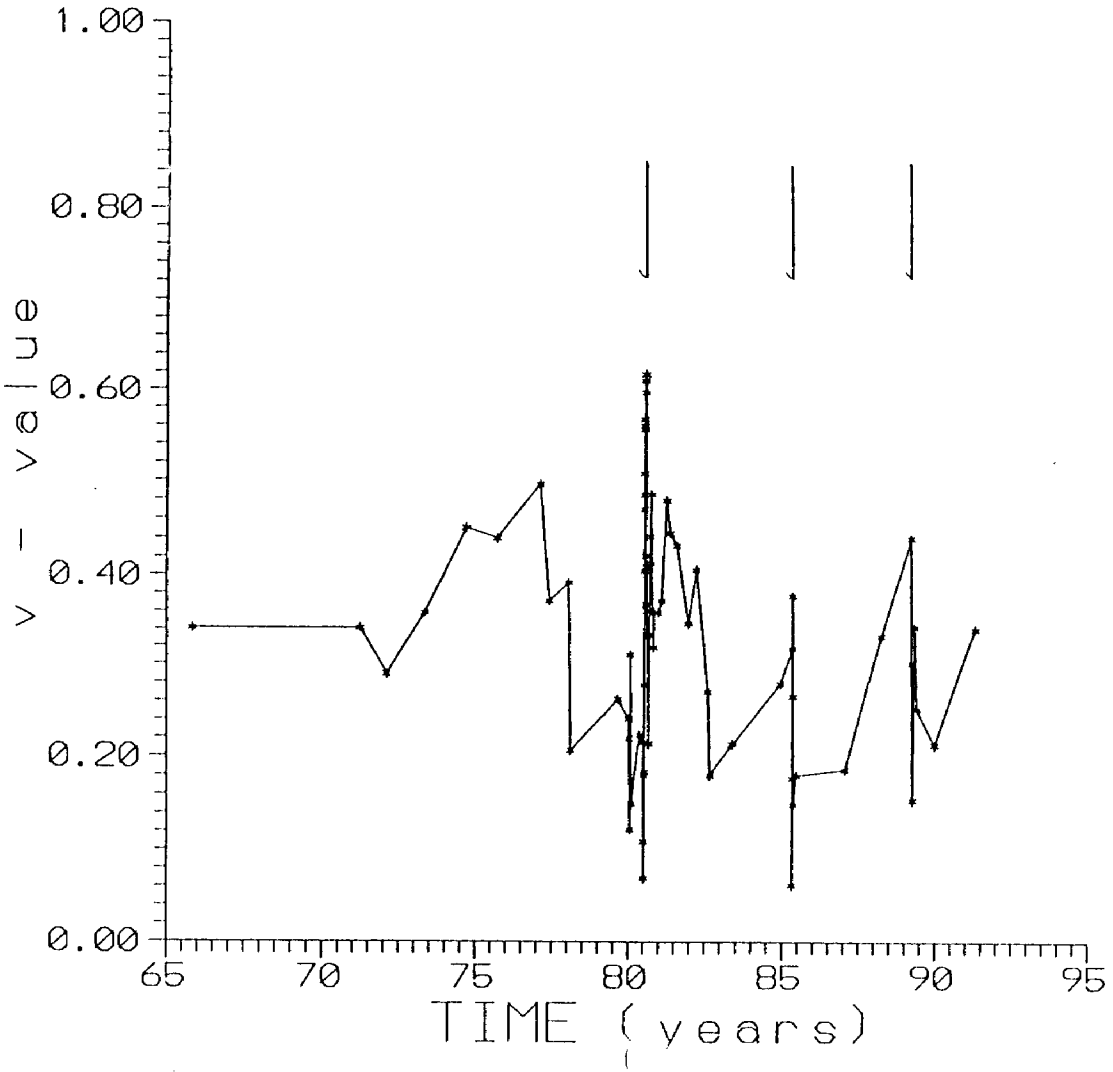
1.00
0.80
0.60
0.40
0.20
0.00
V - value
65
70
75
80
85
90
95
TIME (years)

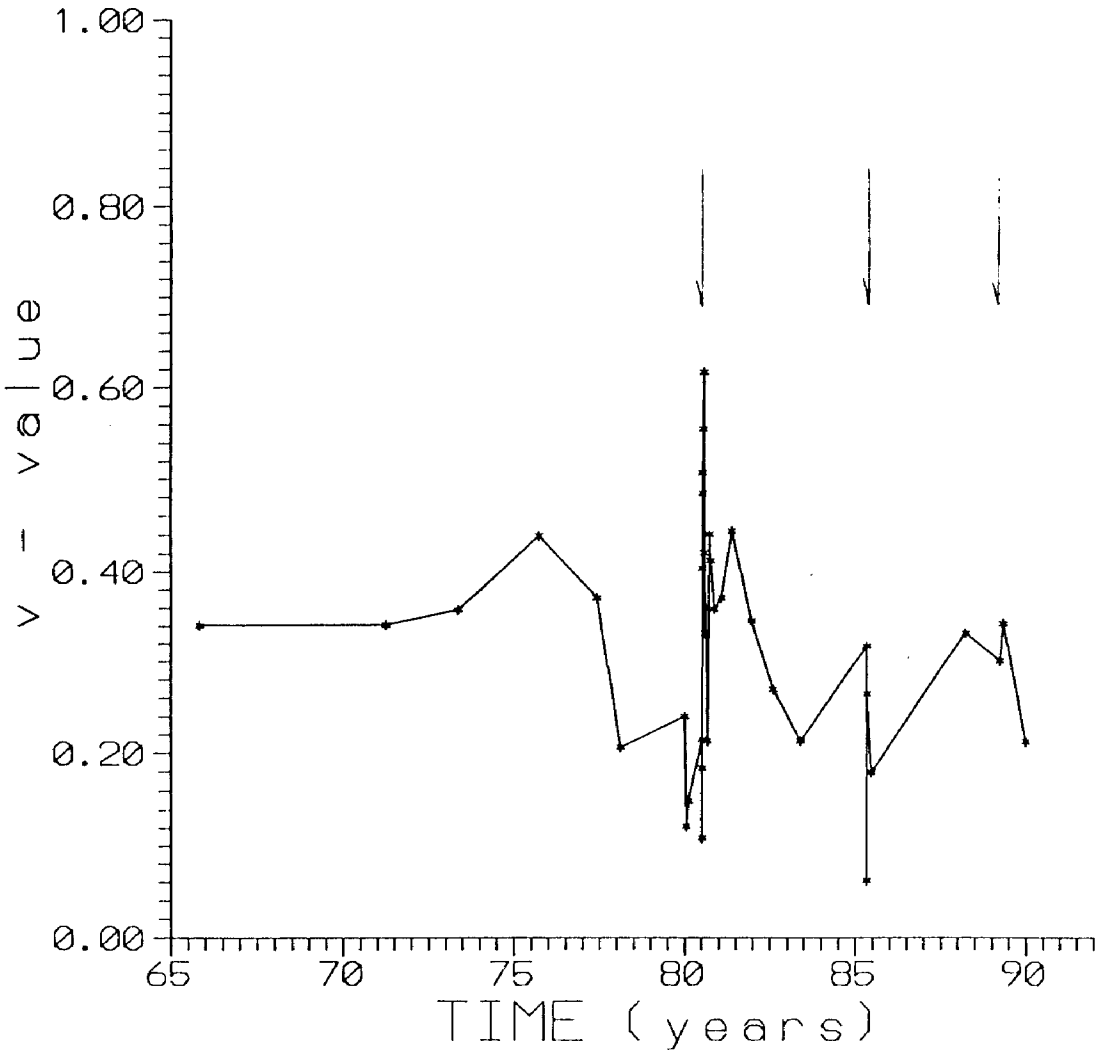
1.00
0.80
0.60
0.40
0.20
0.00
V - value
65
70
75
80
85
90
TIME (years)

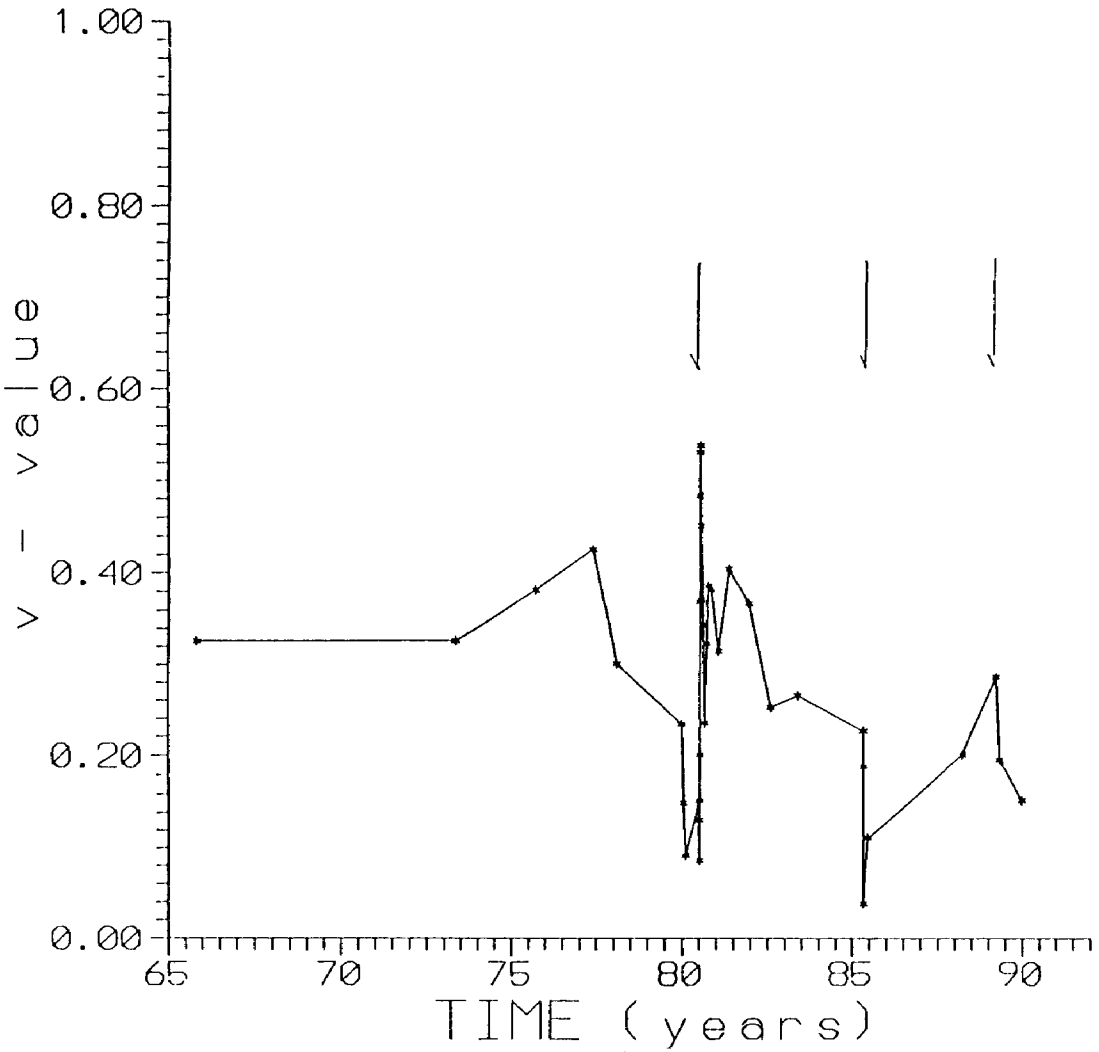
1.00
0.80
0.60
0.40
0.20
0.00
V - value
65
70
75
80
85
90
TIME (years)

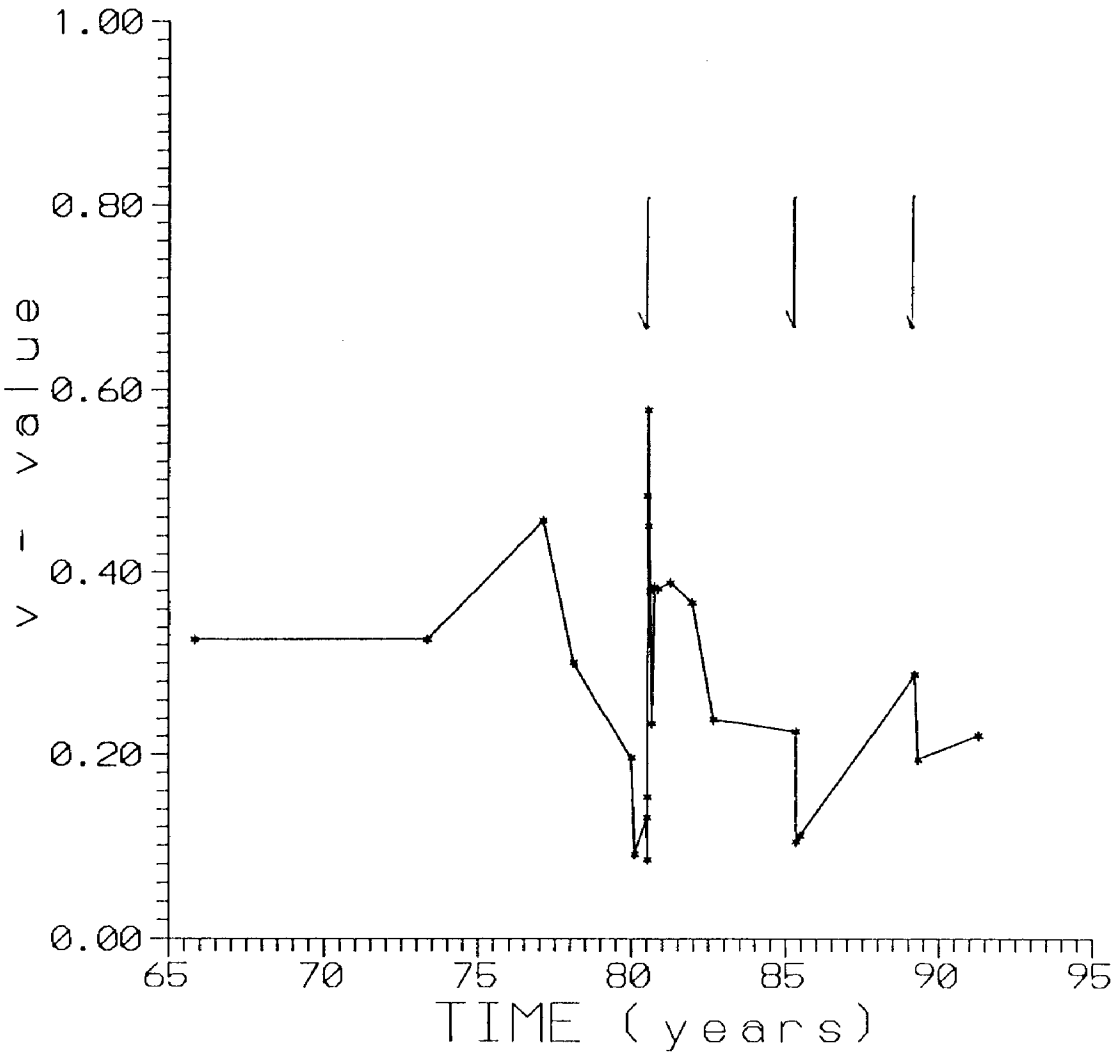
1.00
0.80
0.60
0.40
0.20
0.00
V - value
65
70
75
80
85
90
95
TIME (years)

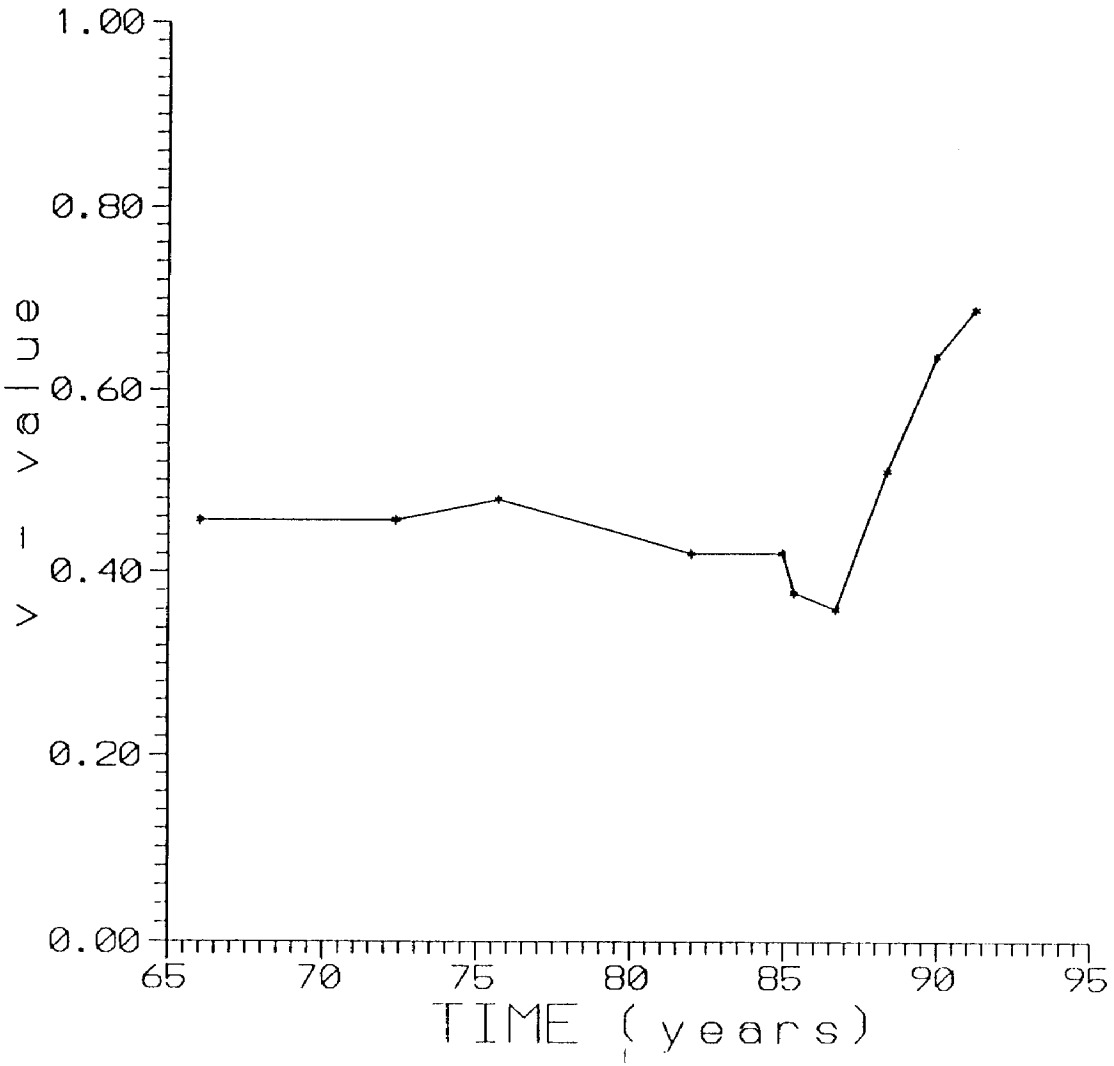
1.00
0.80
0.60
0.40
0.20
0.00
Value
65
70
75
80
85
90
95
TIME (years)

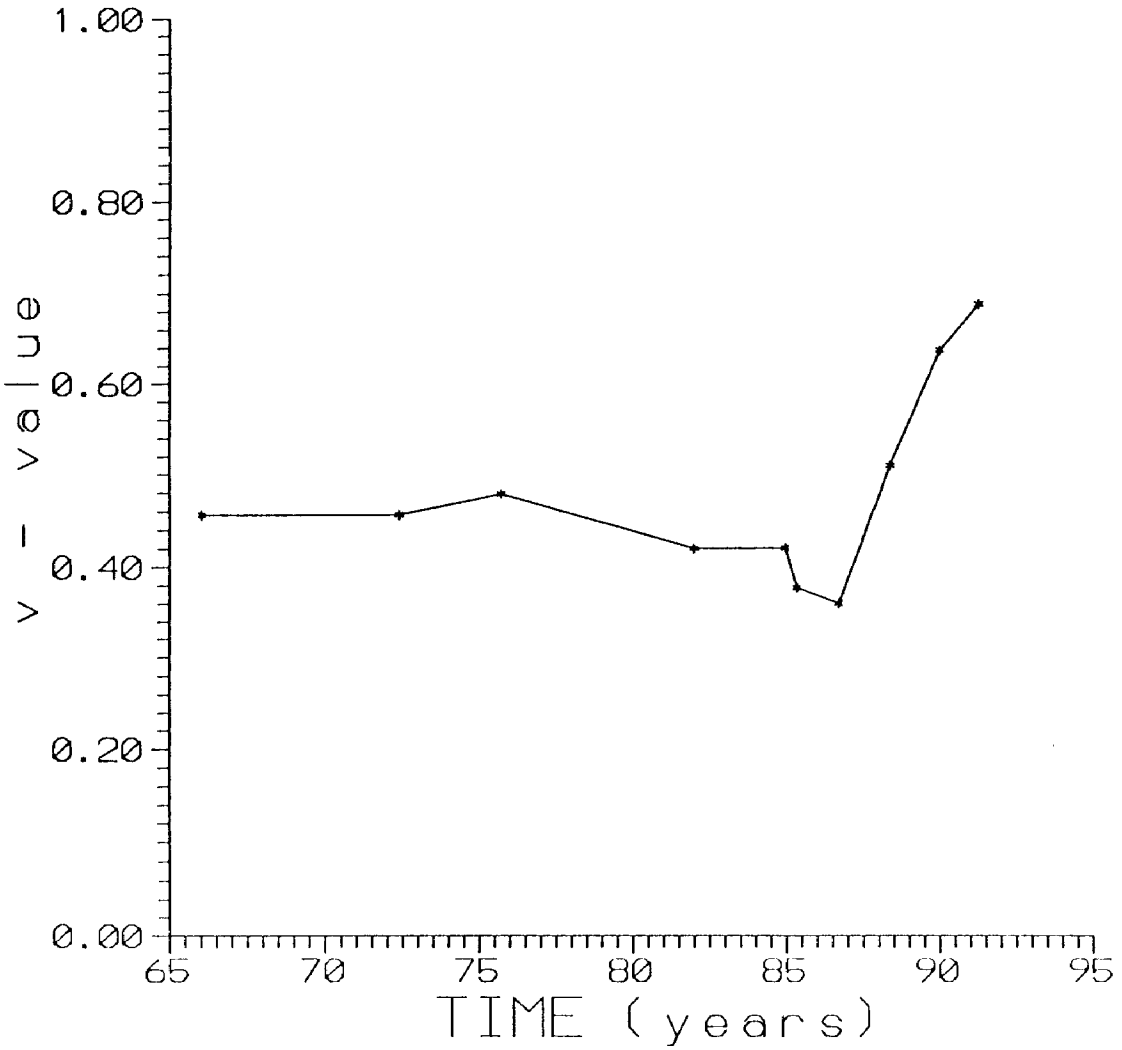
1.00
0.80
0.60
0.40
0.20
0.00
V - value
65
70
75
80
85
90
95
TIME (years)

MAGNETOTELLURICS IN THE EASTERN PART OF CENTRAL GREECE

CHOULIARAS G. and G.N. STAVRAKAKIS

Introduction

The magnetotelluric (MT) method of geophysical prospecting has been applied in this study to detect possible changes in the electromagnetic properties in a specific seismic region in Greece prior to the occurrence of a strong earthquake. The region under investigation is the Volos - Almyros area (22°E - 23.5°E and 39°N - 39.8°N) where eight destructive seismic sequences with main shock magnitudes $M_s \geq 6$ have occurred during the present century.

Of special interest to the MT investigation are the seismotectonic results by Drakopoulos and Delibasis (1982), Papazachos (1983), and Kronberg and Guenther (1977) which indicate a main stress field in a N - S direction and the corresponding normal faults having an E - W strike.

For the purposes of this study, preliminary MT measurements were conducted in several sites in the region of interest, in order to establish noise free data. These measurements showed that the MT results are in good agreement with the seismotectonics of this region and with other MT results from different tectonic regimes.

In general these results indicate that active normal faults in regions of crustal extension, are usually associated with elongate conductors. This is due to the circulation of water through these fault zones.

Further on in this study, a state of the art MT observatory was installed and operated in the Volos - Almyros area. In this manner, continuous magnetotelluric data has been recorded and any possible changes in the earth's electric field (resistivity, geoelectric currents, e.t.c) should be clearly detected. For this purpose, a software package has also been developed and tested in order to analyse the recorded MT data.

Theory

Maxwell's equations imply a linear dependance between electirc and magnetic fields at a particular frequency and spatial wave number. In the frequency domain this relationship may be written as:

$$\begin{bmatrix} E_x \\ E_y \end{bmatrix} = \begin{bmatrix} Z_{xx} & Z_{xy} \\ Z_{yx} & Z_{yy} \end{bmatrix} \begin{bmatrix} H_x \\ H_y \end{bmatrix} \qquad (1)$$

where Z_{xx} , Z_{xy} , Z_{yx} , Z_{yy} are elements of the impedance tensor Z, and depend on the conductivity structure beneath the measuring point. E_x and E are the horizontal electric field components and H_x , H_y the horizontal magnetic field components. The indices x and y refer to the measuring axis in the north-south and east-west direction, respectively.

A relationship similar to equation 1, relating the vertical magnetic field component H_z and the magnetic field components H_x and H_y in the frequency domain, may be written as:

$$H_z = AH_x + BH_y \qquad (2)$$

where A and B are unknown complex coefficients. The pair (A,B) can be thought of as operating on the horizontal magnetic field and tipping a part of it into the vertical. For this reason (A, B) is often referred to as the "tipper"; its application to the interpretation of conductivity structures is described by Vozoff (1972).

The estimation of the impedance tensor elements from measured data as performed by Sims et al. (1971), is obtained as a least squares solution in narrow bands of frequencies so that the noise power in two of the channels is minimized while assuming the remaining two to be noise free. Jepsen and Pedersen (1981) initially developed a computer program which provides solutions for the impedance tensor elements and their random errors, given the recorded time series of the horizontal magnetotelluric components as input. The solutions are in terms of auto and cross spectral estimates in a given frequency band. The following model is considered in the frequency domain:

$$\underline{E}_x = Z_{xx}\,\underline{H}_x + Z_{xy}\,\underline{H}_y + \underline{N}_x \qquad (3)$$

where N_x denotes the noise of the part of the electrical field which is not related to the induction process ($\underline{\ }$ indicates a vector quantity consisting of field values at discrete frequencies within the frequency band). Assuming H_x and H_y to be noise free and Z_{xx} and Z_{yy} to be constant within the frequency range of interest, through the minimization of $|N_x|^2$, a least squares solution Z_{xx} and Z_{xy} for the tensor elements is found

$$\hat{Z}_{xx} = \frac{(\tilde{H}_x\,E_x)\;(\tilde{H}_y\,H_y) - (\tilde{H}_y\,E_x)\;(\tilde{H}_x\,H_y)}{(\tilde{H}_x\,H_x)\;(\tilde{H}_y\,H_y) - (\tilde{H}_x\,H_y)\;(\tilde{H}_y\,H_x)} \qquad (4a)$$

$$\hat{Z}_{xy} = \frac{(\tilde{H}_y\,E_x)\;(\tilde{H}_x\,H_x) - (\tilde{H}_x\,E_x)\;(\tilde{H}_y\,H_x)}{(\tilde{H}_x\,H_x)\;(\tilde{H}_y\,H_y) - (\tilde{H}_x\,H_y)\;(\tilde{H}_y\,H_x)} \qquad (4b)$$

($\tilde{}$ indicates vector transposition and conjugation and $\hat{}$ indicates estimated quantities).

Similarly, Z_{yy}, Z_{yx}, A and B are found. This program, with minor modifications to handle longer time series and estimate the tipper (A, B), was used in the analysis of the magnetotelluric data collected in Greece.

A measure of the dimensionality of the geoelectrical structures is provided by the skew index S (Swift, 1967), where

$$S = \frac{|Z_{xx} + Z_{yy}|}{|Z_{xy} - Z_{yx}|} \qquad (5)$$

For a complete description of dimensionality indicators the reader is referred to a recent review of the topic by Beamish (1986). In general we have :

- for 1-D structure: $Z_{xx} = Z_{xy} = 0$; $Z_{xy} + Z_{yx} = 0$; $A=B=0$; $S=0$ (6)
- for 2-D structure: $Z_{xx} + Z_{yy} = 0$; $Z_{xy} + Z_{yx} \neq 0$; $A \neq B \neq 0$; $S=0$ (7)
- for 3-D structure: $Z_{xx} = Z_{yy} = 0$; $A=0; B \neq 0$ (8)

In order to determine the strike direction from the MT measurements of the horizontal electromagnetic field components we employ the conventional method of Sims and Bostick (1969) modified by Zhang et al. (1987) for a 2-D structure. Accordingly the strike θ_s is found by retrieving the real part of:

$$\tan 2\theta_s = \frac{|Z_{xx} - Z_{yy}|}{|Z_{xy} + Z_{yx}|} \qquad (9)$$

The MT strike determined by the above method is inherently ambiguous by 90° because 2-D structures provide symmetrical properties for the rotated tensor in increments of 90°. Thus from measurements of the horizontal MT components one will find a strike direction or a direction perpendicular to it without being able to tell which is which. To resolve this ambiguity we employ the vertical magnetic field transfer function (A, B) in order to determine the angle Φ_T . According to Vozoff (1972):

$$\Phi_T = \frac{(Re^2\,A + Re^2\,B)\tan^{-1}\dfrac{Re(B)}{Re(A)} + (Im^2\,A + Im^2\,B)\tan^{-1}\dfrac{Im(B)}{Im(A)}}{\sqrt{|A|^2 + |B|^2}} \qquad (10)$$

and this angle will be perpendicular to the strike for a 2-D structure.

In Greece, earthquake prediction by Varotsos and Alexopoulos (1984 a,b) claims an outstanding success rate in predicting sizable earthquakes located within their network of telluric stations. Nevertheless, magnetotelluric disturbances are a very serious shortcoming in the identification of the SES, especially, for an impending earthquake of small magnitude or of large epicentral distance.

Rikitake (1947) suggested that the method of computing the difference between observed earth potentials and those predicted from measurements of the magnetic field should be applied to monitor any anomalous changes in earth currents related to earthquakes. Thus the removal of magnetically induced effects from the telluric measurements should improve the detectability of the SES and thus

make predictions for distant or small earthquakes more reliable.

It is well known that the application of the tensor impedance concept to the analysis of magnetotelluric data as published by Sims et al. (1971) makes it possible to obtain estimates of the tensor elements which describe the local induction effect. The transfer function relating the magnetic field to the electric field from a galvanic source will in general be different from the one describing the induction process analysed by the standard magnetotelluric method. Thus, for noise-free data, the calculated residual electric field should show if an electric potential is generated within the earthquake volume.

This standard magnetotelluric analysis is employed to remove induction effects from the electrical measurements and thus we may observe what is henceforth termed the "residual" electric field.

Instrumentation and Methodology

The preliminary MT measurements were conducted with two pairs of non-polarizing electrodes of the copper-coppersulphate type that were used for detecting the two horizontal components of the electric field in an east-west and north-south direction. The distance between the electrodes was 100 m for each pair. Three induction coil magnetometers were used to measure the time derivatives of the three orthogonal components of the magnetic field in nort-south, east-west and vertical directions.

The output voltages were suitably amplified and filtered with a passband of 0.00027-10 Hz. The five channels were sampled at 48 Hz and recorded digitally on magnetic tapes. Each tape contained 8 hrs of simultaneous recordings of the five magnetotelluric components. 12-V batteries were used for power supply. Tapes were replaced three times a day and during these breaks in the recording the station functions (gains, self-potential compensation etc.) were checked and when necessary adjusted.

For the permanent MT measurements, a new system for long-term magnetotelluric (MT) measurements which has been developed at the Institute of Geophysics, University of Kiel, in the frame of the EPOC-CT 0045 project - Figures 1 and 2. The MT-system is supplied by solar energy, figure 3. It comprises three magnetic channels and four galvanically separated electric channels. Up to 20 samples/sec can be digitized with a resolution of 20 bit; the storage capacity amounts to 120 Mbyte. The magnetometer of the system has been developed by Bartington in 1991. It has a large bandwidth up to 1 kHz, a very low power consumption, and a weak temperature dependence. The self-potential is measured by Cu-CuSO probes. The probes have been successfully used at the institute since two years, and in a test at the laboratory they gave the best long-term stability.

The main steps in the analysis of each 8 hours of simultaneous recording of the time series are:

(1) Each of the five time series is low pass filtered at 0.5 Hz with a Gaussian filter and resampled to provide for a total window length of 32,768 samples.

(2) Linear trends are removed and the time series are subsequently multiplied by a cosine window, at both ends, of 400 samples width. This reduces the effects of discontinuities on the computed spectra.

(3) The time series are Fourier transformed.

(4). Cross and auto spectra are calculated within each band of frequencies. The first nine frequency bands were chosen to be discrete and centred at the corresponding first nine harmonics. The subsequent bands were chosen so that we had ten frequency bands per decade. In total we used forty bands.

(5) Average impedance tensor elements and their standard errors are calculated from band ten onwards. The first nine bands are excluded from further computation sisnce they involve periods above the 1/3600 Hz instrumental filter.

(6) Apparent resistivities and phases are calculated for the average.

(7) The estimated impedance tensor elements and the tipper estimates along with the spectra of the time series are inputs to a subroutine which computes the differences ΔE_x , ΔE_y and ΔH_z between the observed electric and vertical magnetic components and those predicted by the horizontal magnetic field components:

$$\Delta E_x = E_x - \hat{Z}_{xx} H_x - \hat{Z}_{xy} H_y \qquad (11a)$$

$$\Delta E_y = E_y - \hat{Z}_{xx} H_x - \hat{Z}_{xy} H_y \qquad (11b)$$

$$\Delta H_z = H_z - \hat{A} H_x - \hat{B} H_y \qquad (11c)$$

These residuals and the recorded time series are finally transformed into the time domain and plotted.

Results

The MT preliminary results obtained with the induction coil magnetometers are shown in figures 4 and 5.

Figure 4 shows the normalized impedance tensor T and the tipper A and B, for each station. The impedance tensor Z is normalized using the following relationship:

$$T = \begin{bmatrix} T_{xx} & T_{xy} \\ T_{yx} & T_{yx} \end{bmatrix} = \frac{1}{\sqrt{\omega\mu_o}} \begin{bmatrix} Z_{xx} & Z_{xy} \\ Z_{yx} & Z_{yy} \end{bmatrix} \qquad (12)$$

where ω is the angular frequency and μ_o the magnetic premeability in a vacum.

Figure 5 shows the apparent resistivities:

$$\rho_{ax} = |T_{xy}|^2 \qquad (13a)$$

$$\rho_{ay} = |T_{yx}|^2 \qquad (13b)$$

and corresponding phases:

$$\Phi_x = \arg(-iT_{xy}) \qquad i = \sqrt{-1} \qquad (14a)$$

$$\Phi_y = \arg(+iT_{yx}) \qquad (14b)$$

resulting from the analysis.

Based on the dimensionality indicators mentioned in a previous chapter, the results from figures 4 and 5 indicate that a 2-D structure can represent the regional structure which underlays the MT station. Further on in Figure 5 one observes that although the apparent resistivity curves for the high frequencies exhibit low apparent resistivity values 10 - 100 ohm-m for near surface, the curves exhibit very prominent ansotropy which is increasing towards the low frequency end representing the deeper structure.

In order to determine the MT strike of the regional structure we use equation 9 which gives an inherently anbiguous result by 90° as discussed earlier. The value for the MT strike from this equation is $\theta_s = 105° \pm 90°$. To resolve this ambiguity we employ equation 10 which gives the unambiguous tipper angle Φ_T which sould be perpendicular to the true strike θ_s for a 2-D structure.

These results are shown in figure 6 and when this is compared to the orientation of the main structures surrounding our MT station

shown in map 1, we notice that the E-W trending structures agree quite well with the orientation of the MT strike as determined from our data.

Using the estimated impedance tensor and tipper elements shown earlier and the spectra of the recorded time series, from which they were derived, the residual horizontal electric and vertical magnetic fields were computed. An example is displayed for a 2-hour segment recorded data in figure 7. The residual electric fields, ΔE_x and ΔE_y, for both stations show a good prediction of the horizontal electric fields from the corresponding magnetic fields. The same may be said about the prediction of the vertical magnetic field from the two horizontal components as seen by the residual ΔH_z.

Figures 8, 9, 10 show typical recordings of the five MT components at the site of the permanent MT observatory in the Volos region which employs the 'state of the art' MT equipment for the continuous monitoring of the MT fields. The sampling period for figures 8, 9, 10 are 180, 15 and 2 seconds, respectively.

In figure 8 we can see MT recordings over a 3 day period beginning on day 278 of 1993 and starting at 09:36 local time. One easily notices the three daily variations on the magnetic field components between 09:36 - 17:61, 34:00 - 42:00, 58:00 - 65:00 hours.

Figure 9 shows an MT recording sampled every 15 seconds and here we can see that the data quality which reflect the noise conditions near our station is very good. However figure 10 shows a recording sampled every 2 seconds and here we can see that around 16:02 hour, noise saturates our signal in both electric field (E_x , E_y) components. This is a typical noise source arising from a water pump nearby and an example of how this noise is later filtered away in the processing of the actual data is shown in figure 11.

Routine determination of impedance tensor elements, from data having high multiple coherence values has shown only minor changes in the tensor estimates during the recording period. Further on, the analysis of the magnetotelluric data has provided an accurate estimate of the local induction effect. The subsequent removal of such induction effects from the electric field measurements is shown to drastically improve the detection of any local variation in the earth's electric field caused by internal sources.

Discussion

Magnetotelluric (MT) measurements have been performed in the area of Anhialos near Volos in Greece. These measurements consisted of a preliminary recognisance survey in order to evaluate the noise conditions of the area, to determine the resistivity structure of the region and also to evaluate the software for the analysis of the MT data. The results from these measurements show that this region can be represented by a 2-D conductive regional structure strike having a strike approximately in a E-W direction. This result is in agreement with the seismotectonic results of the region which indicate that the principle regional faults have an E-W orientation. Since these faults are shown to be electrically conductive, from the MT results, it is implied that the conductive fluids in the fault zones can act as channels for geoelectric currents and thus are of great importance in the detection of possible precursory geoelectric currents. Further on a software package for the analysis of the MT data, which eliminates the induction effects from the electric field recordings is tested in this study. The results show that the computation of the residual electric field, obtained as the difference between the observed and the estimated inductive part of the electric fields, clearly improves the detection of any local electric field anomaly.

In October 1993 a state of the art MT system was installed in the region for the purpose of continuously monitoring the five components of the magnetotelluric field in order to be directly correlated with the seismicity of the area. So far routine determination of the impedance tensor shows only minor changes during the recording period and no anomalous geoelectric currents have been detected. Ofcourse this should be expected due to the lack of significant seismic activity in this region during the rather short period of monitoring. Nevertheless the results from these magnetotelluric investigation are of great importance in the development of earthquake prediction research in Greece by means of electromagnetic currents.

REFERENCES

Drakopoulos, J. and Delibasis, N., 1982. The focal mechanism of earthquakes in the major area of Greece for the period 1947 - 1981. Univ. of Athens, Seismological Laboratory Publication No. 2.

Jepsen, J.B and Pedersen, L.B., 1981. Evaluation of a tensor AMT measurement system. Geoskrifter, 15: 1-68.

Kronberg, P. and Guenther, R., 1977. Fracture patterns and principles of crustal fracturing in the Aegean region. Proc. VI Colloquium on the geology of the Aegean region, II, Athens 1977.

Papazachos, B.C., Panagiotopoulos, D.G., Tsapanos, T.M., Mountrakis, D.M. and Dimopoulos, G.CG, 1983. A study of the 1980 summer seismic sequence in the Magnesia region of Central Greece. Geophys. J. R. ast. Soc. 75 155-168.

Rikitake, T., 1947. A method for studying the relations between the changes in geomagnetism and earth current. Bull. Earthquake Res. Inst. 25:9-13.

Sims, W.E and Bostick, F. X., 1969. Method of magnetotellurics analysis:Res. Lab. tech rep. 58, Univ. of Texas.

Sims, W.E, Bostick, F.X and Smith, H.W. 1971. The estimation of the magnetotelluric impedance tensor elements from measured data. Geophysics, 36, pp 938-942.

Swift, C.M., 1967. A magnetotelluric investigation of an electrical conductivity anomaly in the SW United States. Ph. D. thesis, MIT.

Zhang, P., Roberts, R.G and Pedersen, L.B., 1987. Magnetotelluric strike rules. geophysics, vol. 52, No. 3, pp 267-278.

Varotsos, P. and Alexopoulos, K., 1984a. Physical properties of the variation of the electric field of the earth preceding earthquakes. I. Tectonophysics, 110:73-98.

Varotsos, P. and Alexopoulos, K., 1984b. Physical properties of the variation of the electric field of the earth preceding earthquakes, II. Determination of epicentre and magnitude. Tectonophysics, 110:99-125.

Vozoff, K., 1972. The magnetotelluric method in the exploration of sedimentary basins. Geophysics, 37:98-141.

FIGURE CAPTIONS

Map 1. Map of the Central Thessaly region in Greece, showing direction of the stress field, major regional structures and lineaments, and location of MT recordings (dark circle).

Figure 1. Overview of the MT station hardware.

Figure 2. Overview of the MT station recording units.

Figure 3. Overview of the MT station power unit.

Figure 4. Normalized impedance tensor and tipper functions from the MT station. Squares denote the real part, triangles denote the imaginary part, crosses are the 68% confidence limits.

Figure 5. Skew values, apparent resistivities and phases from the VOL station. Squares denote the north-south direction, ρ_{a2} and φ_2 and triangles denote the east-west direction, ρ_{a3} and φ_3. Bars denote standard error.

Figure 6. Focal sphere indicating strike of the 2-D regional MT strike θ_s (solid line) and MT 'tipper' angle φ_T (dashed line with arrow).

Figure 7. Recording of the five magnetotelluric components and the computed residuals from the magnetotelluric station. Index **x** refers to the north-south direction, **y** to the east-west direction and **z** to the vertical direction. **H** is the magnetic field component and **E** is the electric field component. **ΔE** and **ΔH** are the computed residuals. Units are A m^{-1} for the magnetic field and V m^{-1} for the electric field.

Figure 8. Recording of the five magnetotelluric components sampled at a period of 180 seconds.

Figure 9. Recording of the five magnetotelluric components sampled at a period of 15 seconds.

Figure 10. Recording of the five magnetotelluric components sampled at a period of 2 seconds.

Figure 11. Recording of the five magnetotelluric components sampled at a period of 2 seconds (as in figure 10) but low pass filtered to eliminate the local noise source.

MAP 1.

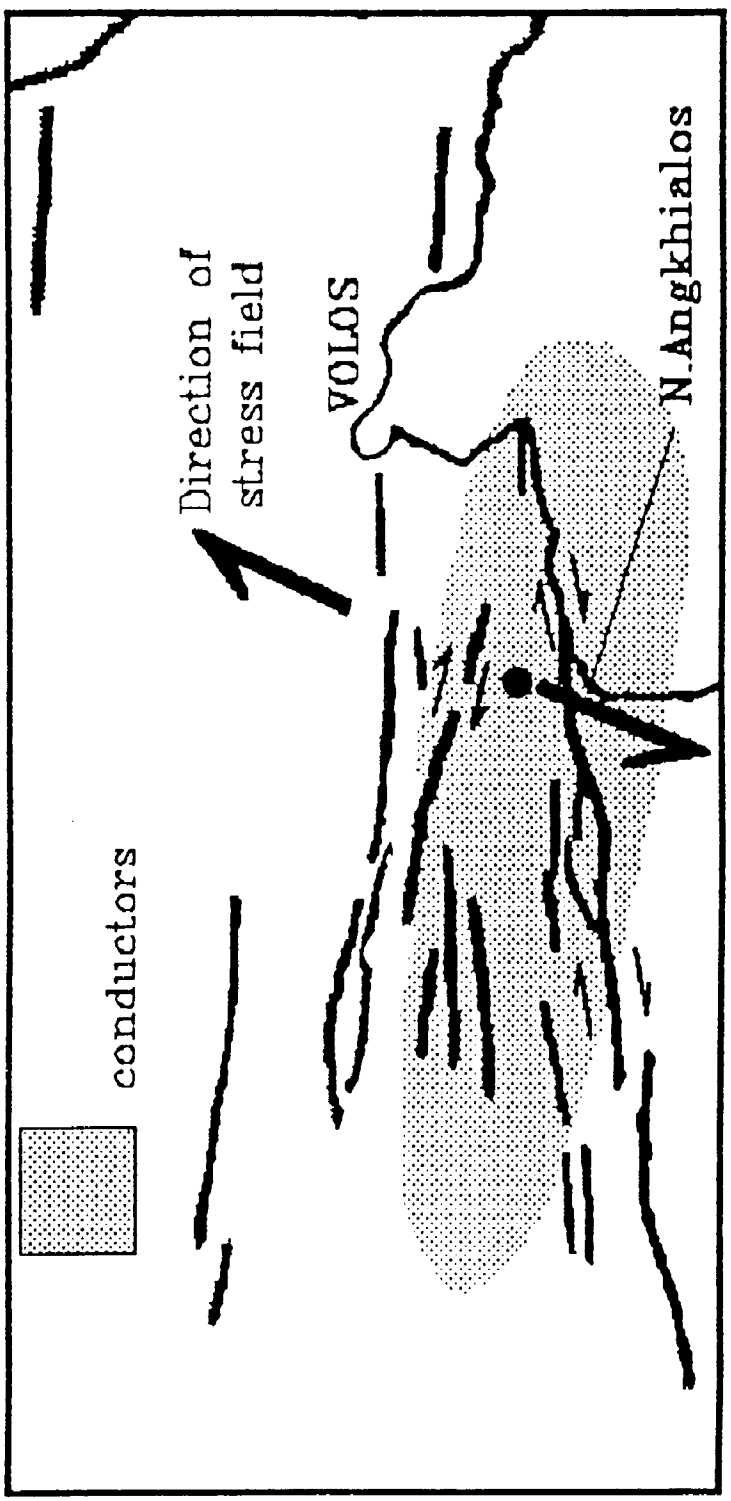

MT-measuring system architecture

Fig.1

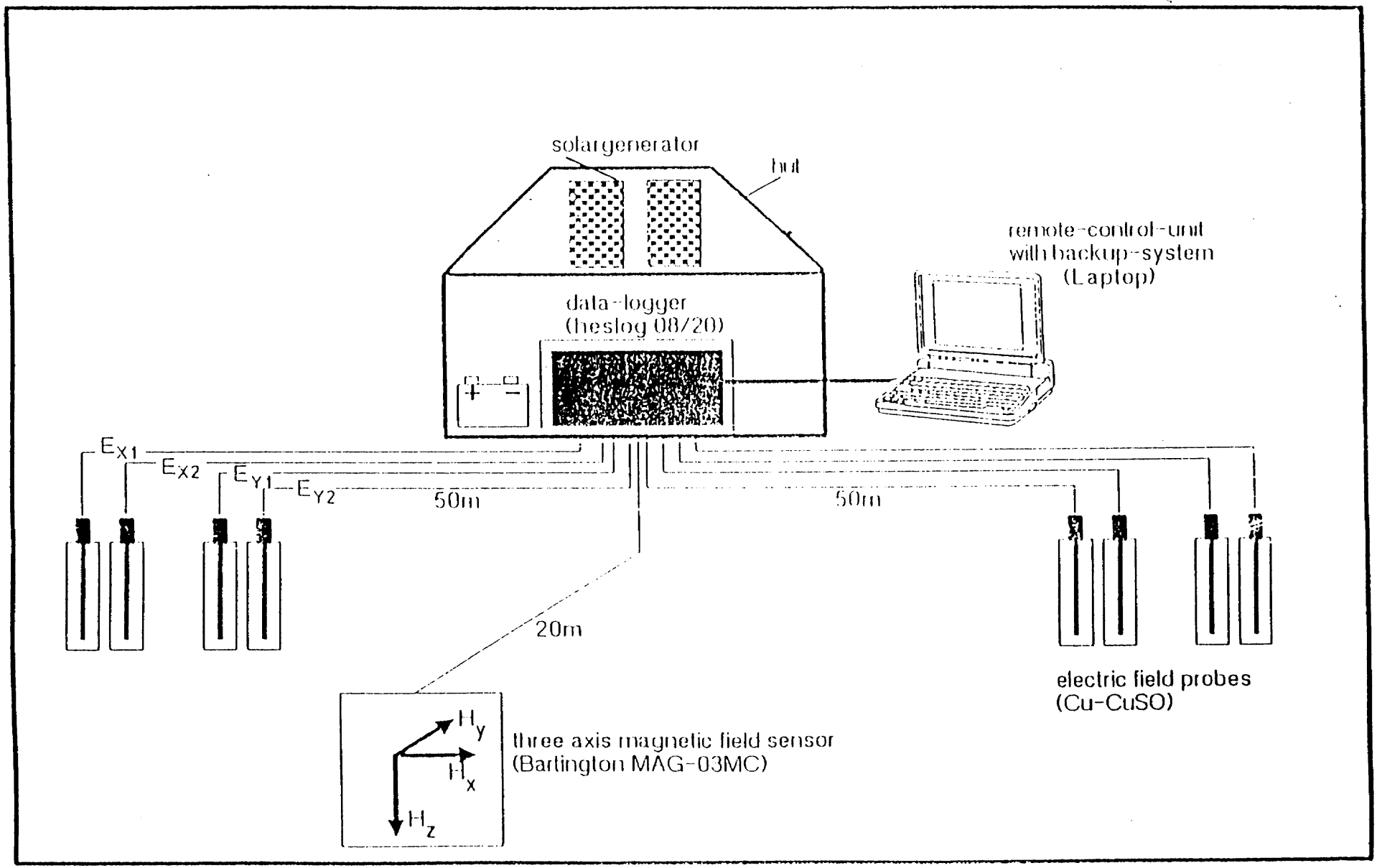

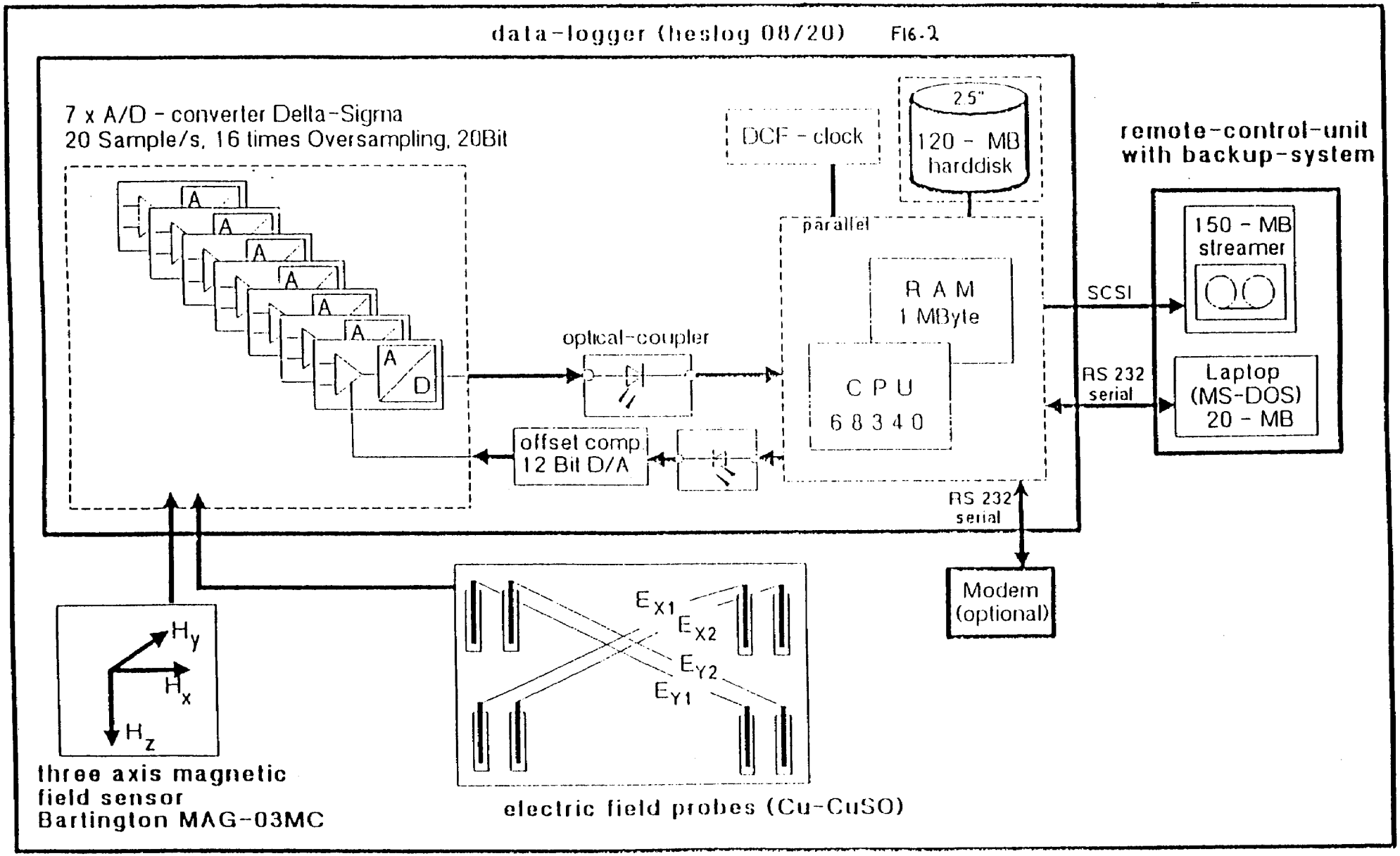

The new developed MT-recording system

solar-power station Fig.3

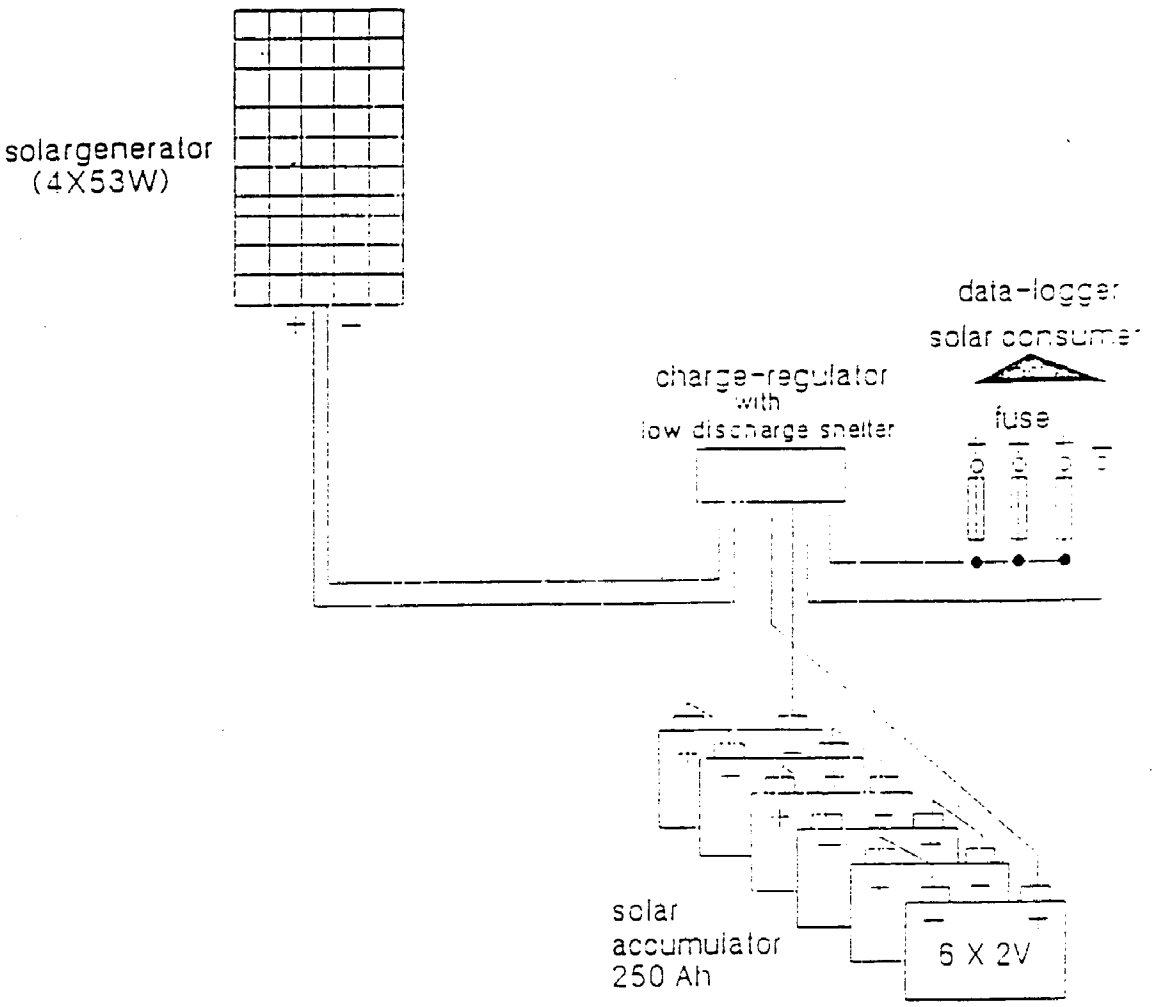

dimensioning: operating voltage 12V

consumer	operating time	current consumption	single capacity
magnetometer	24 h	50 mA	1.20 Ah
data-logger	24 h	700 mA	16.80 Ah
DCF-clock	24 h	120 mA	2.88 Ah
charge-regulator	24 h	2 mA	0.05 Ah
total	24 h	872 mA	20.93 Ah

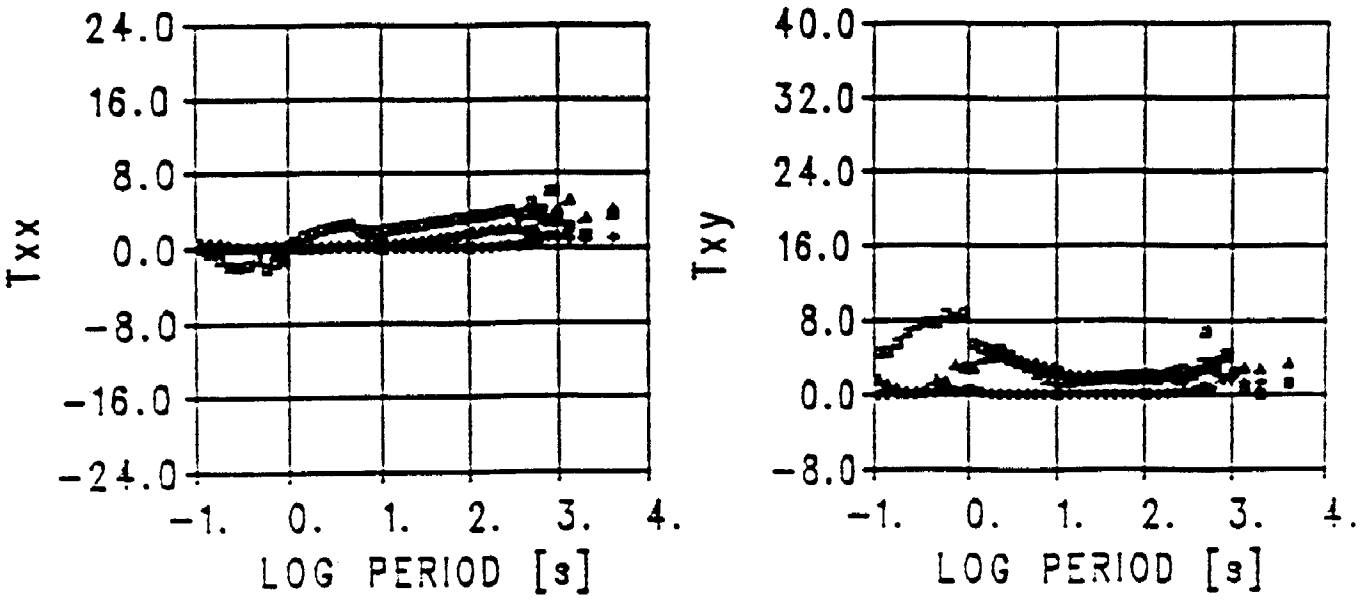
Txx
24.0
16.0
8.0
0.0
-8.0
-16.0
-24.0
-1. 0. 1. 2. 3. 4.
LOG PERIOD [s]

Txy
40.0
32.0
24.0
16.0
8.0
0.0
-8.0
-1. 0. 1. 2. 3. 4.
LOG PERIOD [s]

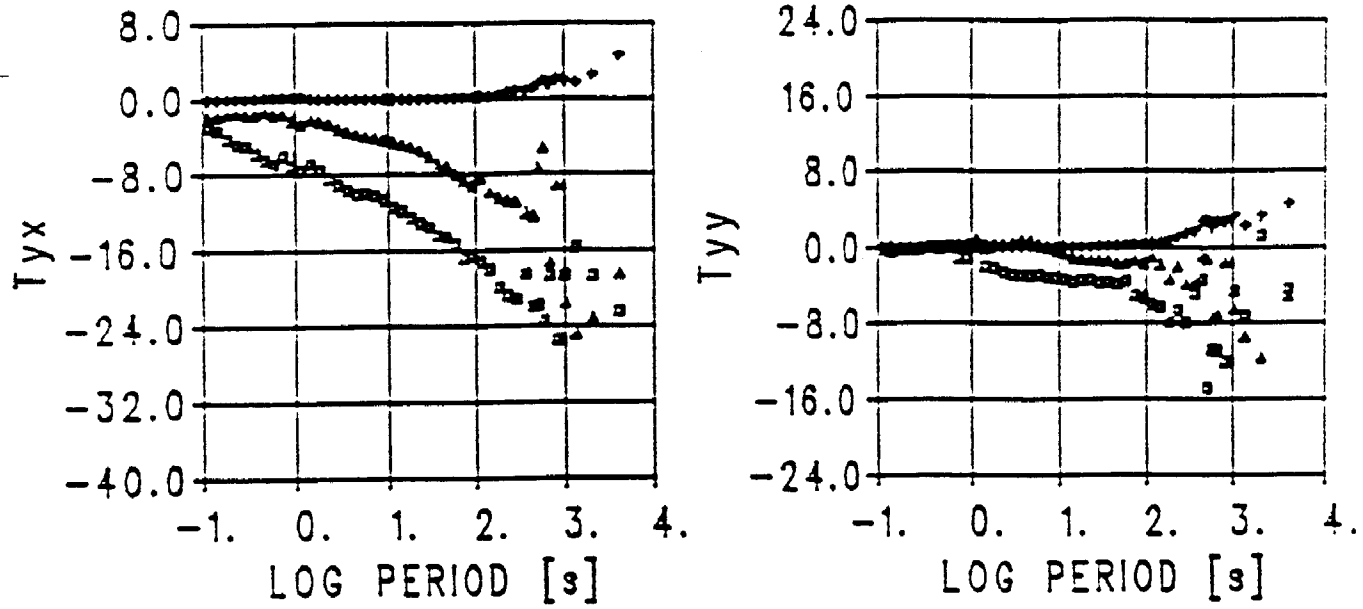
Tyx
8.0
0.0
-8.0
-16.0
-24.0
-32.0
-40.0
-1. 0. 1. 2. 3. 4.
LOG PERIOD [s]

Tyy
24.0
16.0
8.0
0.0
-8.0
-16.0
-24.0
-1. 0. 1. 2. 3. 4.
LOG PERIOD [s]

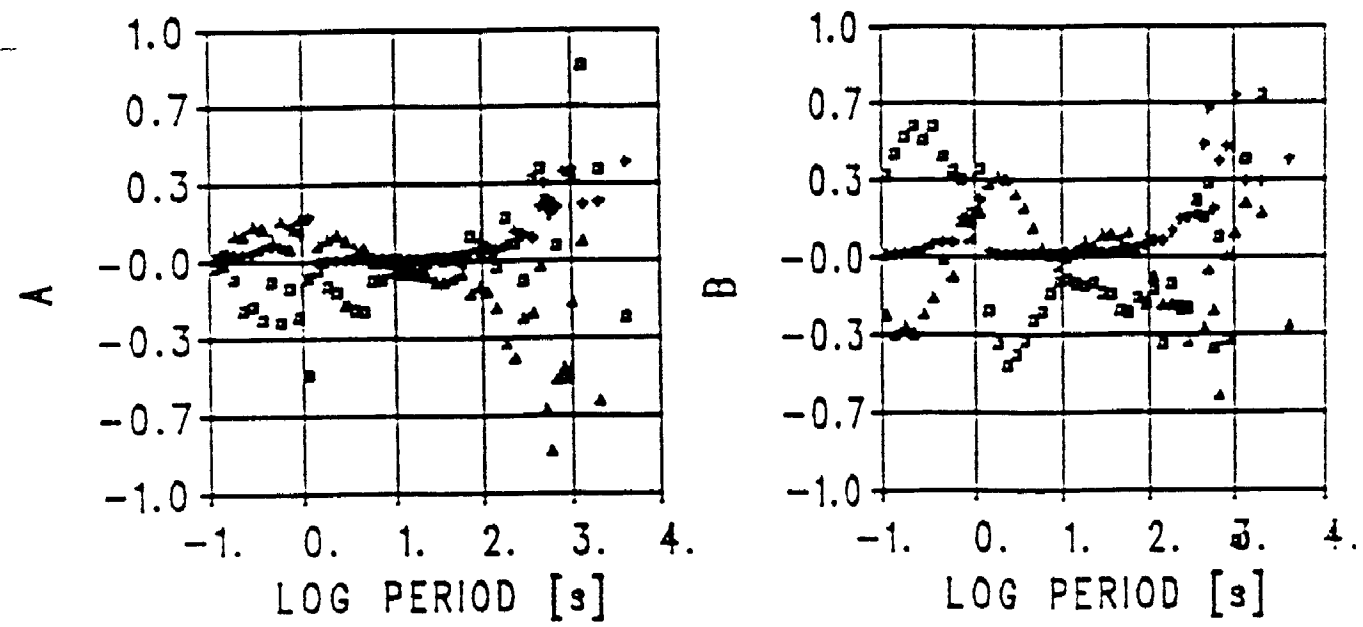
A
1.0
0.7
0.3
-0.0
-0.3
-0.7
-1.0
-1. 0. 1. 2. 3. 4.
LOG PERIOD [s]

B
1.0
0.7
0.3
-0.0
-0.3
-0.7
-1.0
-1. 0. 1. 2. 3. 4.
LOG PERIOD [s]

FIG. 4

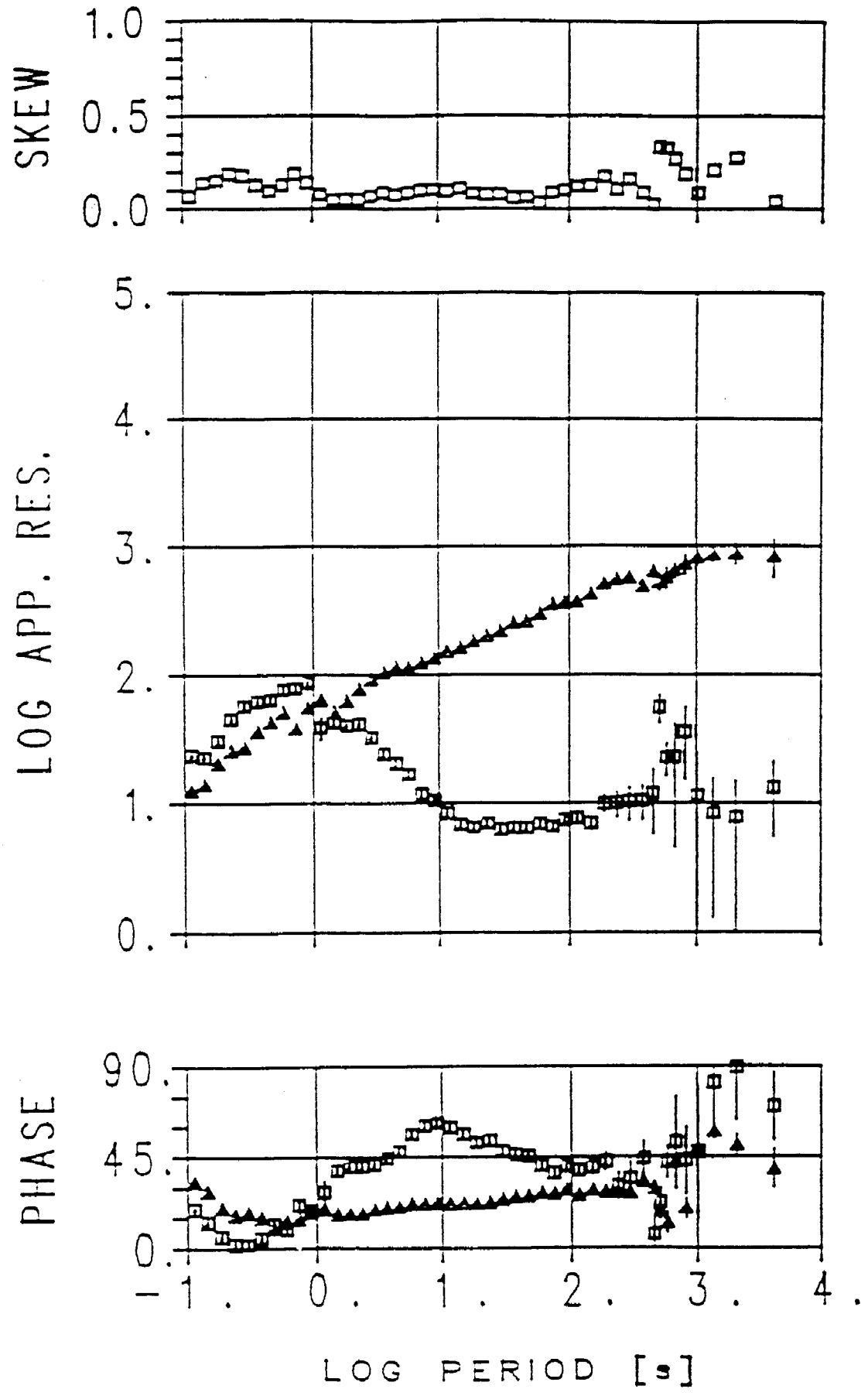
SKEW
1.0
0.5
0.0
LOG APP. RES.
5.
4.
3.
2.
1.
0.
PHASE
90.
45.
0.
-1.
0.
1.
2.
3.
4.
LOG PERIOD [s]

FIG. 5

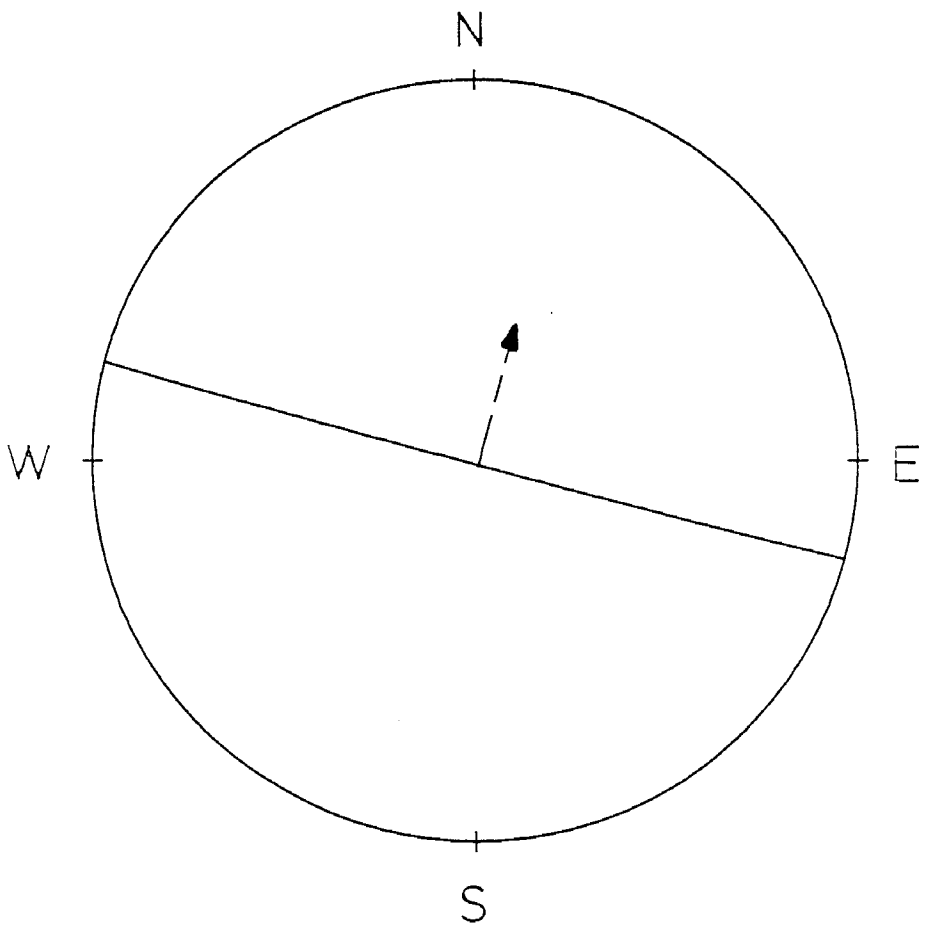

FIG. 6

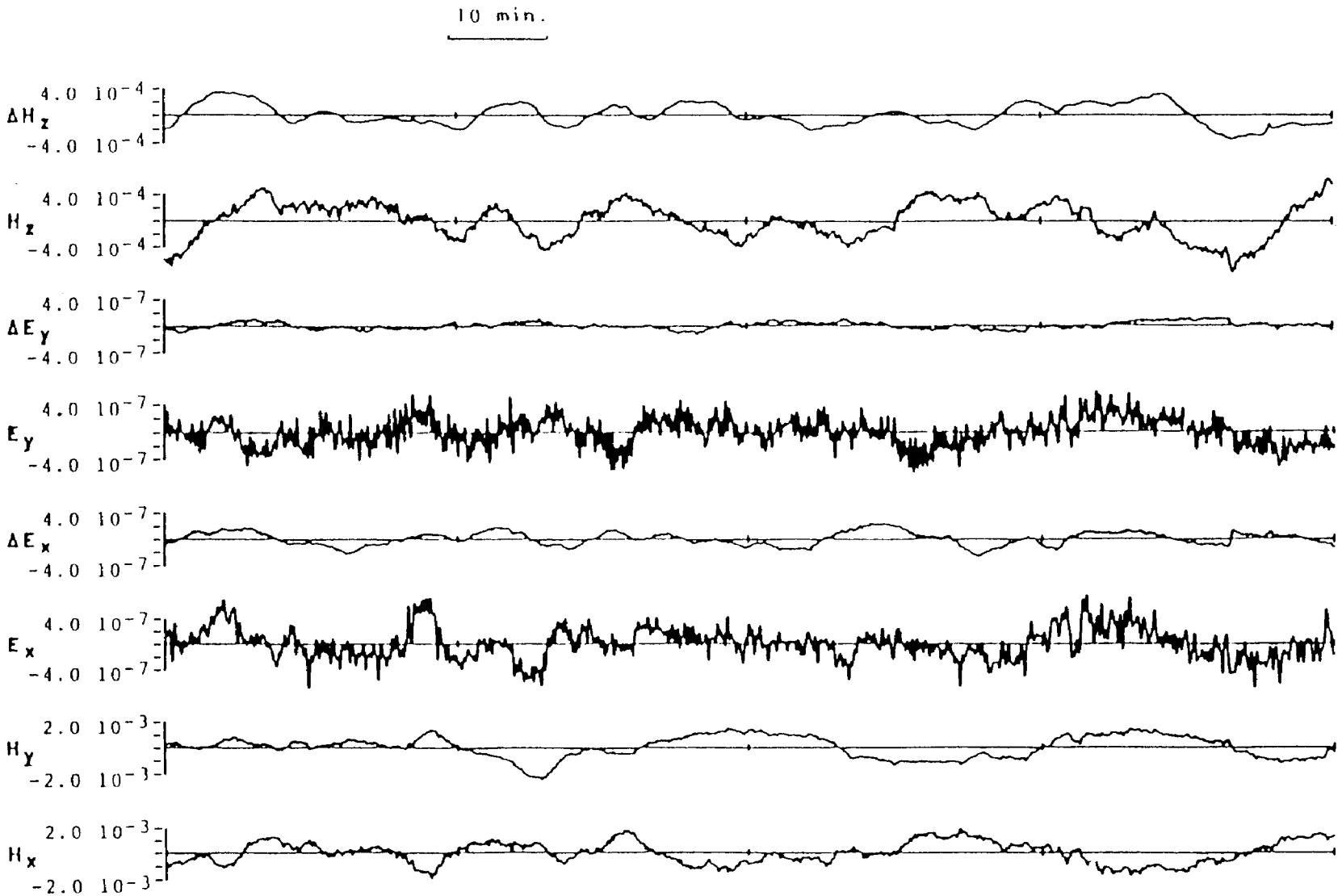
10 min.
ΔHz
4.0 10-4
-4.0 10-4
Hz
4.0 10-4
-4.0 10-4
ΔEy
4.0 10-7
-4.0 10-7
Ey
4.0 10-7
-4.0 10-7
ΔEx
4.0 10-7
-4.0 10-7
Ex
4.0 10-7
-4.0 10-7
Hy
2.0 10-3
-2.0 10-3
Hx
2.0 10-3
-2.0 10-3

FIG. 4

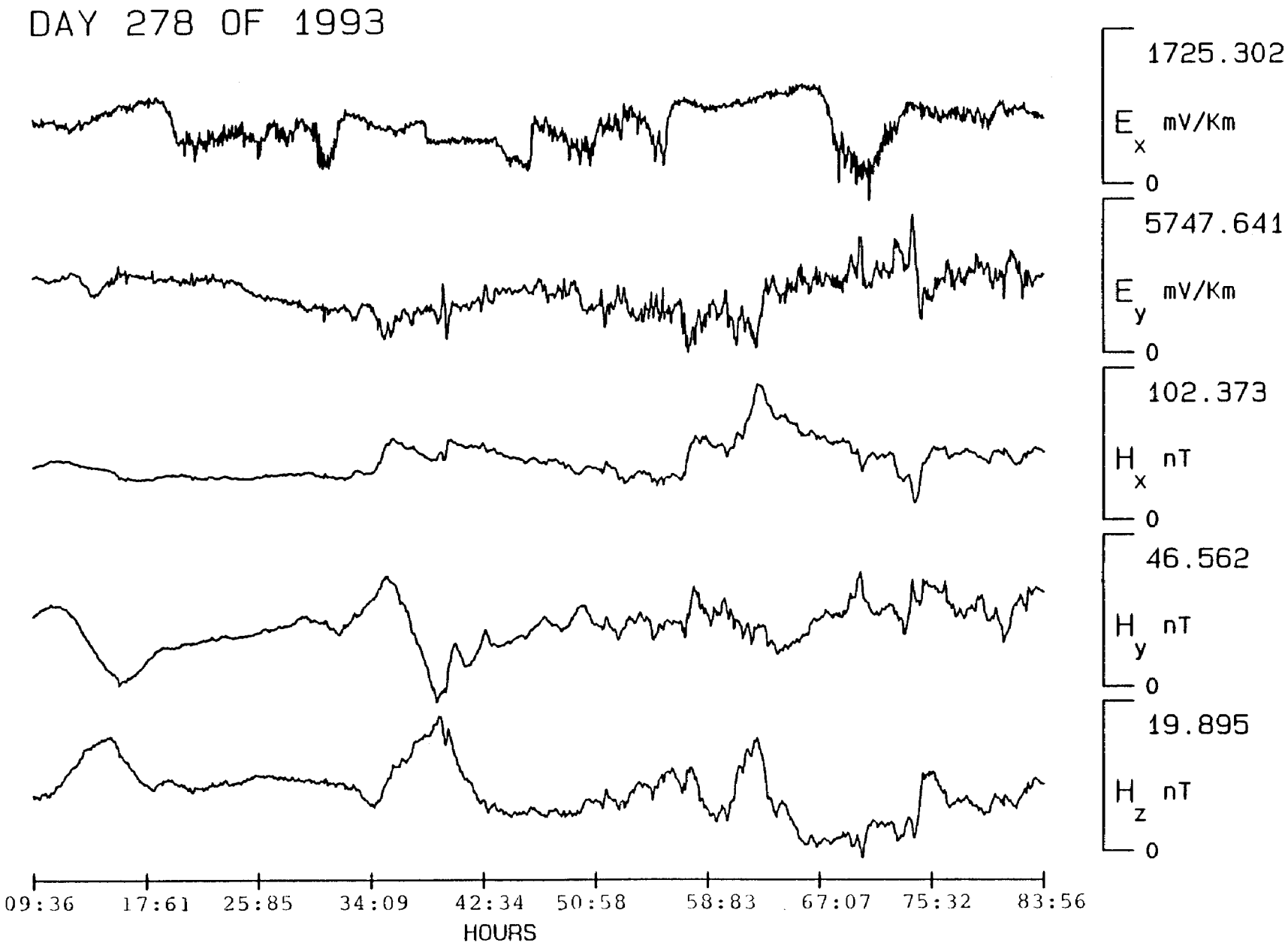
DAY 278 OF 1993
1725.302
E_x mV/Km
0
5747.641
E_y mV/Km
0
102.373
H_x nT
0
46.562
H_y nT
0
19.895
H_z nT
0
09:36
17:61
25:85
34:09
42:34
50:58
58:83
67:07
75:32
83:56
HOURS

Fig. 8

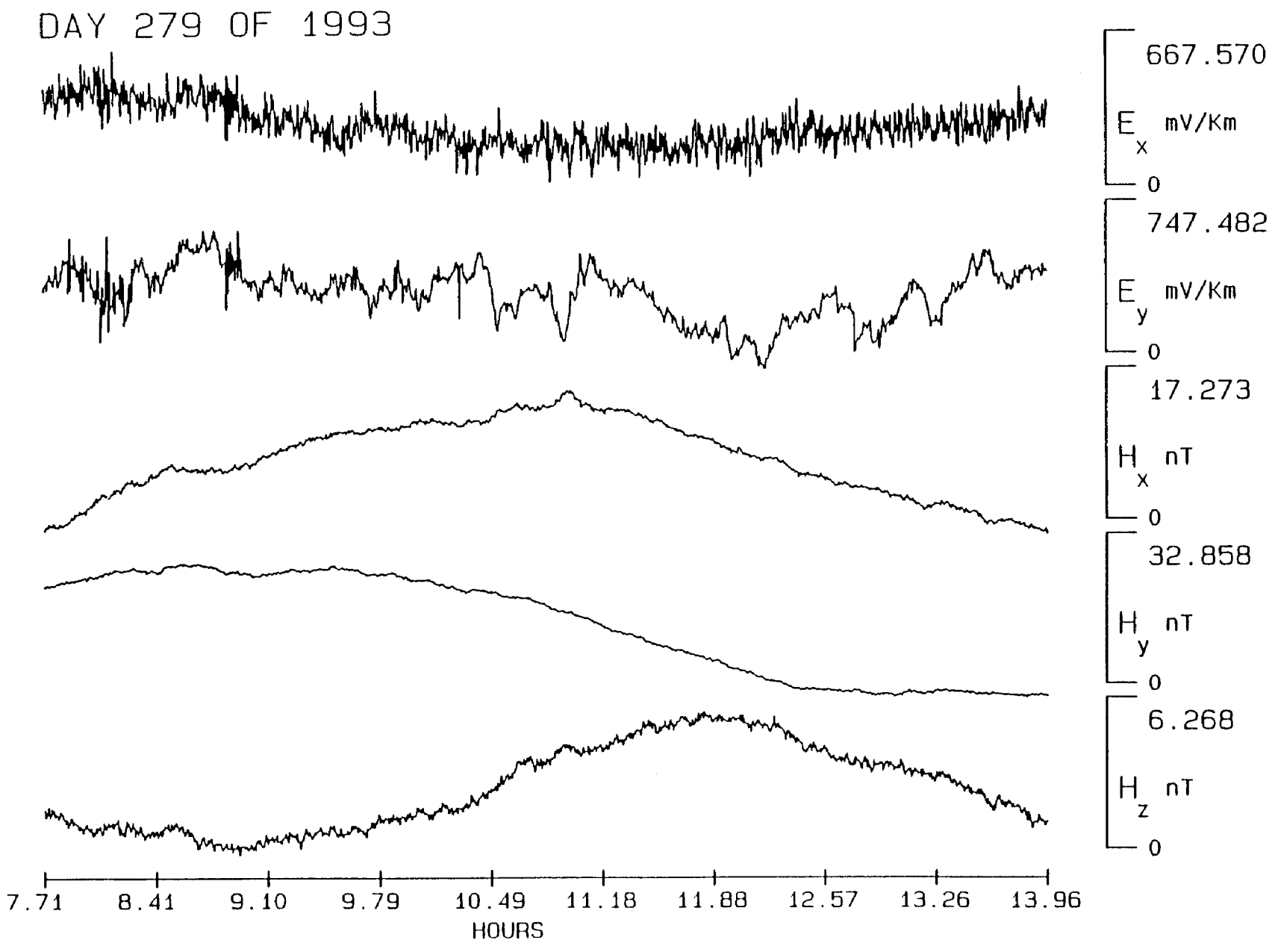
DAY 279 OF 1993
667.570
E_x mV/Km
0
747.482
E_y mV/Km
0
17.273
H_x nT
0
32.858
H_y nT
0
6.268
H_z nT
0
7.71
8.41
9.10
9.79
10.49
11.18
11.88
12.57
13.26
13.96
HOURS

Fig. 9

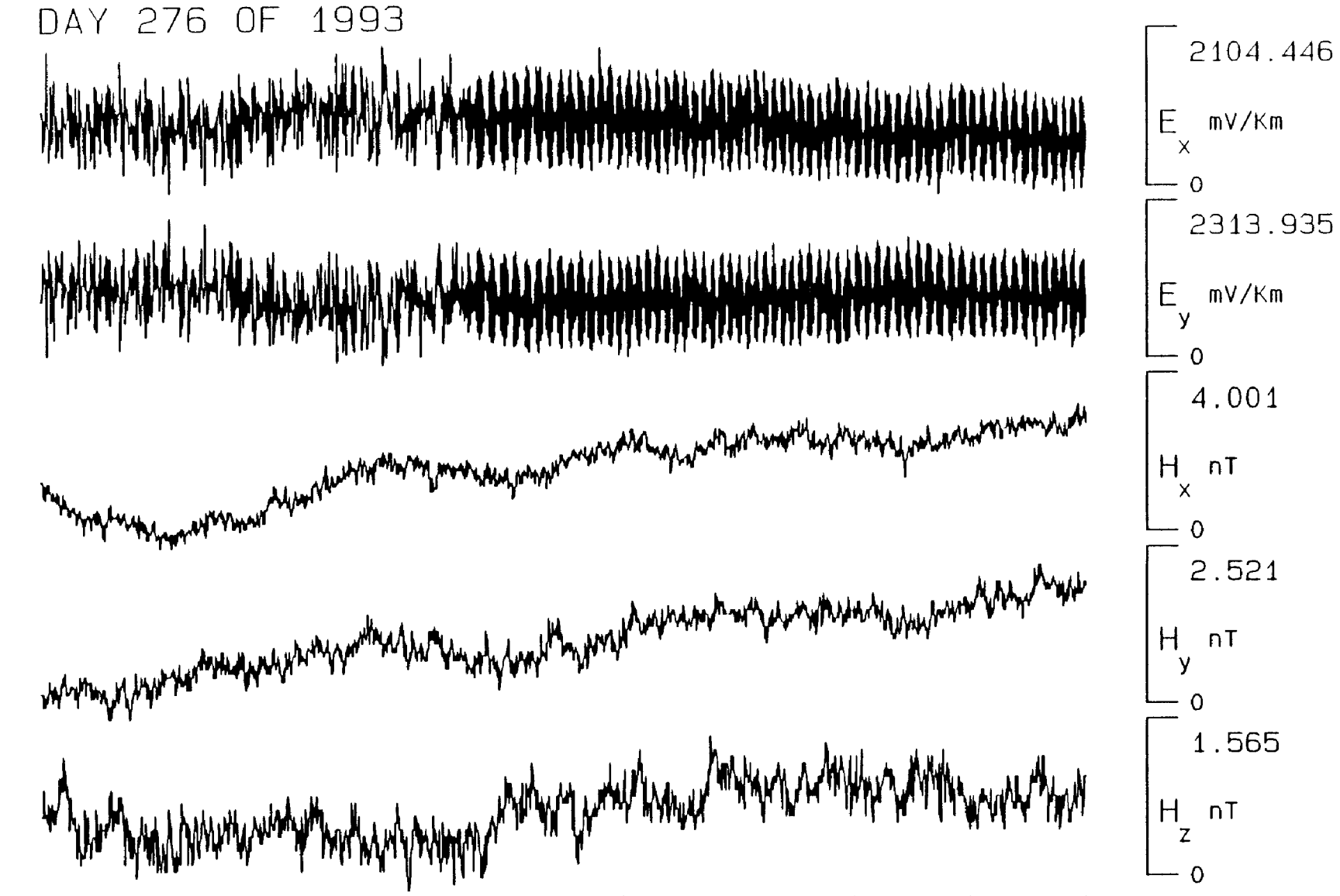
DAY 276 OF 1993
2104.446
E x mV/Km
0
2313.935
E y mV/Km
0
4.001
H x nT
0
2.521
H y nT
0
1.565
H z nT
0
15.88
15.92
15.97
16.01
16.06
16.10
16.15
16.19
16.24
16.28
HOURS

FIG.10

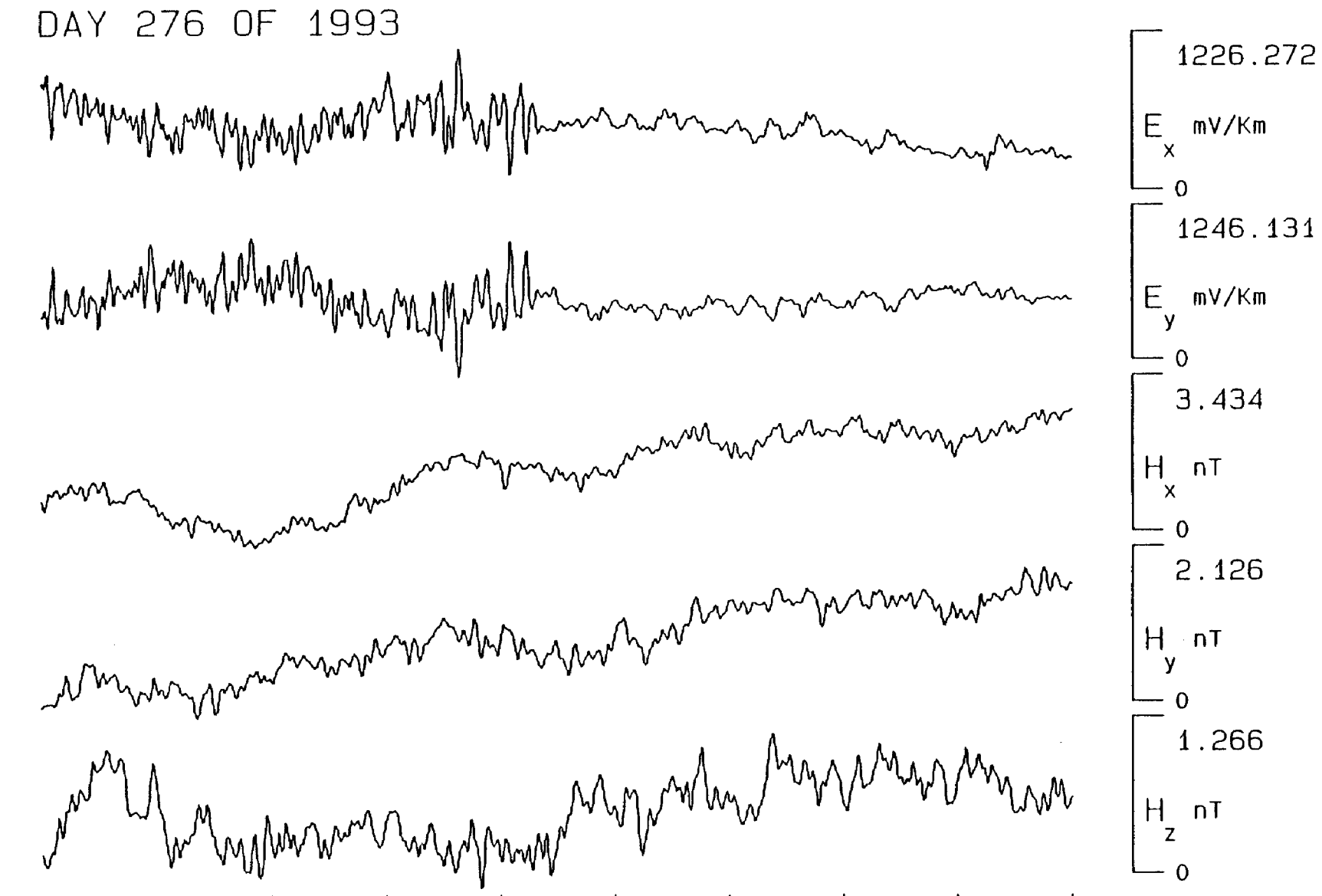
DAY 276 OF 1993
1226.272
E x mV/Km
0
1246.131
E y mV/Km
0
3.434
H x nT
0
2.126
H y nT
0
1.266
H z nT
0
15.84
15.89
15.93
15.98
16.03
16.07
16.12
16.17
16.21
16.26
HOURS

ON INTERMEDIATE TERM EARTHQUAKE PREDICTION IN GREECE BASED ON THE ALGORITHM M8

by

J. LATOUSSAKIS, G.N. STAVRAKAKIS, J.DRAKOPOULOS

National Observatory of Athens, Seismological Institute

P.O.BOX 20048, 118 10 Athens, Greece

ABSTRACT

In the present study an attempt is made to identify the Times of Increased Probability (TIPs) of occurrence of a moderate earthquake ($M_L \geq 5.5$) by premonitory intermediate-term seismic activation in lower- magnitude range, as defined in the algorithm M8. A previous study has shown that 10 out of 11 earthquakes with $M_L \geq 5.5$ which took place in Greece in the time period 1977-1990, occurred within TIPs diagnosed retrospectively indicating that the algorithm M8 can also be applied for smaller earthquakes in regions for which complete catalogues are available.

By scanning the territory of Greece and adjacent areas four regions are diagnosed as candidate for earthquakes of $M_L \geq 5.5$ since they have already entered in TIPs. The results obtained here by no means constitute a definitive earthquake prediction but simply outline the territories which deserve for more detailed and comprehensive analysis. Monitoring of their seismicity would provide further insight to the ongoing research on localization of the impending earthquakes within TIPs.

However, while our paper was rewieving two strong earthquakes occurred within current TIPs diagnosed by the algorithm M8. The observed parameters are in good agreement with the estimated ones, as we analytically describe in the last section.

INTRODUCTION

Several studies of precursors to past events suggest that seismicity patterns can play an important role in earthquake prediction programs of the future. A number of authors have examined seismicity prior to past earthquakes and proposed various patterns as precursors. The first comprehensive review of those studies was made by KANAMORI (1981), McNALLY (1982) who outlined the basic types of seismicity precursors, such as, foreshocks, quiescence, swarms, accelerated activity, and doughnuts. Although seismic quiescence has received the most attention from the seismicity patterns (see review in HABERMANN, 1988; WYSS and HABERMANN, 1988), many reported observations of quiescence seem to have problems either due to the statistical inadequancies in the treatment of the data (REASENBERG and MATTHEWS, 1988) or due to magnitude bias in earthquake catalogs (HABERMANN, 1982).

On the other hand, pattern recognition techniques have been developed (GELFAND et al., 1976; GABRIELOV et al., 1986) in order to examine whether the time interval $(t, t+\tau)$ belongs to a Time of Increased Probability (TIP) of a strong earthquake (τ is considered as a numerical parameter). For

this purpose, two algorithms for diagnosis of TIPs have been proposed and applied to different seismic regions of the world. The first one, the so called CN-algorithm was designed for the analysis of the earthquake catalogs for California and Nevada. In this case, strong earthquakes were defined by the threshold M_o = 6.4 (ALLEN eT al., 1987). The second one, the algorithm M8, based on the concept of self-similarity of earthquakes was designed by KEILIS-BOROK and KOSSOBOKOV (1984, 1986) using a smaller set of functions, and a simpler diagnosis criterion. Moreover, the earthquake catalogues may include lower magnitudes than in algorithm CN.

However, both algorithms are referred to intermediate-term earthquake prediction and have been tested on independent data. The algorithm CN has been successfully applied to several regions of the world (ALLEN et al., 1983; KEILIS-BOROK et al., 1988; KEILIS-BOROK et al., 1990). The algorithm M8 has also been applied to 19 different regions of the world and the results can be summarized as follows: TIPs precede 27 out of 34 strong earthquakes and, in different regions, occupy, on the average, about 24 % of the time interval analysed.

For the area of Greece, and especially along the Hellenic arc several studies have been made to investigate the seismicity patterns, including seismic gap, drop of seismicity rate, inactivity of the seismogenetic layer, seismic periodicity (WYSS and BAER, 1981a,b; PAPAZACHOS and COMNINAKIS, 1982; PURCARU and BERKCHEMER, 1982;

PAPADIMITRIOU and PAPAZACHOS, 1985; PAPADOPOULOS 1986,1988). However, AMBRASEYS (1981) pointed out, at that time, that the limited data on spatial and temporal variations in seismicity in the Hellenic arc do not seem to justify specific predictions. It is noteworthy that all previous studies have been based on historical and instrumental data by using only large or moderate earthquakes, and that the occurrence time of the forthcoming large earthquake along the Hellenic arc was given in the long-term sense, i.e. next decade or so.

On the other hand, the algorithm M8 depicts the activation of the earthquake flow in the lower magnitude range. A TIP is declared when (i) all the characteristic functions are defined and (ii) all the functions achieve large values during a common time interval. To fullfill the first condition at least six years data from the beginning of the catalogue are needed and at least six years data to distinguish long seismicity level from a short one.

Therefore, the application of the algorithm M8 to the area of Greece and especially to the Hellenic arc by using solely recent complete regional data from 1971 onwards will essentially contribute to earthquake prediction problem in this region.

UTLINE OF THE ALGORITHM M8

For convenience of the reader, we briefly repeat the functions which are used in the algorithm M8. More details are given by KEILIS-BOROK and KOSSOBOKOV (1986).

The functions are defined on a sequence of main shocks. Each main shock is defined by the vectors of six components, $\{t_i, \varphi_i, \lambda_i, h_i, M_i, B_i(e)\}$, where i is the sequence number of the main shock, t is the origin time, φ is the latitude, h is the focal depth, M is the earthquake magnitude, and B(e) is the number of aftershocks that occurred in the first e days after the main shock.

The function N(t:m,s) defines the current level of seismic activity, in other words it depicts the number of main shocks with $M \geq m$ in the time interval (t-s, t).

The function K(t:m,s) defines the increment of seismic activity and is given by:

$$K(t:m,s) = N(t:m,s) - N(t-s:m,s).$$

The function V(t:m,s,u) defines the variation of seismic activity and is given by:

$$V(t:m,s,u) = \Sigma[N(t_{i+1}:m,s)-N(t_i:m,s)]$$

The function L(t:m,s,t_o) defines the deviation of seismic activity from a long-term linear trend and is given by:

$$L(t:m,s,t_o)= N(t:m,t-t_o)-N(t-s:m,t-s-t_o)(t-t_o)(t-s-t_o)^{-1}$$

The concentration of main shocks in space is defined in the following way. Let $S(t:m,M',s,\alpha,\beta) = \Sigma 10^{\beta(M_i-\gamma)}$ be a weighted sum of the main shocks within (t-s,t) time and (m,M') magnitude intervals. Each weight depends on the magnitude and is roughly proportional to the length of source. Specifically, we have used $\beta = b/3$, where b is the coefficient in the magnitude energy relation $\log E = \alpha+bM$. The parameter α normalizes the weights. The average length of a source is proportional to S/N, and the average distance between them is proportional to $S/N^{-1/3}$ in the case of uniform distribution. Their ratio characterizes concentration and can be roghly estimated by the function

$$Z(t:m,M',s,\alpha,\beta)=S(t:m,M',s,\alpha,\beta) \;/\; [N(t:m,s)-N(t:M',s]^{2/3}$$

The function B defines the clustering of earthquakes and $B(t:m,M',s,M_o,e)$ is the maximal number of aftershocks with $M \geq M_o$ in the first e days after a main shock within intervals (t-s,t) and (m,M').

Because the seismic activity in the regions considered is obviously different, we normalize it by adjusting the magnitude threshold M so that the everage yearly rate of occurrence of main shocks with $M \geq m$ in area is equal to a certain common value. For one set of functions designated as

N_1, L_1, and Z_1 the constant is 10 years, and it is 20 per year for another set N_2, L_2, and Z_2. For all these six function the duration of a time interval s is 6 years. The upper magnitude threshold M is defined to M_o. For the function Z we have used $M' = M_o - 0.5$. For B the threshold were $m = M_o - 2$ and $M' = M_o - 0.2$.

To diagnose a TIP at time t we require that over the preceeding 3 years:

(i) each group $\{N_1, N_2\}, \{L_1, L_2\}, \{Z_1, Z_2\}, \{B\}$ contains functions with extremely large values, and

(ii) at least 6 out 7 functions $\{N_1, N_2, L_1, L_2, Z_1, Z_2, B\}$ have extremely large values. Extremely large refers to values in the upper Q% quantile range (Q=25 for B and Q=10 for all other functions).

Finally, the vector $F_u(t)$ of the above mentioned functions is computed for discrete times $\{t_i\}$ with a half-a-year step. The time interval $\{t_i, t_i+\tau\}$ is a TIP when the conditions (i) and (ii) occur at t_{i-1} and t_i.

PREVIOUS RESULTS

For the area of Greece and adjacent territories the algorithm M8 has been applied for M_o = 7.0 (LATOUSSAKIS and KOSSOBOKOV, 1990). It has been revealed, retrospectively, that the three strongest earthquakes of Ms≥7.0 which occurred in Greece during the time interval 1973-1988 were preceded by a specific increase of the earthquake activity in the lower magnitude range which was depicted by the algorithm M8.

Furthermore, for the same area an attempt was made by LATOUSSAKIS and STAVRAKAKIS (1992) to investigate whether the algorithm M8 could be applied to smaller earthquakes. i.e M_L≥5.5 which are of major practical importance due to their frequent occurrence in the area of Greece. The obtained results seem to be promising in terms of intermediate -term earthquake prediction.

Especially, the above authors examined 15 earthquakes of M_L≥5.5 which took place in Greece and surrounding region from 1977 to 1990. Ten out of them occurred within TIPs. The algorithm failed in diagnosing TIPs in four cases, because the relevant events occurred in regions, i.e. Albania, West Turkey, for which a complete earthquake catalog was not available to the authors. Only in one case, namely that of the Thessaloniki (northern Greece) earthquake of June 20, 1978 the algorithm M8 did not diagnose any TIP. It might also be explained in terms of the completeness of the NOA catalog (National Observatory of Athens) for northern Greece at that time. This fact indicates how critical the

selection of the area is within which TIPs are sought.

Once we have examined the applicability of the algorithm M8 to smaller earthquakes in Greece, we continue to explore the possibility of identifying current TIPs of occurrence of earthquakes with $M_L \geq 5.5$ for the same area. The obtained results are discussed in terms of the seismic history of the regions.

APPLICATION OF THE ALGORITHM M8

As we mentioned above, by considering a threshold magnitude, M_o, equal to 5.5 then the algorithm M8 requires complete data for events with magnitudes M_o-2.0 (3.5) and above. In the present study we used the NOA catalog which is complete for earthquakes with local magnitude greater than 3.2 for the time period 1971-1990 (PAPANASTASSIOU et al., 1989, see also fig.I). This catalogue contains about 14,000 earthquakes with local magnitude in the range 3.0 to 6.8 for the above mentioned time period. Figure 1 shows the epicenter distribution of the events with $M_L \geq 4.5$ which occurred in Greece and adjacent region from 1971-1990. Since the algorithm M8 requires main shocks, we remove the aftershocks from the catalog following the criteria given by LATOUSSAKIS and STAVRAKAKIS (1992).

After that, the territory (31°-41°N, 21°-27°E) was firstly scanned by overlapping circles of diameter $D = \exp(M_o-5.6)+1$ in degrees of the Earth meridian, that is a radius of 105 km for a $M_o = 5.5$, with a step of one degrees

in latitude and longitude, respectively. The seismicity is considered within each area, and several integral traits of an earthquake activity are estimated as functions of a sliding time window. If most of them (at least six out of seven) become extremely large within a certain narrow time interval a TIP is diagnosed for 5 years. In light of the above first scanning of the territory, by 72 overlapping circles, a first diagnosis of TIPs for M_o = 5.5 was done.

The results have shown that 14 circles (see fig.2) contain current TIPs. These circles delineate four volumes as illustrated in fig.2, and we look for the stability of the diagnosis for each volume separately as follows.

(a) Volume I (Southwestern Aegean Sea Region)

Volume I consists of four overlapping circles with centers C1 (34°N, 24°E), C2(35°N,22°E), C3(35°N, 23°E), and C4(36°N,23°E) of radius equal to 105 km. Each circle contains current TIP diagnosed for events with $M_L \geq 5.5$ as shown in figure 3a. The TIP is considered to be equal to 5 years (KEILIS-BOROK and KOSSOBOKOV, 1986), consisting of ten periods τ_i (i = 1, 10) of duration of six months each one.

Furthermore, we looked for whether the current TIP could be diagnosed in this region by considering higher threshold magnitudes, i.e. M_o = 6.0, 6.5, 7.0, and 7.5. For this purpose, the volume I was also scanned by overlapping circles with a center the geographical centre (35°N-23°E) of

the circles C1,C2,C3,C4,C5 and of various radius corresponding to higher M_o as shown in figure 4. Table 1 summarizes the seismicity parameters which have been used to compute the characteristic functions of the algorithm M8 for each region delineated by a circle. The results obtained are illustrated in figure 3b. As can be seen, for M_o = 7.5 no current TIP was identified, indicating probably an upper bound magnitude for the imminent earthquake or even the present seismic potential of this region. Due to space limitations, we represent only the results which were obtained for the largest M_o. Figure 5 shows the variation of the seven characteristic functions vs time for Mo = 7.0. The vertical line depicts the starting of the current TIP. Table 2 summarizes the corresponding values of the seven functions used for the diagnosis of the TIP for Mo = 7.0, in this region.

Summarizing the results obtained for the Volume I, a TIP stably appears in the southwestern part of the Hellenic arc for different M_o = 5.5-7.0, which according to the algorithm M8 has to be filled from now (1991) till the end of 1993. The TIP diagnosed for this region includes the seismic gap identified by WYSS and BAER (1981a,b), PAPAZACHOS and COMNINAKIS (1982), and has been used for a long-term prediction in this region.

In figure 4 the distribution of the earthquakes of $M_s \geq 6.5$ occurred in this region during the time period 1500-1990 is also shown. The historical earthquakes of the

period 1500-1899 were taken from PAPAZACHOS and PAPAZACHOS (1989), the instrumental data of the period 1900-1985 from MAKROPOULOS et al. (1989). Considering this spatial distribution as well as the conclusions made by various authors (see introduction) for this region, it is reasonable to assume that the most probable location is near 36.0°N - 23.0°E, within the so called Anticithira gap (fig.1 and 4), (between West Crete and Anticithira).

At this point we should like to clarify that only one TIP has been diagnosed in the southwestern part of the Hellenic arc, despite of the four circles which are shown in figure 4. Each circle, as we have mentioned above, corresponds to a different M_o. We made such an analysis to assess the earthquake magnitude expected in this region. It does not mean that four earthquakes will occur within the relevant circles. Based on this fact, we expect a surface waves magnitude to be in the range $6.0 \leq M_s < 7.5$. The lower limit comes out from the threshold local magnitude (equal to 5.5, and $M_s = M_L + 0.5$) considered in the presesent study, and the upper bound from the threshold magnitude for which no TIP was identified.

(b) Volume II (Southeastern Aegean Sea Region)

The same procedure was followed to delineate the volume II which contains four circles with centers C5(36°N, 26°), C6(37°N, 25°E), C7(37°N, 26°E), and C8(37°N, 28°E) and of

radius equal to 105 km (M_o = 5.5) (fig.2). Each circle contains a TIP for $M_o \geq 5.5$ as illustrated in fig.6a.

Furthermore, the volume II was scanned by overlapping circles (fig.7) with a center the geographical centre of C5,C6,C7,C8 and of various radius corresponding to higher M_o in order to investigate whether TIPs appear in this region for higher magnitudes. Again, it does not mean that four earthquakes will follow the TIPs. Actually, one current TIP was diagnosed and the different circles delinate the candidate areas for different magnitudes. Table 3 summarizes the seismicity parameters that have been used to compute the functions including in the algorithm M8 for each region delineated by a circle. Figure 6b shows the obtained results. For $M_o > 7.0$, no TIP was identified, indicating probably an upper bound magnitude for volume II. Figure 8 illustrates the variation of the seven functions vs. time for the largest M_o (= 6.5). The vertical line represents the beginning of the TIP. Table 4 summarizes the corresponding values obtained by the algorithm M8 for M_o = 6.5.

Based on the spatial distribution of the large events (fig.7), and by considering the conclusion made by WYSS and BAER (1981a,b) it is reasonable to consider as the most probable location near 36.5°N - 27.5°E (broad region of Kos island) with a surface magnitude $6.0 < M_s < 7.0$. It is of great importance to emphasize at this point, that an abnormal nucleation of subcrustal earthquakes in the vicinity of Kos island has been observed for the time period 1971-1985

(GALANOPOULOS, 1989). Especially, during the above time period, 57 out of 122 events of m_b>3 and with focal depths greater than or equal to 100 km occurred in the vicinity of Kos island. In several cases it has been reported that deep-focus earthquake activity sometimes increases preceding large shallow earthquakes (MOGI, 1973). We consider this observation as an additional fact which enhances our estimation for the location of the earthquake expected to occur in the southeastern part of the Hellenic arc.

Volume III (North - Central Aegean Sea Region)

This region (fig.2) was also delineated by following the same procedure as above. It contains four circles with centers C9(38°N-25°E), C10(38°N-26°E), C11(39°-25°E), and C12(39°-26°E) and of radius equal to 105 km (M_o = 5.5). Each circle contains a TIP as illustrated in figure 9a.

Furthermore, this volume was scanned by overlapping circles with center 38.5°N-25.5°E (fig.10) and various radii, corresponding to higher M_o to look for TIPs of larger events by using the seismicity parameters summarized in Table 5. Figure 9b shows the obtained results. No TIPs for M_o>7.0 were diagnosed indicating an upper bound of the magnitude expected in this region. Table 6 summarizes the values obtained for the seven functions of the algorithm M8 for M_o = 6.5 and figure 11 illustrates their time variation.

Based on the spatial distribution of the large events

(fig.10) and by considering the seismic history of this region, we may define as the most probable location near 38.5°N-25.5°E for a shallow earthquake of surface magnitude $6.0<Ms<7.0$.

Volume IV (Mainland of Greece)

This volume (fig.2) is delineated by two circles with centers C13(39°N-22°E) and C14(40°N-21°E) and of radius equal to 105 km (M_o = 5.5). Each circle contains a TIP as shown in fig.12a. To ensure that the current TIPs do not appear by random, the volume IV was also scanned by overlapping circles with center 39.5°N-21.5°E (fig.13) and various radius corresponding to higher M_o, by using the seismicity parameters summarized in table 7. When $M_o>6.5$ the TIPs were not identified (fig.12b). Table 8 gives the values obtained for the seven functions and figure 14 illustrates their time variation for M_o = 6.0.

It is evident that the characteristic earthquake magnitude M_o for which current TIPs were not diagnosed is different for each volume indicating also a different upper bound magnitude consistent with the seismic history of each region. Furthermore, it might indicate the present seismic potential of each volume.

By a further consideration of the seismic history of the region (see and fig.13) we expect as a probable location near

39°N - 22.5°E for the forthcoming earthquake of surface magnitude 6.0<Ms<7.0.

The stability of the results based on the NOA-catalogue has been examined by LATOUSSAKIS and KOSSOBOKOV (1990). These authors varied the lower magnitude threshold in the count of aftershocks B(e) from 3.0 to 4.5, and the interval for this count e from 2 to 14 days. They, also, used other space and tim limits in the definition of aftershocks, taking them from GARDNER and KNOPOFF (1974). Finally, they applied the same algorithm M8 to the extented catalog for the area of Greece (MAKROPOULOS et al., 1989). In all these experiments the TIPs were stable.

DISCUSSION AND CONCLUSIONS

Once the applicability of the algorithm M8 has retrospectively been tested for earthquakes of M_o = 5.5 occurred in Greece, we further explored the possibility of identifying current TIPs for this area. For this purpose, the territory was scanned by overlapping circles of radius equal to 105 km corresponding to a M_o = 5.5. In this way, a first diagnosis was made aiming at delineating subregions for which current TIPs are sought by considering higher magnitudes M_o and different seismicity parameters.

Volume I includes the southwestern part of the Hellenic arc for which current TIPs were diagnosed for M_o = 5.5 to 7.0. For higher magnitudes no TIP was found indicating,

probably, the present seismic potential of this region. The TIP consists of ten periods of duration of six months each one. According to the results obtained for volume I, the current TIP for the highest magnitude (M_o = 7.0) started at the end of 1988. Because seven periods have already elapsed, it is reasonable to assume that the probability of occurrence of the forthcoming large event in this region became extremely high, to fill the TIP. The impending earthquake may occur at any time from now (1991) till the end of 1992. We make such an estimation because of the following reasons.

Firstly, to be filled the current TIP in this region, a time interval of about six months is left. Practically, it means that the TIP can be filled at any time from the moment at which we diagnose this TIP till the end of the TIP's duration (that is, end of 1992). Secondly, there is no way to estimate more accurately the occurrence time of a strong earthquake within a TIP. It is obvious that, if we had made the present analysis in 1988, then we would have defined as a possible time of occurrence the whole interval 1988-1992, once there is no other way to estimate the time of occurrence within a TIP. For this reason, we emphasized the need of establishment of a dense seismological network in the candidate region to detect, if possible, any seismic short-term precursor, which could help for a better assessment of the time of occurrence. Of cource, one could propose monitoring of other geophysical parameters for the same purpose.

As far as the location of the forthcoming large earthquake within the current TIP is concerned, it was significantly reduced by considering the seismic history of the investigated region. As we have pointed out, the most probable location is the area between Anticithira island and off the western coast Crete, and not anywhere within the circles.

Volume II includes the southeastern part of the Hellenic arc for which a current TIP was also diagnosed, but for smaller magnitude (M_o = 6.5) of the impending earthquake. It might be an indication that the seismic potential of the western part of the Hellenic arc is higher than that of the eastern one. It is also interesting to notice that the current TIP for M_o = 6.5 in this area started very recently (at the beginning of 1991) in contrast to the TIP for the West Hellenic arc for which only six months have left. By considering the seismic history of this region, especially the recent abnormal nucleation of deep focus earthquakes in the vicinity of Kos island we assume this area as the candidate one for the next large earthquake in the East Hellenic arc.

For volumes III and IV, current TIPs were declared for M_o = 6.5 and 6.0, respectively. Also in these cases, the locations expected of the forthcoming large earthquakes were given in terms of the seismic history of the corresponding regions.

VERIFICATION OF OUR PREDICTION

While our paper was under the normal procedure of making the corrections and suggestions proposed by two anonymous reviewers, the following strong earthquakes occurred in Greece (Prelininary Determinations of the National Observatory of Athens):

(i) On November 6, 1992 (19h06m, GMT) an earthquake of local magnitude equal to 5.7 (surafce magnitude = 6.2) took place at 38.02°N - 27.16°E at a focal depth of 39 km (see fig.15). That is within the shaded area delineated within the circles of figure 10. We believe that this event occurred within the current TIP diagnosed for volume III of the present study. As the reader himself can realize , the "predicted parameters", given in the text:

" probable location near 38.5°N - 25.5°E, shallow event, surface waves magnitude $6.0<M_s<7.0$" with the observed ones are in a satisfactory agreement by means of the cabability of the algorithm M8. We would like to emphasize once again that the TIP has been strictly diagnosed with the algorithm M8, while the lower and upper magnitude bounds where estimated by using the criterion of magnitude for which the current TIP disappears. (i.e. for $M_o > 7.0$ for volume III). The location mentioned above was based on personal judgment by considering the spatial distribution of the large earthquakes took place in volume III in the past. It is interesting to note that the last large event in this area took place on July 16, 1955 and

was of magnitude M_s = 7.0.

Moreover, on November 21, 1992 (05h07m, GMT) a strong earthquake of surface magnitude equal to 6.5 took place at 35.38°N - 22.37°E at a focal depth of 99 km (see fig.16). That is the shaded area delineated within the circles of figure 4 of Volume I (southwestern Hellenic Arc). This event also occurred within the TIP diagnosed by the algorithm M8. For this case we have estimated the probable location near to 36.0°N - 23.0°E, the surface waves magnitude greater than 6.0, once the threshold local magnitude was equal to 5.5 and an upper bound 7.5, since for higher magnitudes no TIP was diagnosed. Comparing the estimated parameters with the observed ones, it is evident that they are in good agreement, by means of the algorithm M8 and in the sense of indermediate-term earthquake prediction. It is worth reminding that we also stressed that the current TIP in the southwestern part of Hellenic arc is expected to be filled by the end of 1992, by emphasizing the high probability since only six months are left. Actually, it happened.

As we have mentioned in the abstract of the present paper, "the results obtained here by no means constitute a definitive earthquake prediction but simply outline the territories in Greece which deserve particular attention". The occurrence of the two strong earthquakes on November 6 and Nov.21, 1992 verifies our statement. Additionally, it shows that the algorithm M8 could contribute substantially to intermediate-term earthquake prediction research. The present

case encourages us to emphasize the current TIPs which have been found by KEILIS-BOROK et al. (1990) for Central Italy and by KEILIS-BOROK and KOSSOBOKOV (1990) for Central Japan. Based on what very recently in Greece happened, we believe that these regions deserve particular attention.

Acknowledgements

This study was a part of a research project and was financially suported by the European Centre on Prevention and Forecasting of Earthquakes (Council of Europe), under the contract number 122/1/11/91.

REFERENCES

ALLEN, C., HUTTON, K., KEILIS-BOROK, V.I., KNOPOFF, L., KOSSOBOKOV, I.V., and ROTWAIN I.M. (1983), Selfsimilar Premonitory Seismicity Patterns, Abstract, XVIII Congress of IUGG, Hamburg, Germany.

ALLEN,C.R., KEILIS-BOROK,V.I., ROTWAIN,I.M., HUTTON,K. (1987). A set of long-term seismological precursors; California and some other regions. In: Computational Seismology, vol.19 (translation from Russian), Allerton Press, N.Y., 24-35.

AMBRASEYS,N.N. (1981). On the long-term seismicity of the Hellenic arc. Boll.Geof. Teor. Appl., 23, 355-359.

GABRIELOV,A.M., et al. (1986). Algorithms of Long-Term Earthquakes' Prediction, CERESIS,Lima, Peru, 61pp.

GALANOPOULOS, A.G. (1989). Abnormal nucleation of subcrustal events in the vicinity of Cos island. Prakt. Academy of Athens, Vol.63, 288-297.

GARDNER,J.K. and L. KNOPOFF, (1974). Is the sequence of earthquakes in southern California, with aftreshocks removed, Poissonian? Bull. Seism. Soc. Am.,64, 1363-1367.

GELFAND,I.M., GUBERMAN, Sh.A., KEILIS-BOROK, V.I., KNOPOFF,L., PRESS,F.,RANZMAN,I.,Ya.,ROTWAIN,I.M., SADWSKY, I.M. (1976).Pattern recognition applied to earthquake epicenters in California. Phys. Earth Planet. Inter.,11,227-283.

HABERMANN, R.E. (1982). Consistency to teleseismic reporting since 1963. Bull. Seism. Soc. Am.,71, 93-194.

HABERMANN, R.E. (1988). Precursory seismic quiescence: Past,

present, and future. Pageoph, 126, 279-318.

KANAMORI, H. (1981). The nature of seismicity patterns before large earthquakes. In: Earthquake prediction. An International Review, Maurice Ewing Series, vol.4, (eds. D. Simpson, P. Richards), AGU, Washington DC, 1-19.

KEILIS-BOROK, V.I. and V.G. KOSSOBOKOV (1984). A complex of long-term precursors for the strongest earthquakes of the world. In proceedings of the 27th Geological Congress, vol. 61, Earthquakes and Hazard Prevention,Nauka, Moscow, 56-61.

KEILIS-BOROK, V.I. and V.G. KOSSOBOKOV (1986). Time of increased probability for the great earthquakes of the world. Comput. Seismology, 19, 48-58.

KEILIS-BOROK, V.I. and V.G.KOSSOBOKOV (1988). Premonitory activiation of seismic flow: Algorithm M8, Lecture Notes of the workshop on Global Geophysical Informatics with Applications to Research in Earthquake Prediction and Seismic Risk. Rep.H4,SMR/303-10, Int.Cent. for Theor. Phys., Trieste, Italy, 17pp.

KEILIS-BOROK, V.I., KNOPOFF, L., ROTWAIN, I.M., and ALLEN, C.R. (1988). Intermediate -term prediction of occurrence times of strong earthquakes. Nature, 335, (61192), 690-694.

KEILIS-BOROK,V.I. and V.G. KOSSOBOKOV (1990). Times of incresed probability of strong earthquakes (M>7.5) diagnosed by algorithm M8 in Japan and adjacent territories. Journal of Geoph. Res., Vol.95, NO.B8, 12413-12422.

KEILIS-BOROK, V.I., I.V. KUZNETSOV, G.F. PANZA,I.M. ROTWAIN, and G. Costa (1990). On intermediate-term earthquake prediction

in central Italy. Pageoph, Vol.134, 79-92.

LATOUSSAKIS,J. and V.G. KOSSOBOKOV (1990). Intermediate term earthquake prediction in the area of Greece: Application of the algorithm M8. Pageoph, Vol.134, No.2, 261-282.

LATOUSSAKIS,J. and G. N. STAVRAKAKIS (1992). Times of increased probability of strong earthquakes (M_L>5.5) diagnosed by algorithm M8 in Greece. Tectonophysics, 210, 315-326.

MAKROPOULOS, C., DRAKOPOULOS, J., and LATOUSSAKIS, J.(1989), A revised and extended earthquake catalogue for Greece since 1990 Geophys. J. Int., 98, 391-394.

McNALLY, K.C.(1982) Variations in seismicity as a fundamental tool in earthquake prediction. Bull. Seism. Soc. Am., 72, S351-S366.

MOGI, K. (1973). Relationship between shallow and deep seismicity in the Western Pacific region. Tectonophysics, Vol. 17, 1-22.

PAPADIMITRIOU, E.E. and PAPAZACHOS, B.C. (1985). Seismicity gaps in the Aegean and surrounding area. Boll. Geofis. Teor. Appl., 27, 185-195.

PAPADOPOULOS, G.A. (1986). Long-term earthquake prediction in the Western Hellenic arc. Earthq. Predict. Res., Vol. 4, 131-137.

PAPADOPOULOS, G.A. (1988). Long-term accelerating foreshock activity may indicate the occurrence time of a strong shock in the Western Hellenic arc. Tectonophysics, Vol.152, 179-192.

PAPANASTASSIOU,D., DRAKOPOULOS, J., LATOUSSAKIS, J., STAVRAKAKIS, G., and DRAKAKTOS, G. (1989), The new telemetric

seismological network of the National Observatory of Athens. Proc. of XXI Gen. Assembly of European Seism. Com., Aug. 23-27- Sofia, Bulgaria, 228-243.

PAPAZACHOS, B.C. and P.E. COMNINAKIS (1982). Long-term earthquake prediction in the Hellenic Trench-Arc system. Tectonophysics, Vol. 86, 3-16.

PAPAZACHOS, B. and PAPAZACHOS, C. (1989). The earthquakes in Greece. Edit. Ziti, Thessaloniki, 356pp (in Greek with English summaries).

PURCARU, G. and BERCKHEMER, H. (1979). Patterns of occurrence of large earthquakes in the region of the Mediterranean. Intern. Symp. Earthq. Pred., UNESCO, 1979, Paris, Paper III-7, Publ. Sc./79/conf.802/, 15pp.

REASENBERG, P.A. and MATTHEWS, M.V. (1988). Precursory seismic quiesence: a preliminary assessment of the hypothesis. Pageoph, 126, 373-406.

WYSS,M. and M. BAER(1981a). Seismic quiescence in the Westren Hellenic Arc may foreshadow large earthquakes. Nature 298, 785-787.

WYSS,M. and M.BAER (1981b). Earthquake hazard in the Hellenic arc. In Earthquake Prediction-An International Review (eds. Simson,B.W., and Richards,B.) ,EGU,4, 54, (Maurice Ewing Series Washington), 153-172.

WYSS, M. and HABERMANN, R.E. (1988). Precursory seismic quiescence. Pageoph, 126, 319-356.

CAPTION OF TABLES

TABLES 1,3,5,7:

Seismicity parameters used for normalization of the functions of the algorithm M8, for volumes I, II, III, and IV, respectively. $a(3.2)$ is the average annual number of the evnts with magnitude greater than or equal to 3.2. $M_{1th}(N)$, $M_{2th}(N)$ are the magnitude thresholds chosen such that the average yearly rate of occurrence of the main shocks is equal to N_1, N_2, respectively.

TABLES 2, 4, 6, 8

Values of the seven functions of the algorithm M8 for volumes I, II, III, and IV, respectively. Extremely large values of the functions are marked with "*". Symbol ▪ marks the score which started the TIPs.

CAPTIONS OF FIGURES

Fig.I: Annual number of earthquakes occurred in Greece after 1968 onwards detected by the National Seismological Network

FIG.1: Epicenter map of earthquakes with $M_L>4.5$ for the time period 1971-1990.

FIG.2: The four volumes which are delineated after the territory had been scanned by 72 overlapping circles of radius of 105 km using a step of 1 degrees in latitude and longitude.

FIG.3: (a) Current TIPs for M_o = 5.5 in volume I (circles C1-C4). Rectangles depict the duration of a TIP. The black area corresponds to the ellapsed time and the white one to the time left. (b). Current TIPs in volume I for higher M_o. No TIP is declared for M_o = 7.5.

FIG.4: Large earthquakes ($M_s \geq .5$) in the southwestern part of the Hellenic arc (Volume I) for the time period 1500-1987. The radius of the overlapping circles corresponds to M_o = 5.5, 6.0, 6.5, and 7.0, respectively. The shaded area depicts the most probable location for the next large shock in this region.

FIG.5: Time variation of the seven functions used to diagnose a current TIP for M_o = 7.0 in volume I. Vertical line represents the beginning of the TIP.

FIG.6 :(a) Current TIPs for M_o =5.5 in volume II (circles C5-C8 in fig.2). See and caption of fig.3a.

(b) Current TIPs in volume II for higher magnitudes in volume II. No TIPs are declared for $M_o>7.0$.

FIG.7: Large events ($M_s \geq .5$) in volume II for the time period 1500-1987. The radius of the overlapping circles corresponds to

M_o = 5.5, 6.0, and 7.0. The shaded area depicts the most probable location of the next large shock in this region.

FIG.8: Time variation of the seven functions used to diagnose a current TIP for M_o = 6.5 in volume II. Vertical line represents the duration of the TIP.

FIG.9: (a) Current TIPs for M_o = 5.5 in volume III (circle C9-C12 in fig.2). See and caption of fig.3a.

(b) Current TIPs for higher M_o in volume III. No TIPs are declared for M_o>7.0.

FIG.10: Large events ($M_s \geq .5$) in volume III for the time period 1500-1987. The radius of the overlapping circles corresponds to M_o = 5.5, 6.0, and 6.5. The shaded area depicts the most probable location of the next large shock in this region.

FIG.11: Time variation of the seven function used to diagnose a current TIP for M_o = 6.5 in volume III.

FIG.12: (a) Current TIPs for M_o = 5.5 in volume IV (circle C13-C14 in fig.2). See and caption of fig.3a.

(b) Current TIPs for higher M_o in volume IV. No TIPs are declared for $M_o \geq 6.5$.

FIG.13: Large events ($M_s \geq 6.5$) in volume IV for the time period 1500-1987. The radius of the overlapping circle corresponds to M_o = 5.5, and 6.0, respectively. The shaded area depicts the most probable location of the next large earthquake in this region.

FIG.14: Time variation of the seven functions used to diagnose a current TIP for M_o = 6.0 in volume IV. Vertical line

represents the beginning of the TIP.

FIG.15: Earthquakes with $M_L \geq 3.5$ occurred in Volume I after the starting time of TIP (1987) till the occurrence of the strong earthquake (M_S = 6.5) of Nov.21, 1992. Its epicenter is depicted by the black triangle.

FIG.16: Earthquakes with $M_L \geq 4.0$ occurred in Volume III after the TIP had started (1987) till the occurrence of the strong (M_S =6.2) event of Nov.06, 1992. Its epicenter is shown with the black triangle.

TABLE 1

No.	Mo	R(km)	a(3.2)	N_{1th}	N_{2th}	$M_{1th}^{(N)}$	$M_{2th}^{(N)}$
1	5.5	105	18	3	6	4.2	4.0
2	6.0	138	26	6	12	4.1	3.9
3	6.5	192	44	10	20	4.0	3.8
4	7.0	280	80	10	20	4.2	4.0

TABLE 3

No.	Mo	R(km)	a(3.2)	N_{1th}	N_{2th}	$M_{1th}^{(N)}$	$M_{2th}^{(N)}$
1	5.5	105	15	3	6	4.0	3.8
2	6.0	138	23	6	12	4.0	3.8
3	6.5	192	43	10	20	4.1	3.9

TABLE 5

No.	Mo	R(km)	a(3.2)	N_{1th}	N_{2th}	$M_{1th}^{(N)}$	$M_{2th}^{(N)}$
1	5.5	105	30	3	6	3.8	3.5
2	6.0	138	46	6	12	3.8	3.5
3	6.5	192	75	10	20	3.8	3.6

TABLE 7

No.	Mo	R(km)	a(3.2)	N_{1th}	N_{2th}	$M_{1th}^{(N)}$	$M_{2th}^{(N)}$
1	5.5	105	27	6	12	3.8	3.6
2	6.0	138	52	10	20	3.9	3.6

TABLE 2

G:H	M_{MAX}	TIME	N_1	N_2	L_1	L_2	Z_1	Z_2	B
0: 0	4.5	1971 7 1	5	9	–	–	156	170	–
0: 0	4.4	1971 12 31	11	22	–	–	204	228	–
0: 0	6.1	1972 6 30	17	33	–	–	333	325	1
0: 0	4.6	1972 12 30	19	39	–	–	340	333	1
0: 0	5.2	1973 7 1	25	50	–	–	372	365	5
0: 0	5.5	1973 12 30	28	58	–	–	400	388	5
0: 0	4.6	1974 7 1	33	66	–	–	408	400	5
0: 0	4.8	1974 12 31	35	71	–	–	415	408	–
0: 0	4.4	1975 7 1	38	82	–	–	418	417	–
0: 0	5.0	1975 12 31	44	91	–	–	449	442	3
0: 0	4.8	1976 6 30	49	100	–	–	455	452	3
0: 0	4.7	1976 12 30	51	106	–	–	460	457	–
0: 0	4.3	1977 7 1	48	103	–	–	458	453	–
1: 1	5.9	1977 12 30	50	100	39	79	504	482	13*
1: 1	5.4	1978 7 1	52	99	37	70	487	472	13*
1: 1	4.4	1978 12 31	55	104	39	72	487	476	1
1: 1	5.4	1979 7 1	53	99	34	61	488	474	0
1: 1	4.9	1979 12 31	54	98	34	57	477	468	0
1: 1	4.7	1980 6 30	51	95	29	51	480	467	–
1: 1	4.9	1980 12 30	57	109	34	64	488	477	–
0: 0	4.6	1981 7 1	65	119	42	69	494	487	–
0: 0	4.9	1981 12 30	69	127	43	75	492	490	–
0: 0	4.5	1982 7 1	69	134	42	79	491	490	–
0: 0	5.7	1982 12 31	70	138	43	82	508	503	1
2: 4	5.2	1983 7 1	74	144	47*	88*	524*	517*	1
2: 4	5.2	1983 12 31	70	140	40	81	504	501	0
3: 6	5.9	1984 6 30	75*	150*	43	89*	516	513	4
3: 6	4.7	1984 12 30	74	148	41	84	517	513	4
3: 6	5.1	1985 7 1	73	148	39	84	513	510	0
3: 6	4.8	1985 12 30	72	152*	38	87	513	511	0
3: 4	4.6	1986 7 1	76*	161*	42	96*	514	516*	–
4: 5	5.5	1986 12 31	75*	154*	39	84	523	520*	18*
■ 4: 6	5.3	1987 7 1	67	140	28	64	540*	523*	18*
■ 4: 6	4.7	1987 12 31	63	133	21	53	529*	513	0
■ 4: 6	4.8	1988 6 30	63	128	21	45	531*	513	–
▮▮▮ 4: 6	4.5	1988 12 30	65	133	23	49	514	505	–
▮▮▮ 3: 5	4.9	1989 7 1	65	135	22	49	507	501	–
▮▮▮ 2: 3	4.6	1989 12 30	65	137	22	52	491	491	–
▮▮▮ 1: 1	4.4	1990 7 1	55	125	9	35	448	458	–
▮▮▮ 1: 1	4.6	1990 12 31	62	132	16	42	457	468	–

TABLE 4

G:H	M_{MAX}	TIME	N_1	N_2	L_1	L_2	Z_1	Z_2	B
0: 0	4.2	1971 7 1	2	11	-	-	107	153	-
0: 0	4.8	1971 12 31	4	15	-	-	168	189	1
0: 0	4.8	1972 6 30	10	29	-	-	228	244	2
0: 0	5.0	1972 12 30	15	39	-	-	264	277	2
0: 0	4.2	1973 7 1	18	43	-	-	269	285	1
0: 0	4.9	1973 12 30	20	50	-	-	292	304	0
0: 0	4.8	1974 7 1	27	59	-	-	326	332	1
0: 0	4.3	1974 12 31	32	66	-	-	331	340	1
0: 0	5.0	1975 7 1	39	75	-	-	353	361	0
0: 0	5.1	1975 12 31	42	79	-	-	371	375	1
0: 0	4.3	1976 6 30	50	88	-	-	381	387	1
0: 0	4.4	1976 12 30	56	98	-	-	389	398	-
0: 0	4.6	1977 7 1	60	95	-	-	399	405	0
1: 2	5.2	1977 12 30	62	100	58*	86*	406	412	0
1: 2	5.4	1978 7 1	60	96	51	71	410	414	0
1: 2	4.5	1978 12 31	60	96	48	64	404	409	0
1: 2	5.0	1979 7 1	60	98	46	65	412	415	1
2: 3	5.1	1979 12 31	65	102	50	66	427	428	3*
2: 3	5.6	1980 6 30	63	100	45	60	434	433	3*
1: 1	4.7	1980 12 30	60	98	39	56	437	433	1
1: 1	5.1	1981 7 1	59	99	35	54	442	437	1
1: 1	4.3	1981 12 30	62	103	38	57	433	432	1
1: 1	4.5	1982 7 1	60	105	32	57	435	432	1
1: 1	4.4	1982 12 31	57	101	27	49	434	429	1
0: 0	5.2	1983 7 1	56	101	25	48	437	431	0
1: 1	5.2	1983 12 31	60	103	28	47	454*	444	0
1: 1	4.6	1984 6 30	69	111	36	53	452*	447	2
1: 1	4.3	1984 12 30	69	111	35	51	450	445	2
1: 1	4.4	1985 7 1	72	118	38	57	447	444	-
1: 1	4.9	1985 12 30	71	115	35	52	434	434	2
2: 2	4.8	1986 7 1	72	118	36	54	424	428	3*
2: 2	4.5	1986 12 31	75	125	39	61	424	431	3*
1: 1	4.7	1987 7 1	83	135	46	69	432	440	1
1: 1	4.7	1987 12 31	82	134	44	67	437	444	0
1: 1	4.5	1988 6 30	83	133	44	64	435	443	0
1: 1	4.9	1988 12 30	89	142	50	73	445	452	0
4: 7	5.1	1989 7 1	96*	151*	56*	82*	455*	462*	1
3: 6	4.9	1989 12 30	96*	152*	55*	81	445	455*	2
4: 7	4.7	1990 7 1	98*	154*	54	79	449	459*	42*
4: 7	5.0	1990 12 31	97*	157*	52	81	454*	463*	42*

TABLE 6

G:H	M_{MAX}	TIME	N_1	N_2	L_1	L_2	Z_1	Z_2	B
0: 0	4.0	1971 7 1	3	7	–	–	89	104	–
0: 0	4.5	1971 12 31	10	20	–	–	152	159	0
0: 0	4.7	1972 6 30	17	31	–	–	192	194	2
0: 0	4.4	1972 12 30	26	44	–	–	217	219	2
0: 0	4.3	1973 7 1	30	52	–	–	228	231	–
0: 0	4.9	1973 12 30	33	58	–	–	242	243	1
0: 0	4.8	1974 7 1	40	67	–	–	264	263	1
0: 0	4.5	1974 12 31	46	80	–	–	276	275	1
0: 0	4.3	1975 7 1	53	91	–	–	288	288	0
0: 0	4.5	1975 12 31	56	99	–	–	296	296	0
0: 0	4.7	1976 6 30	64	109	–	–	311	310	2
0: 0	4.8	1976 12 30	71	122	–	–	325	323	3
0: 0	5.0	1977 7 1	74	123	–	–	339	333	5
1: 2	5.3	1977 12 30	72	115	62*	96*	351	341	5
1: 2	4.7	1978 7 1	72	115	57*	88*	347	339	1
1: 2	4.2	1978 12 31	64	107	43	71	341	331	1
2: 3	5.5	1979 7 1	74	118	51*	79	369	356	14*
2: 3	4.0	1979 12 31	72	116	48	75	364	350	14*
2: 3	4.0	1980 6 30	67	111	40	66	353	340	–
2: 3	4.9	1980 12 30	74	120	44	69	368	354	15*
2: 2	4.9	1981 7 1	74	117	42	62	370	355	15*
2: 2	6.3	1981 12 30	77	119	45	62	365	352	5
1: 1	6.4	1982 7 1	76	120	41	60	357	346	–
1: 1	4.5	1982 12 31	74	115	36	51	350	339	3
1: 1	4.8	1983 7 1	75	125	36	60	350	340	3
1: 1	6.6	1983 12 31	75	134	35	69	335	330	1
0: 0	5.3	1984 6 30	77	141	35	73	355	345	10
1: 1	5.2	1984 12 30	85*	149	45	81	365	355	10
1: 1	4.6	1985 7 1	81	151	36	78	349	343	0
1: 2	4.8	1985 12 30	88*	159*	44	87	361	354	3
4: 6	5.3	1986 7 1	93*	167*	50	95*	385*	373*	37*
4: 6	4.6	1986 12 31	85*	153	38	75	371	361	37*
4: 6	4.0	1987 7 1	82	154	34	76	363	354	2
4: 6	4.8	1987 12 31	81	157*	32	77	373	361	3
4: 6	4.6	1988 6 30	78	154	28	73	376	361	3
4: 6	4.5	1988 12 30	79	157*	29	75	378	363	15*
3: 5	5.3	1989 7 1	76	147	25	62	381*	364*	48*
3: 4	4.9	1989 12 30	79	146	28	58	396*	376*	48*
3: 4	4.5	1990 7 1	79	149	26	58	382*	367*	5
3: 4	4.1	1990 12 31	75	147	21	54	373	359	0

TABLE 8

G:H	M_{MAX}	TIME	N_1	N_2	L_1	L_2	Z_1	Z_2	B
0: 0	4.8	1971 7 1	7	14	-	-	173	169	1
0: 0	4.2	1971 12 31	10	25	-	-	184	189	1
0: 0	4.3	1972 6 30	15	37	-	-	199	207	0
0: 0	4.9	1972 12 30	22	48	-	-	241	241	1
0: 0	4.2	1973 7 1	28	56	-	-	251	254	1
0: 0	5.4	1973 12 30	31	62	-	-	278	274	3
0: 0	4.2	1974 7 1	33	67	-	-	280	278	3
0: 0	4.9	1974 12 31	38	79	-	-	304	298	2
1: 1	5.4	1975 7 1	41	89	-	-	328	316	31*
1: 1	5.1	1975 12 31	47	97	-	-	354	336	31*
1: 1	5.2	1976 6 30	53	105	-	-	375	358	4
1: 1	5.0	1976 12 30	57	116	-	-	384	362	4
1: 1	4.0	1977 7 1	53	108	-	-	372	352	1
1: 1	4.3	1977 12 30	54	104	44	80	373	353	7
1: 1	4.5	1978 7 1	54	102	41	70	376	356	7
0: 0	4.6	1978 12 31	51	96	33	57	367	348	3
0: 0	4.1	1979 7 1	48	94	27	52	366	345	3
0: 0	5.1	1979 12 31	52	96	30	52	364	346	2
0: 0	5.1	1980 6 30	63	107	41	62	387	369	7
1: 1	6.0	1980 12 30	66	111	44	61	398	375	16*
1: 1	5.3	1981 7 1	78	120	53	66	405	389	36*
1: 1	5.3	1981 12 30	79	121	52	65	401	388	36*
1: 1	4.3	1982 7 1	80	120	51	62	388	378	2
1: 1	4.8	1982 12 31	82	119	52	58	395	384	2
1: 1	5.0	1983 7 1	84	123	54	62	403	391	3
1: 1	4.6	1983 12 31	87	129	56	66	405	392	9*
1: 1	5.1	1984 6 30	92	136	60	71	416	403	25*
4: 6	5.1	1984 12 30	99*	150*	66*	86	431*	416*	25*
4: 7	5.3	1985 7 1	105*	162*	72*	97*	445*	428*	13*
4: 7	4.8	1985 12 30	103*	163*	68*	97*	442*	425*	13*
4: 7	4.1	1986 7 1	94*	157*	55	87*	424*	408*	1
4: 7	4.1	1986 12 31	87	149	45	75	408	394	0
4: 7	4.9	1987 7 1	77	136	32	57	389	376	2
4: 7	4.1	1987 12 31	74	134	28	54	375	365	2
4: 7	4.6	1988 6 30	72	135	25	55	384	370	1
3: 5	4.6	1988 12 30	71	133	23	52	375	365	1
0: 0	4.3	1989 7 1	71	134	23	52	371	362	1
0: 0	4.5	1989 12 30	67	128	18	44	369	359	1
0: 0	4.7	1990 7 1	63	126	12	41	358	349	5
0: 0	4.5	1990 12 31	57	118	4	27	334	330	5

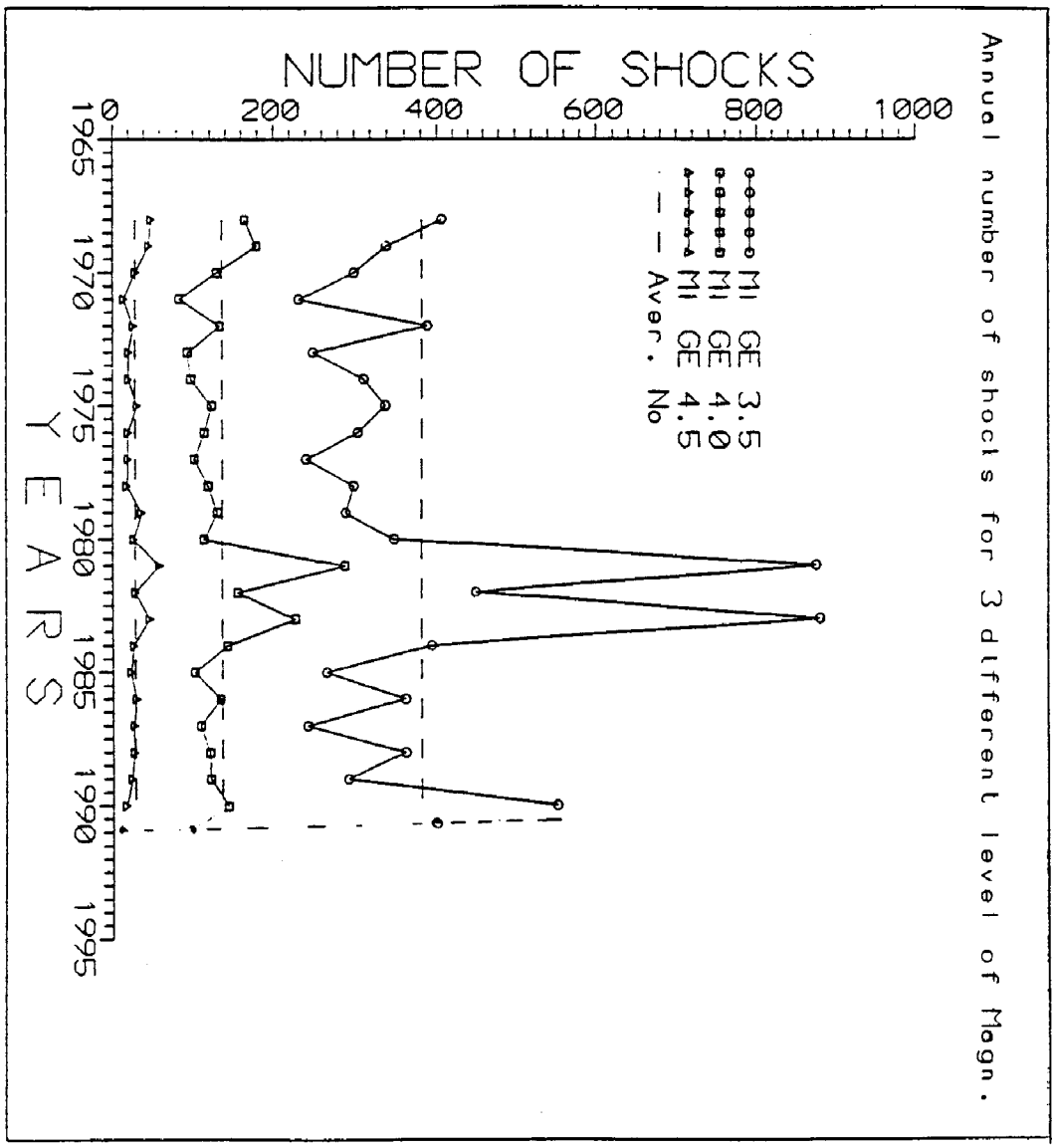
Annual number of shocks for 3 different level of Magn.
NUMBER OF SHOCKS
0
200
400
600
800
1000
1965
1970
1975
1980
1985
1990
1995
YEARS
MI GE 3.5
MI GE 4.0
MI GE 4.5
Aver. No

Fig. I

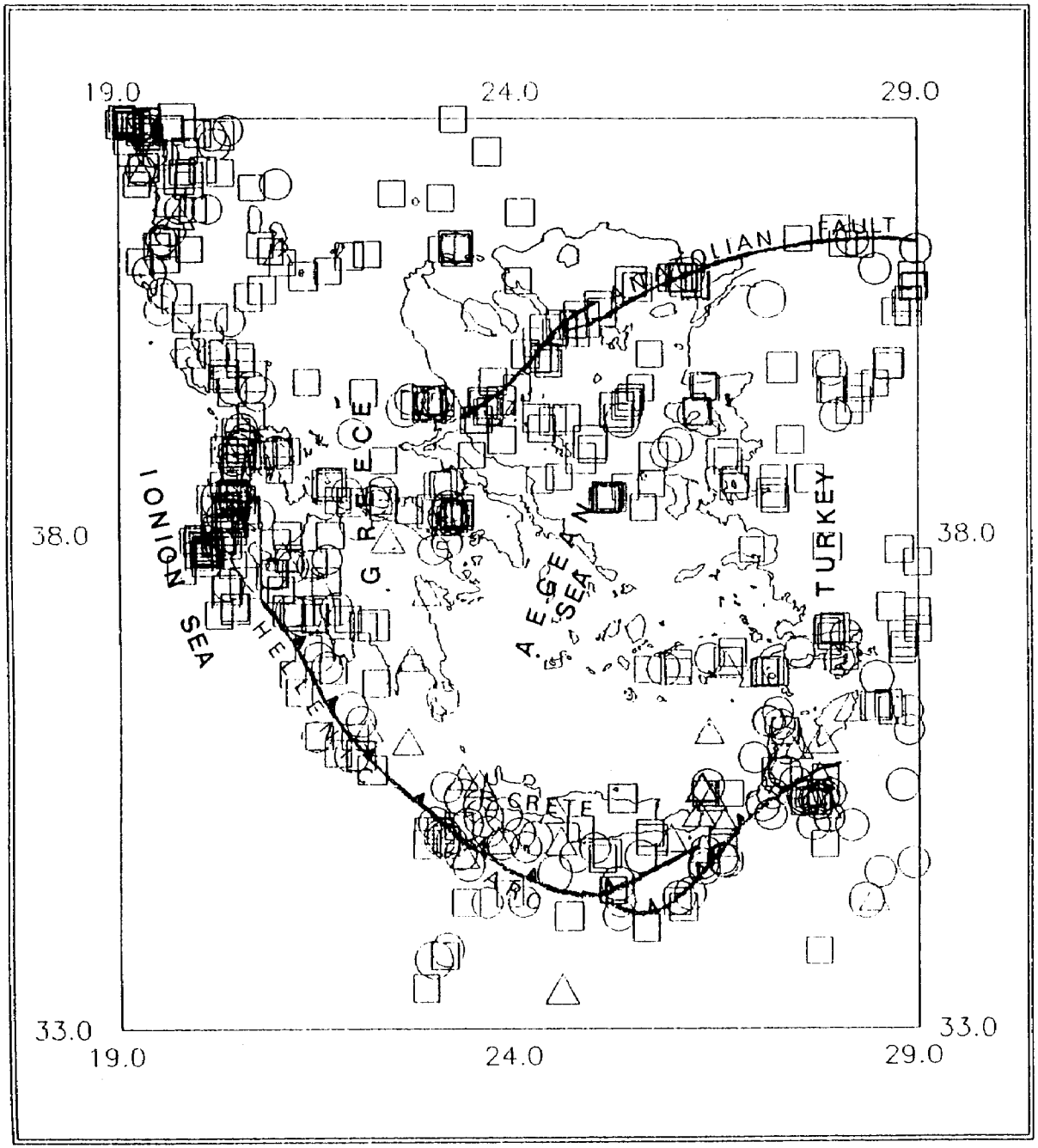

Epicenters with $M_L \geq 4.5$

529 Events

Scale 1 : 3000000

Depth(km)

□ < 30

○ 30 <and< 60

△ 60 <

M= 7.0

M= 6.0

M= 5.0

M= 4.0

0 200

km

Fig. 1

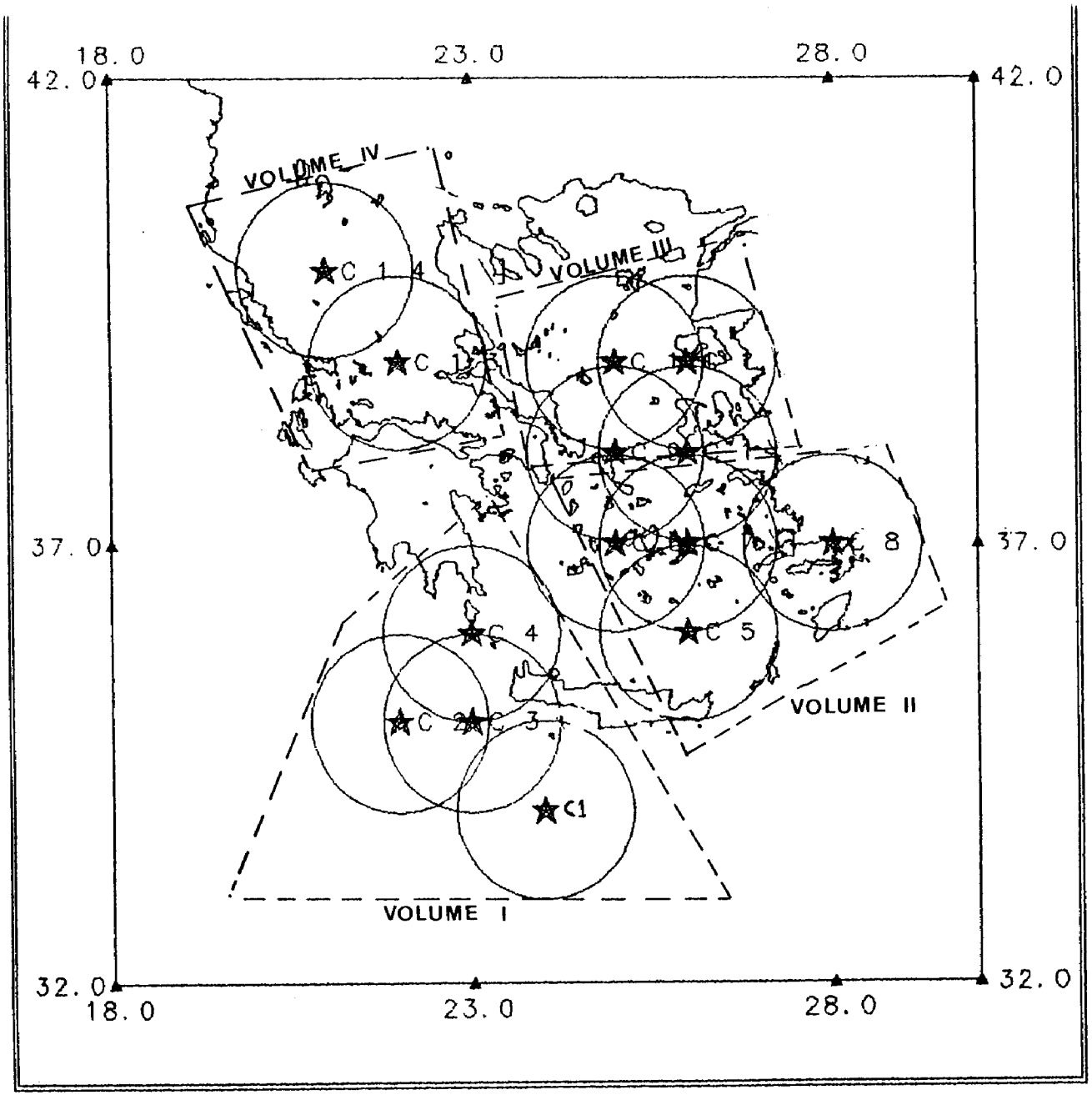

Fig. 2

Scale 9000000

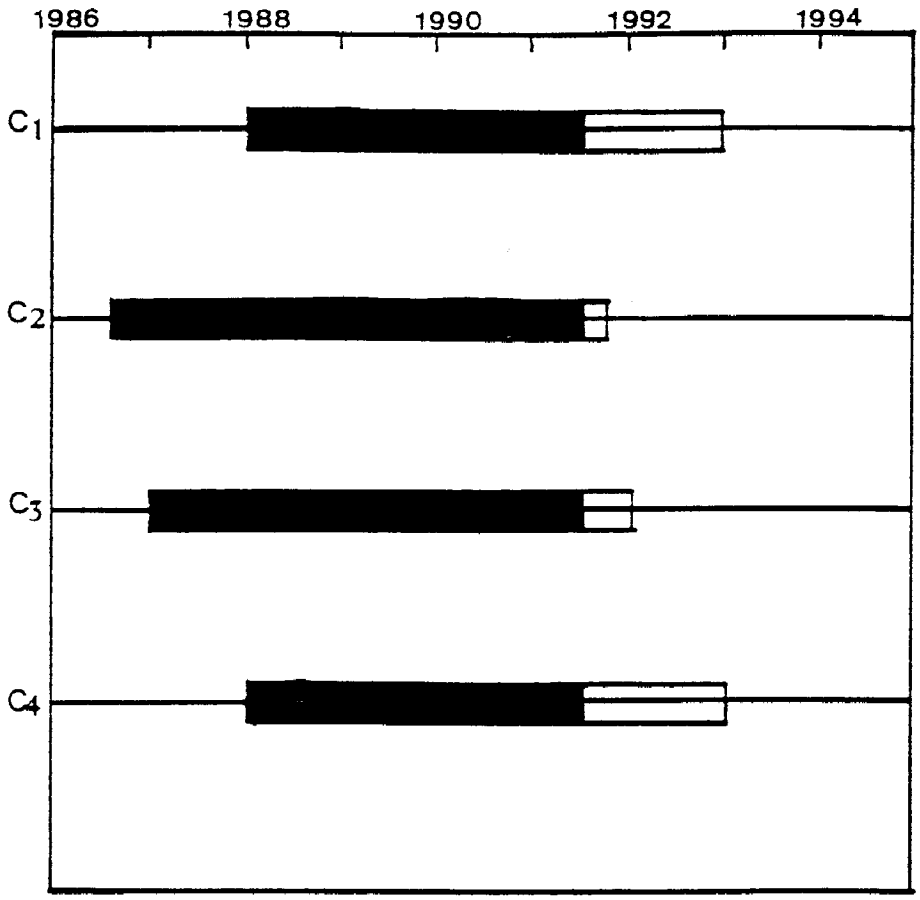

(a)

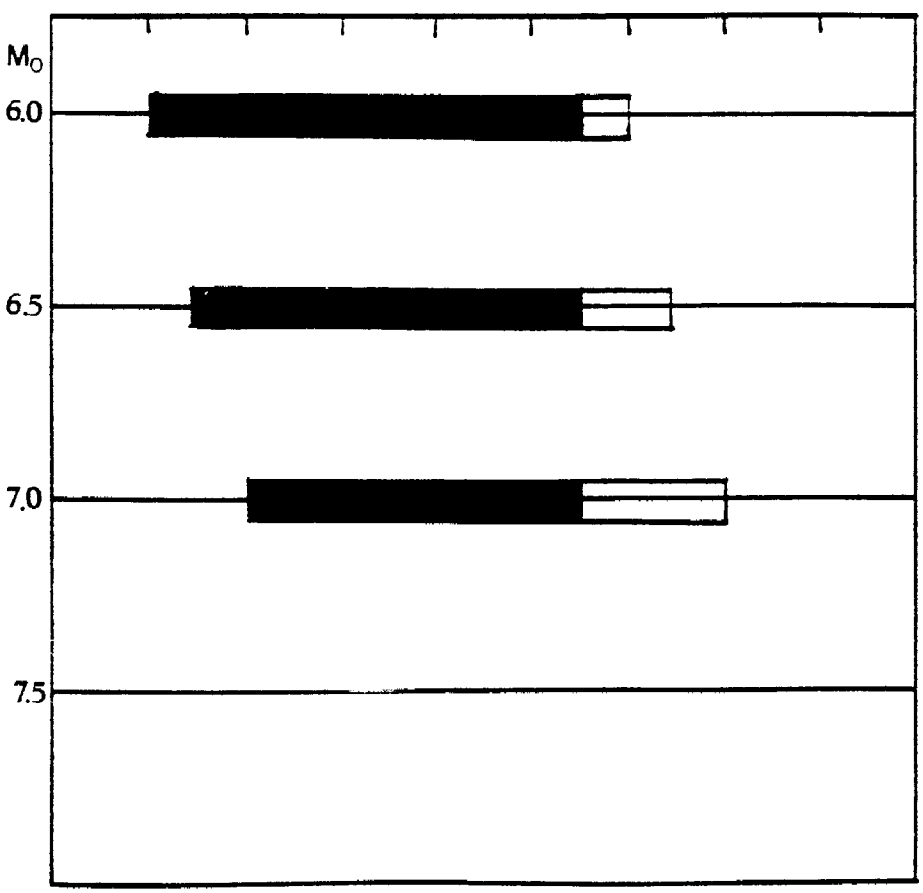

(b)

Figure 3

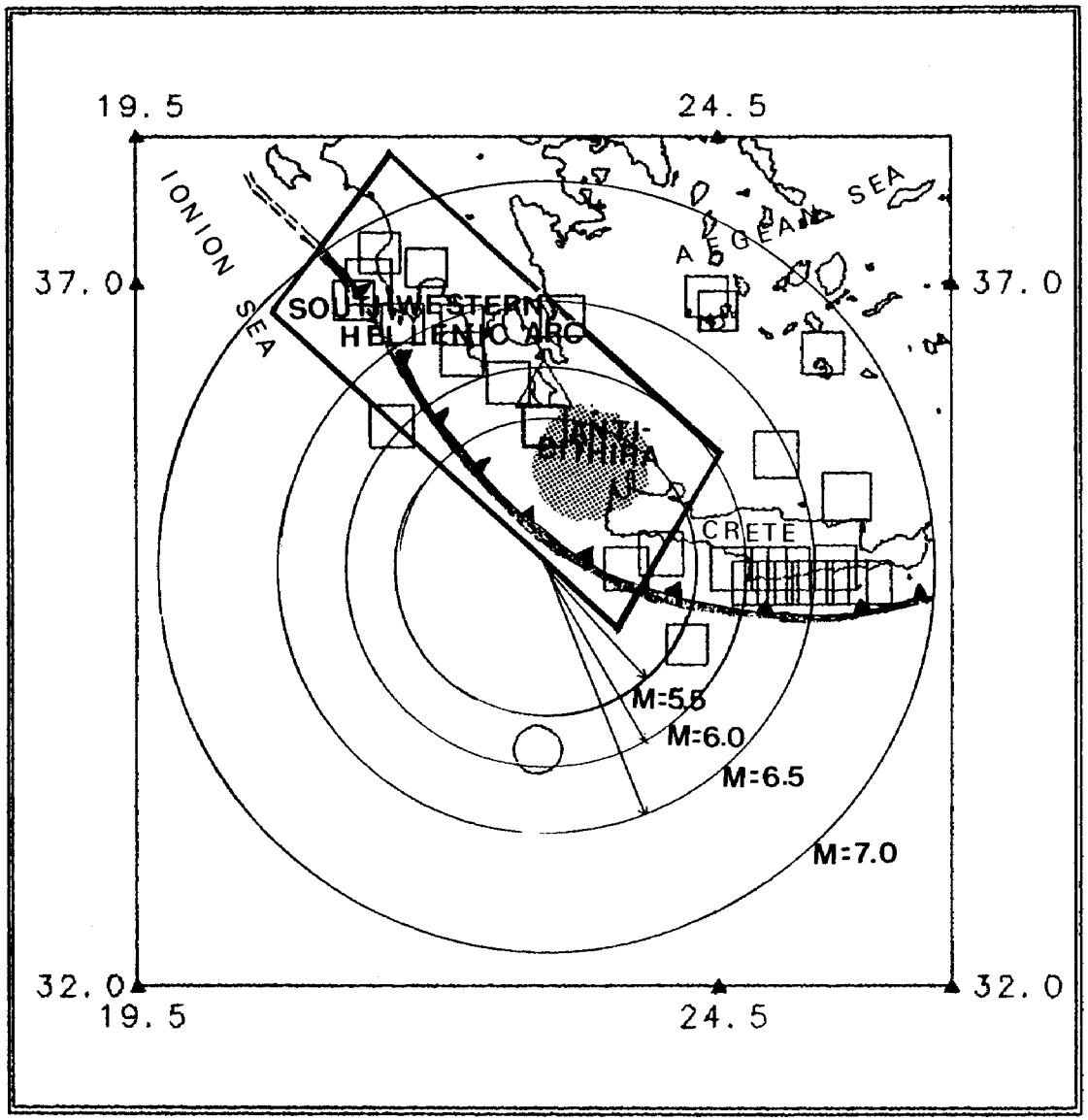

34 Events

Scale 1:700000

Fig. 4

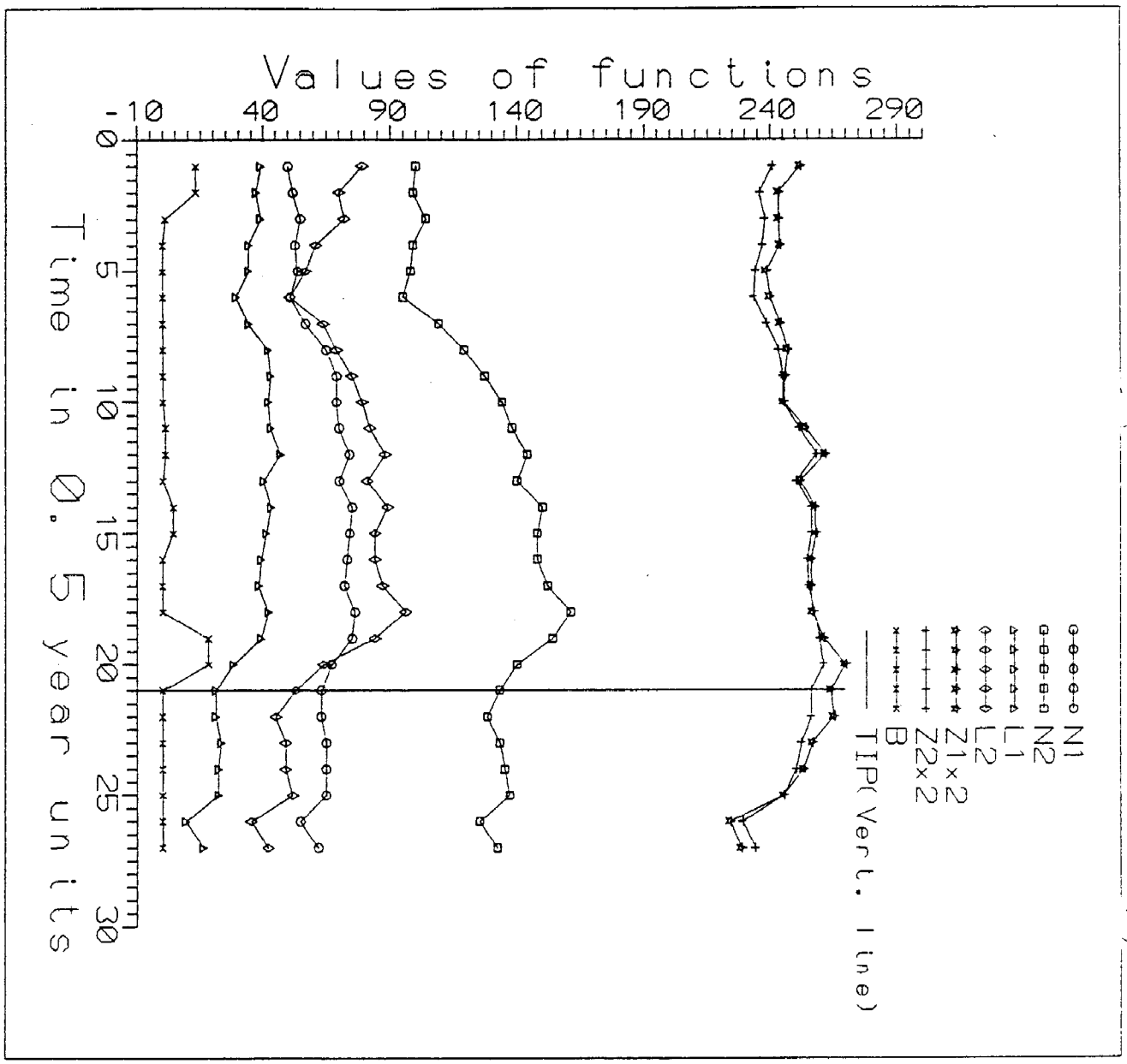
Values of functions
-10
40
90
140
190
240
290
0
5
10
15
20
25
30
Time in 0.5 year units
N1
N2
L1
L2
Z1x2
Z2x2
B
TIP(Vert. line)

Fig. 5

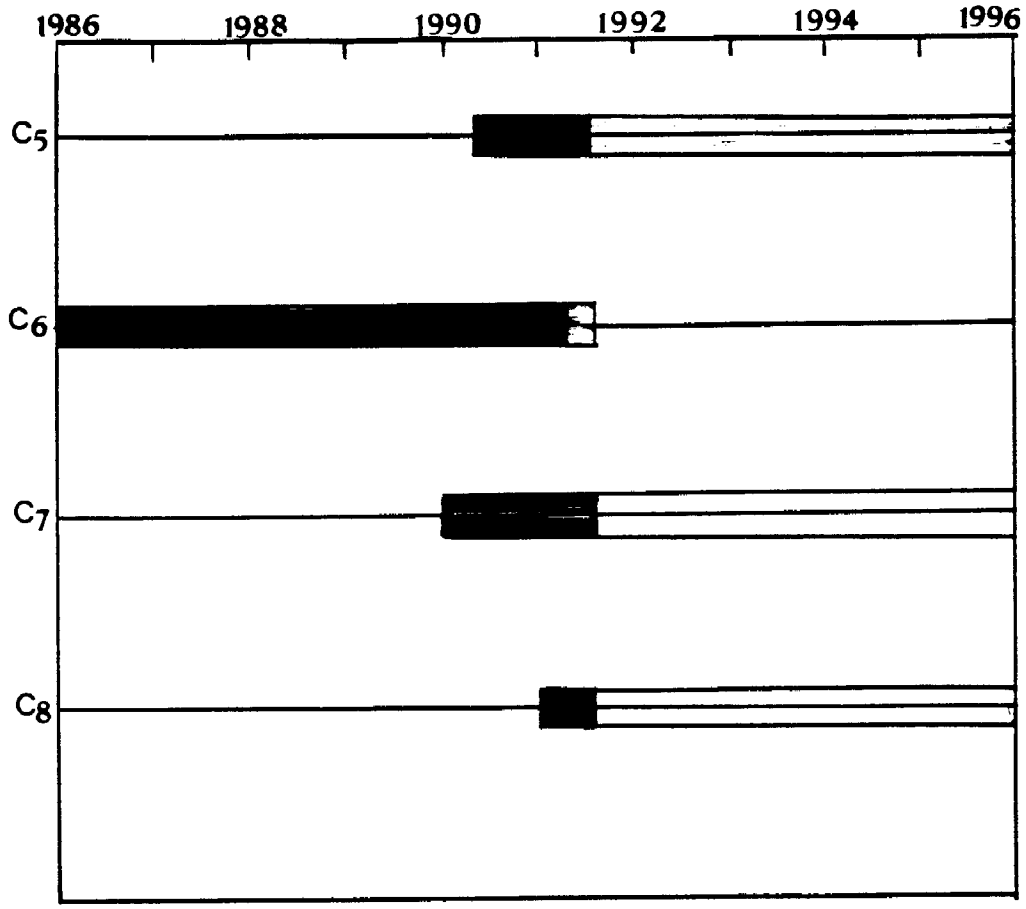

(a)

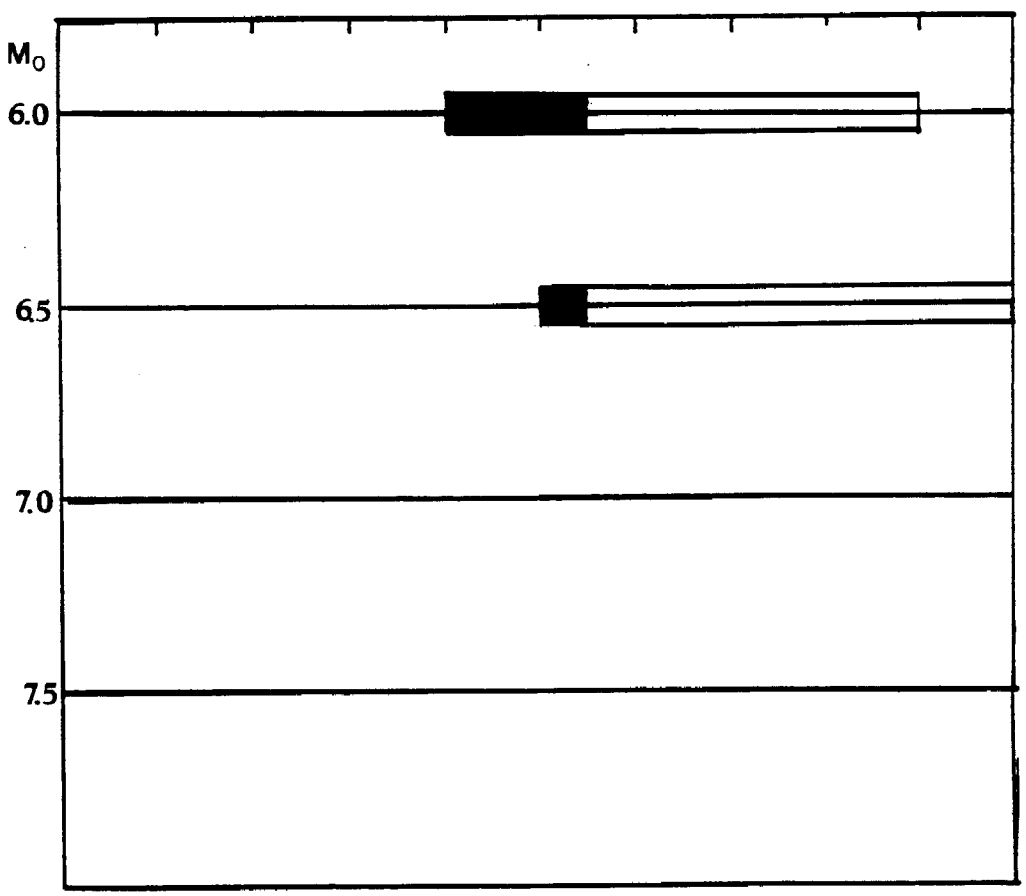

(b)

Figure 6

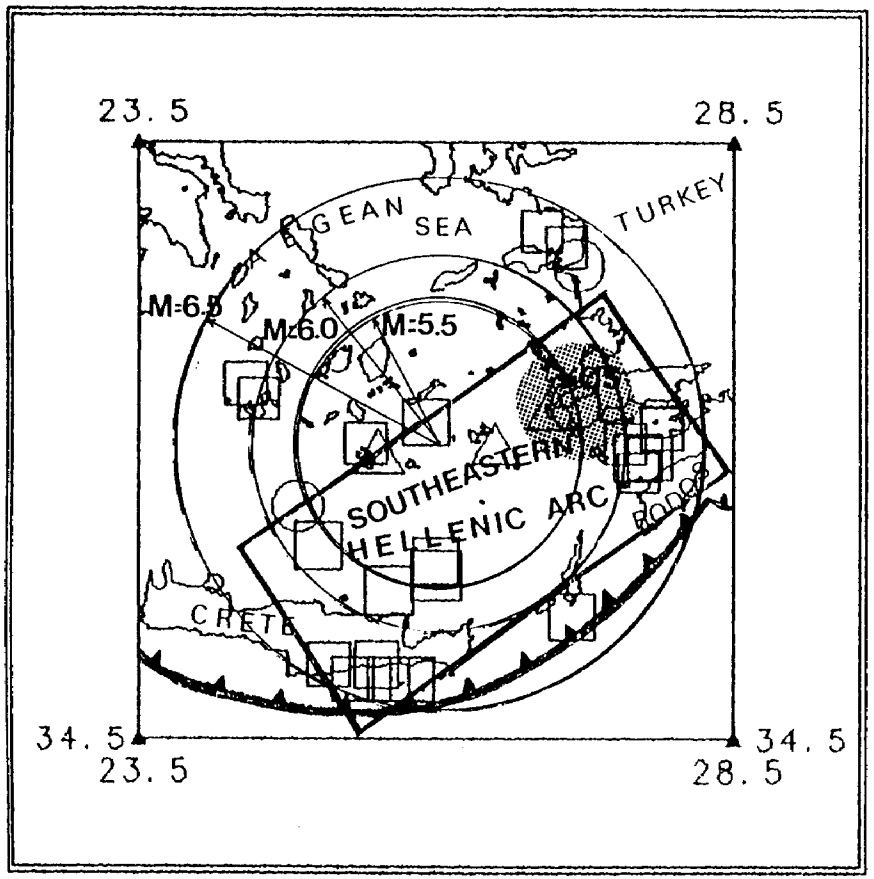

27 Events
Scale 1:7000000

Depth (km)
□ < 30
○ 30 < and < 70
△ 70 <

M= 9.0
M= 8.0
M= 7.0
M= 6.0

0 200
km

Fig. 7

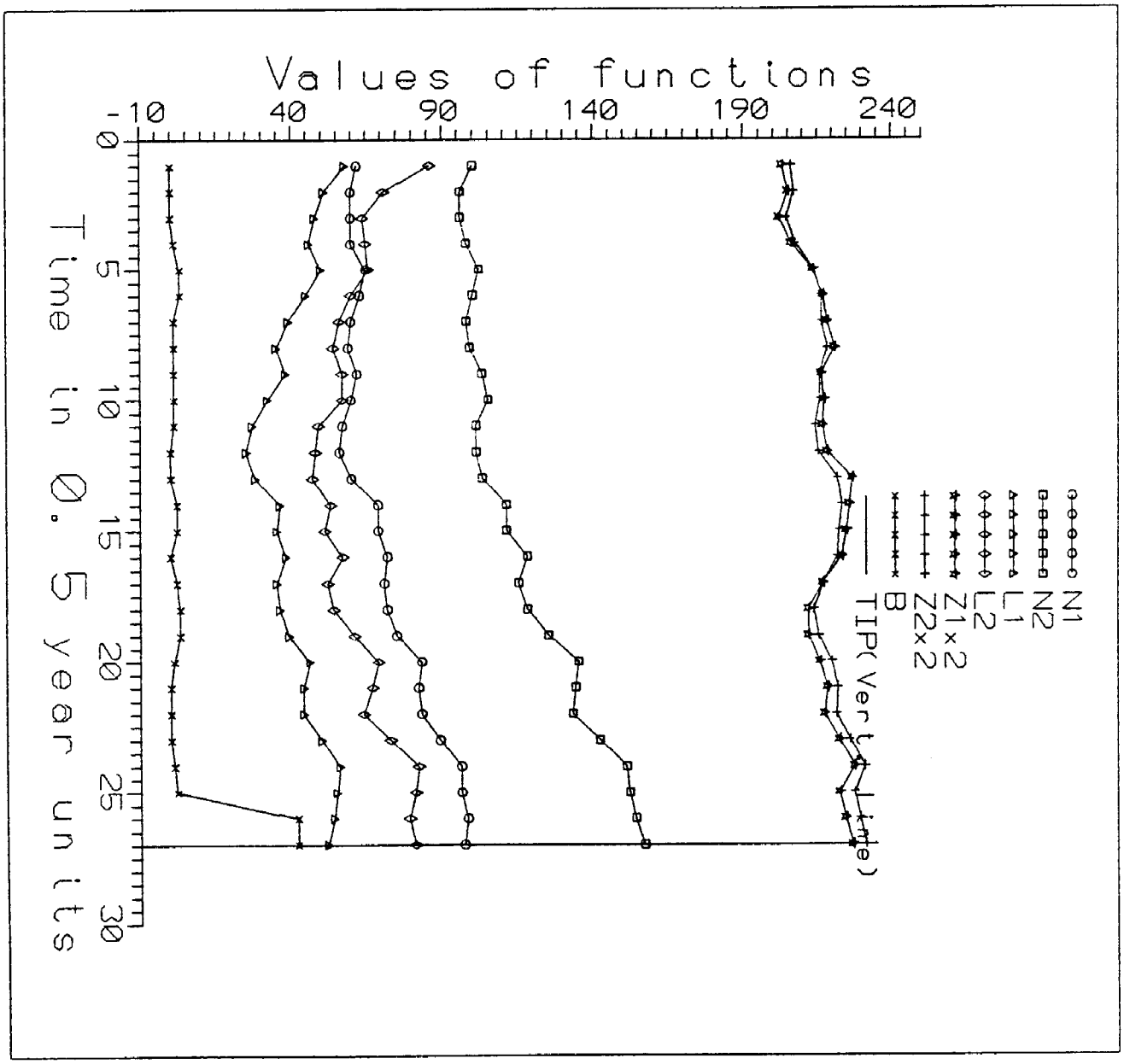
Values of functions
-10
40
90
140
190
240
0
5
10
15
20
25
30
Time in 0.5 year units
N1
N2
L1
L2
Z1x2
Z2x2
B
TIP(Vertical line)

Fig. 8

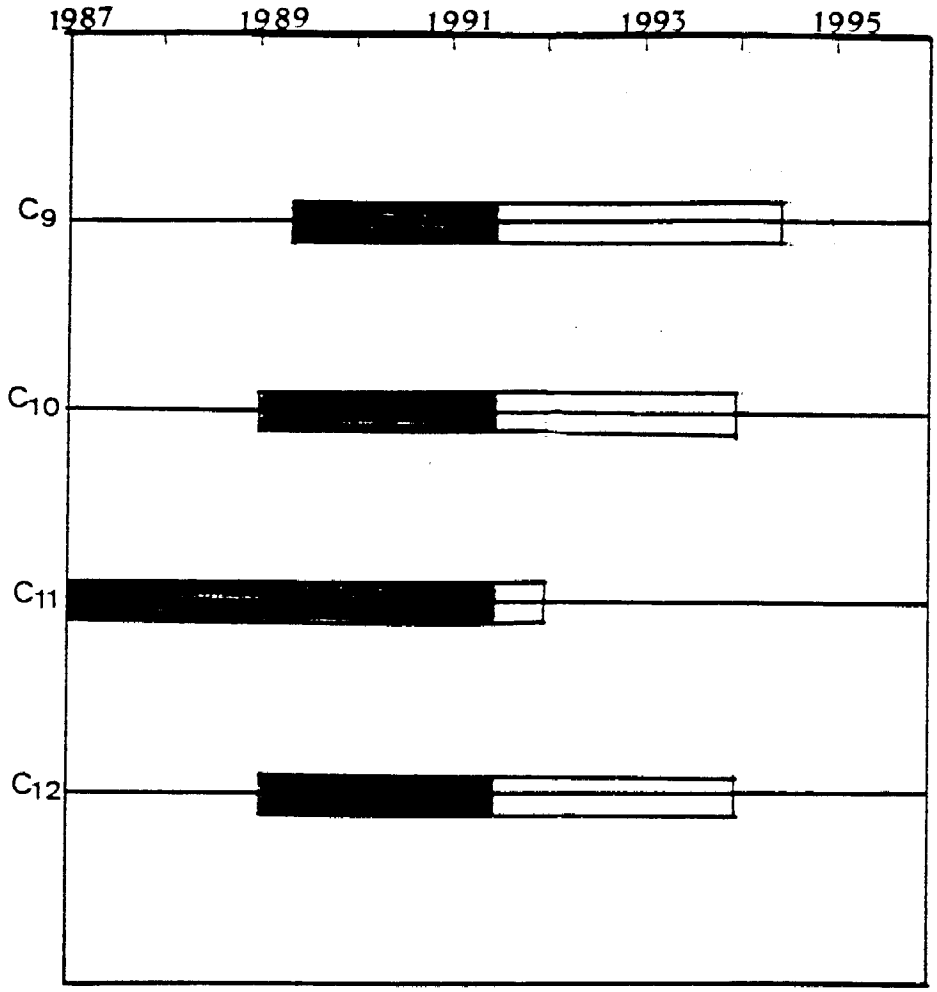

(a)

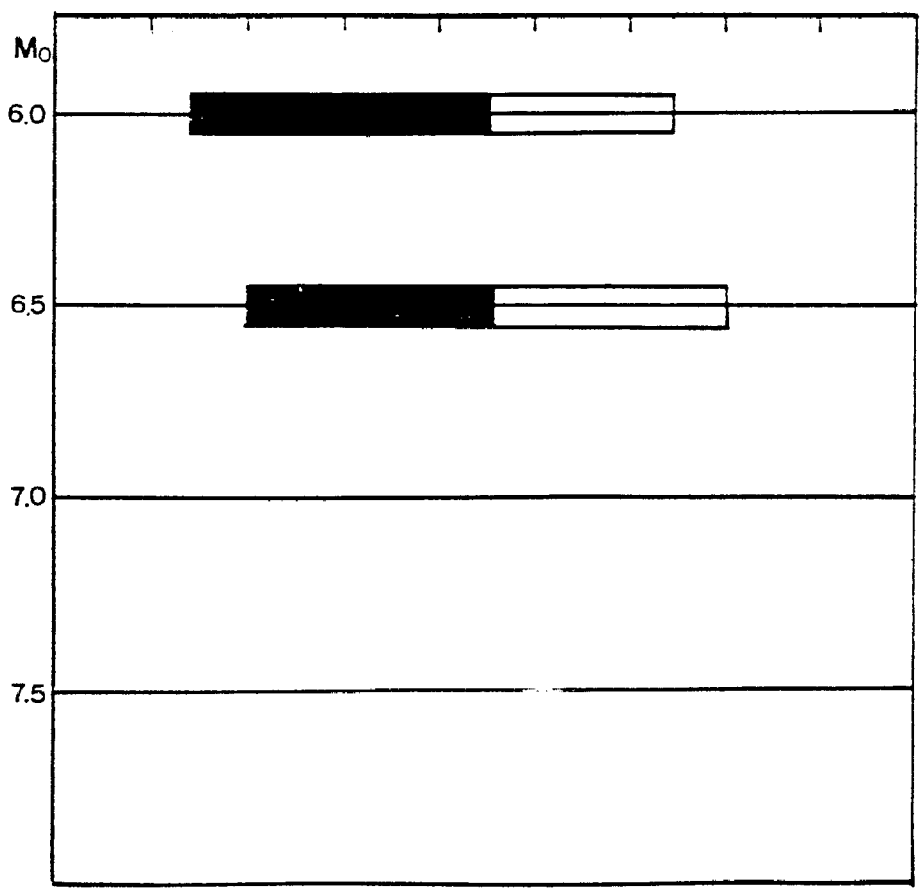

(b)

Figure 9

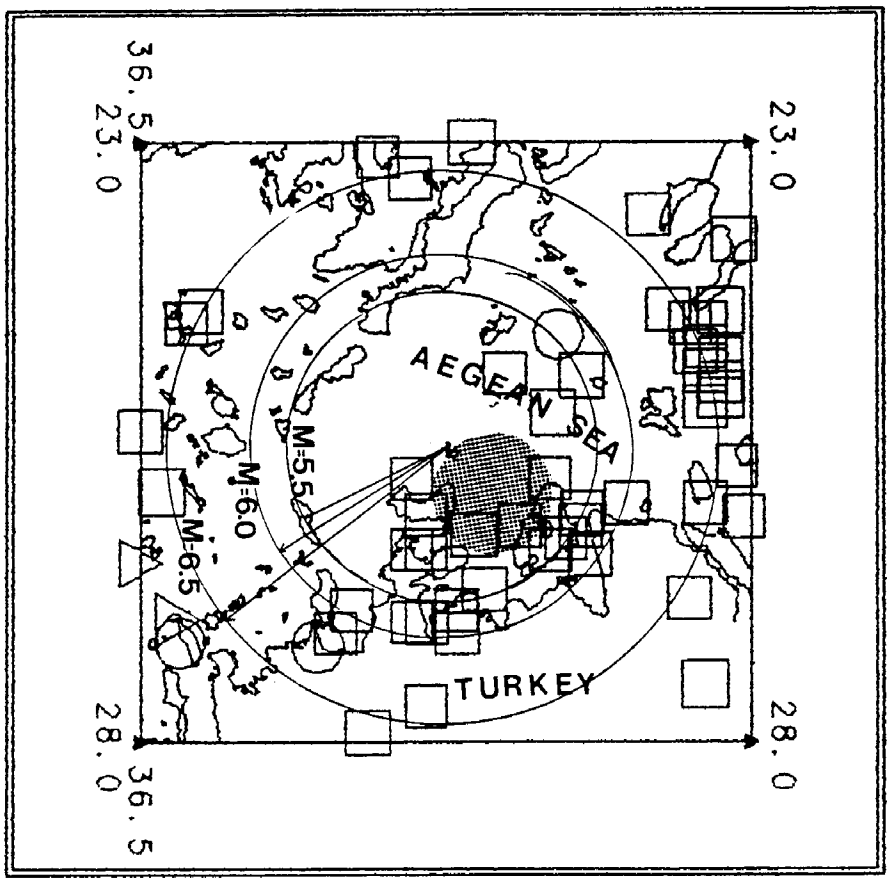
36.5
23.0
23.0
28.0
28.0
36.5
AEGEAN SEA
TURKEY
M=5.5
M=6.0
M=6.5

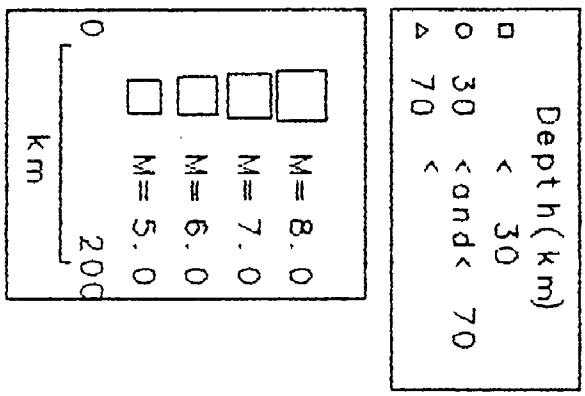
Depth(km)
< 30
30 <and< 70
70 <
M= 8.0
M= 7.0
M= 6.0
M= 5.0
0
200
km

Fig. 10

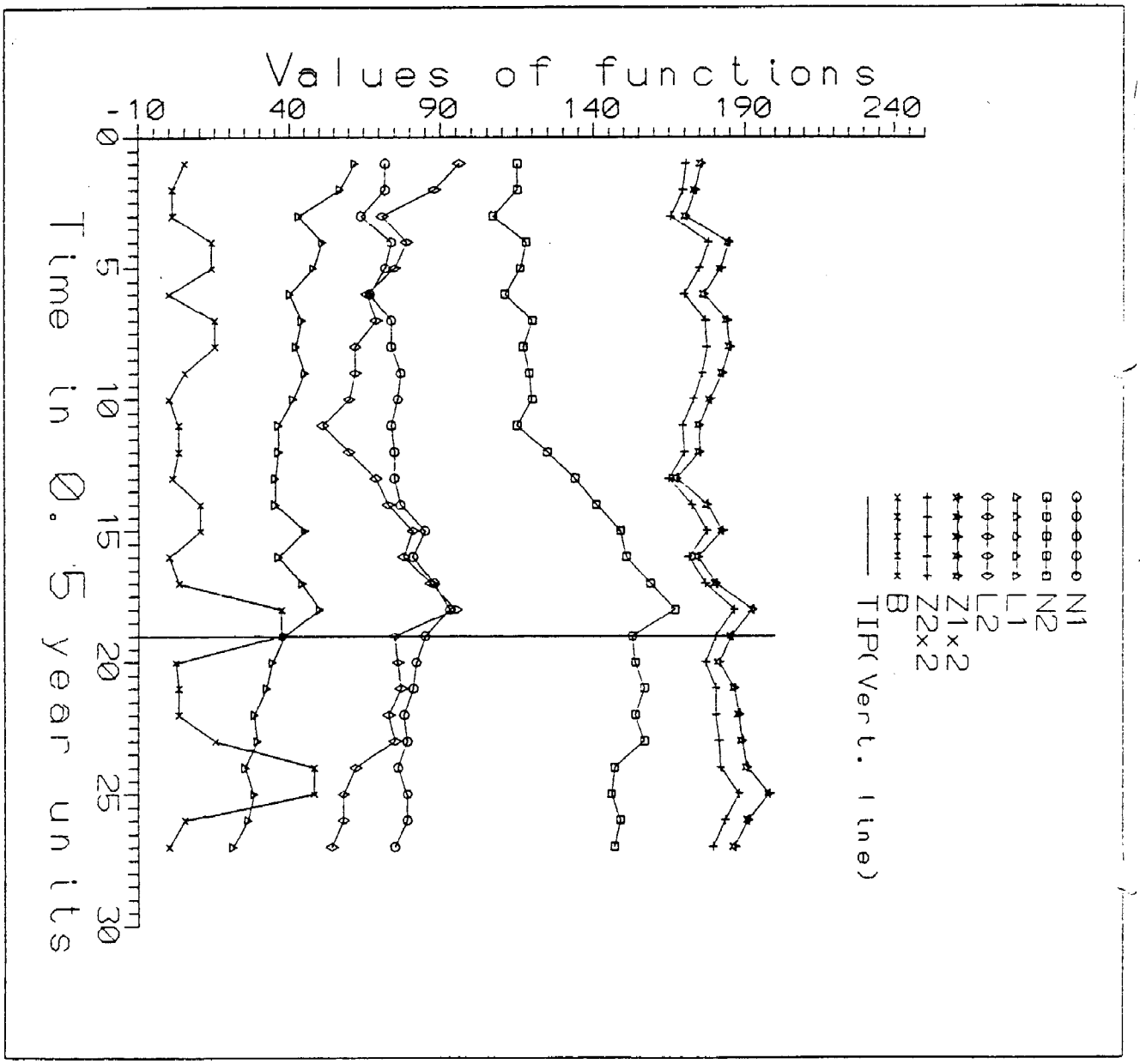
Values of functions
-10
40
90
140
190
240
0
5
10
15
20
25
30
Time in 0.5 year units
N1
N2
L1
L2
Z1x2
Z2x2
B
TIP(Vert. line)

Fig. 11

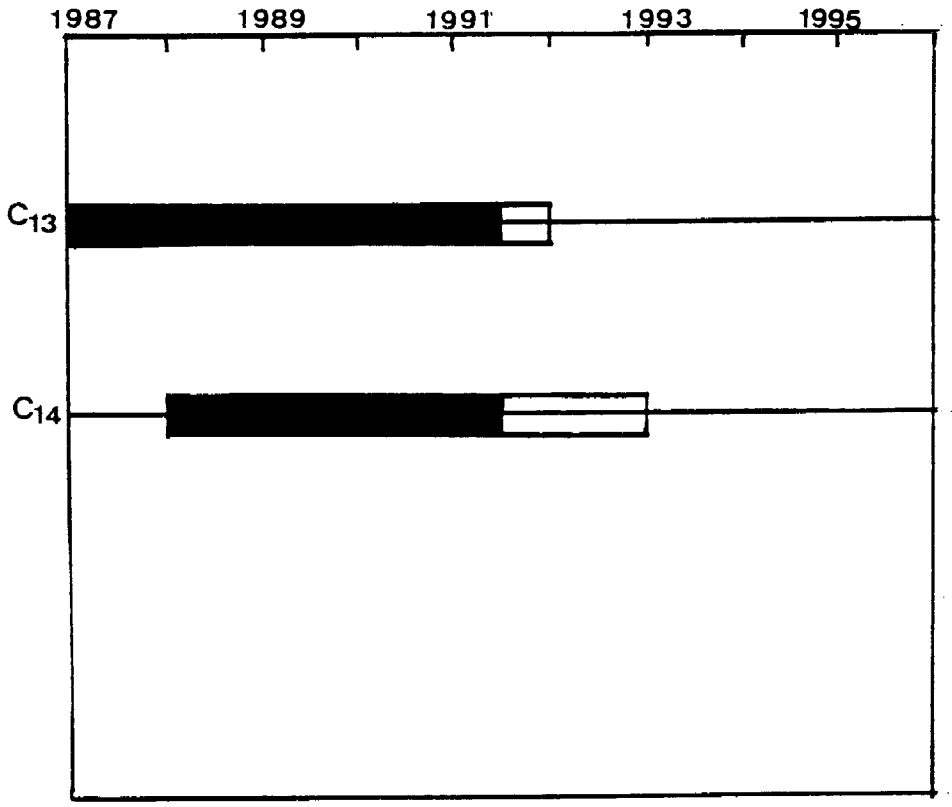

(a)

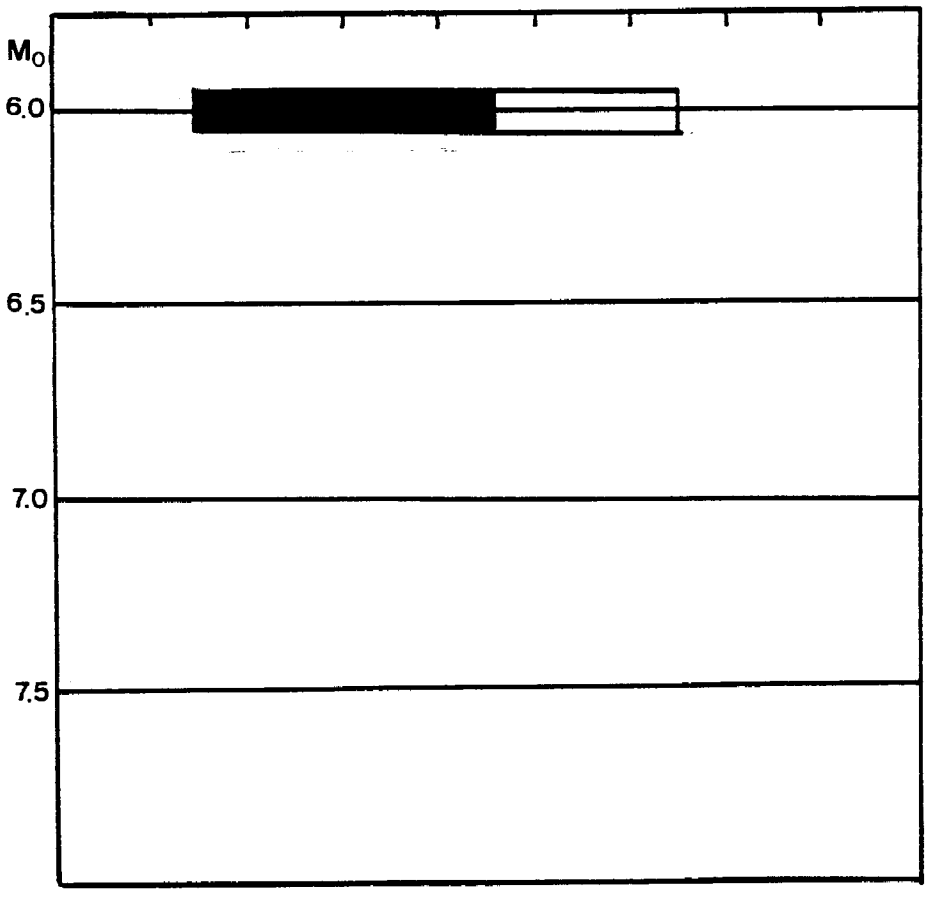

(b)

Figure 12

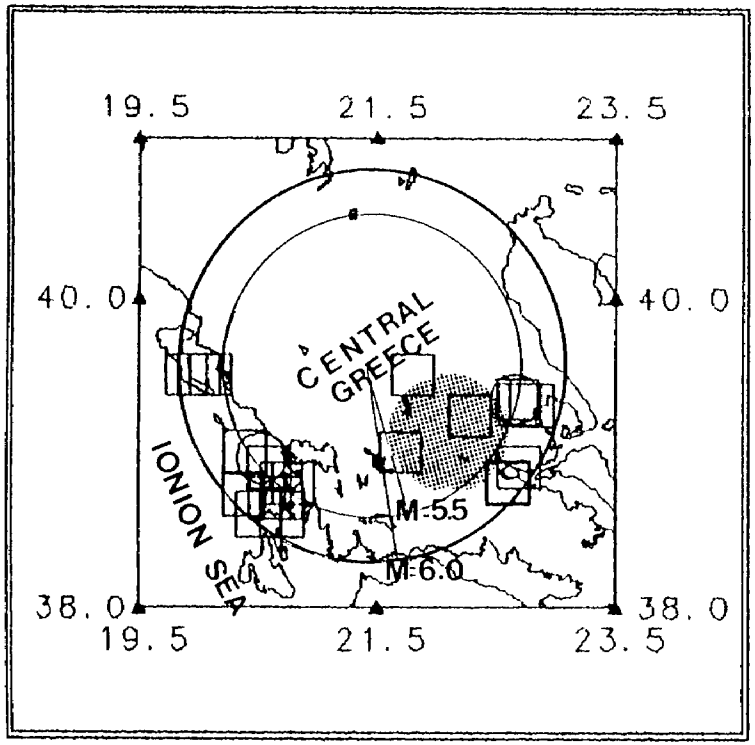

25 Events
Scale 1:7000000

Depth(km)
□ < 30
○ 30 < and < 70
△ 70 <

M= 7.0
M= 6.0
M= 5.0
M= 4.0
0 200
km

Fig. 13

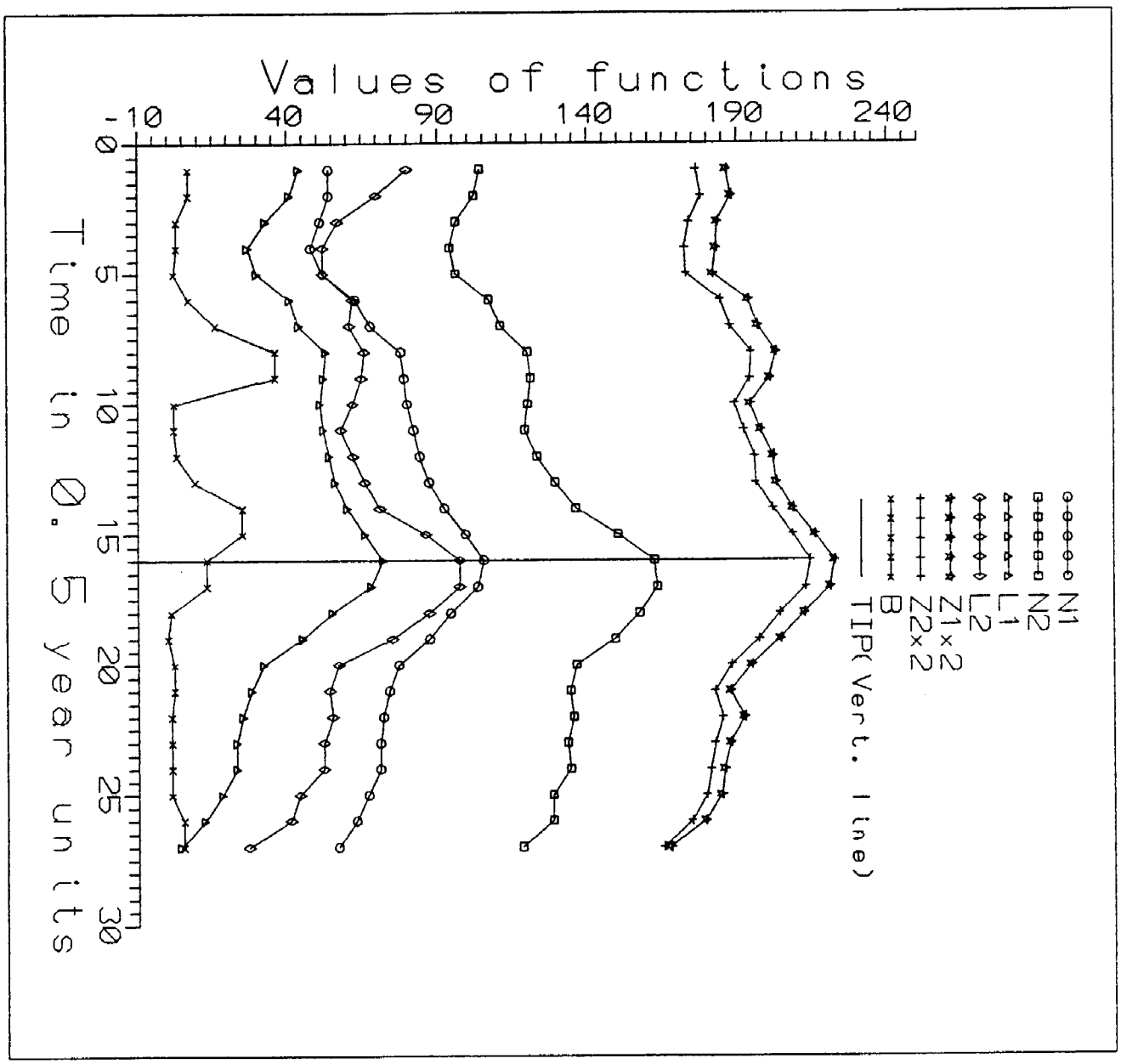
Values of functions
-10
40
90
140
190
240
0
5
10
15
20
25
30
Time in 0.5 year units
N1
N2
L1
L2
Z1x2
Z2x2
B
TIP(Vert. line)

Fig. 14

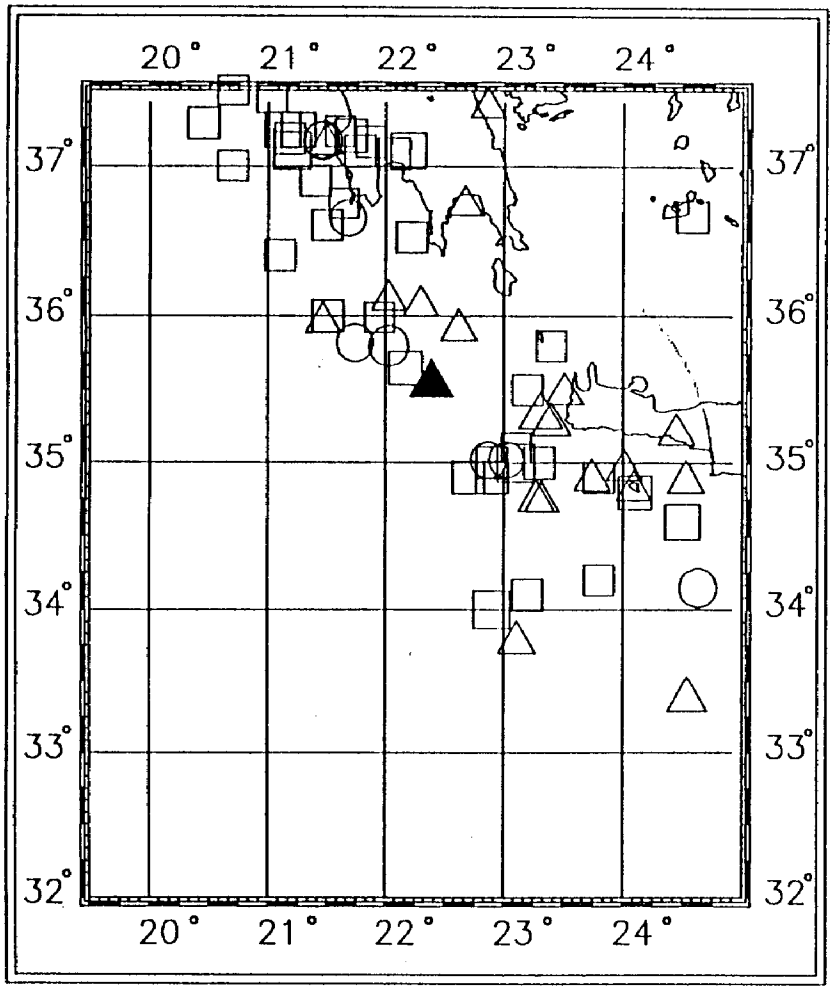

65 Events

Scale 1: 7000000

Depth(km)

□ < 10

○ 10 <and< 30

△ 30 <

□ M= 6.0

□ M= 5.0

□ M= 4.0

□ M= 3.0

0 200

Km

Fig. 15

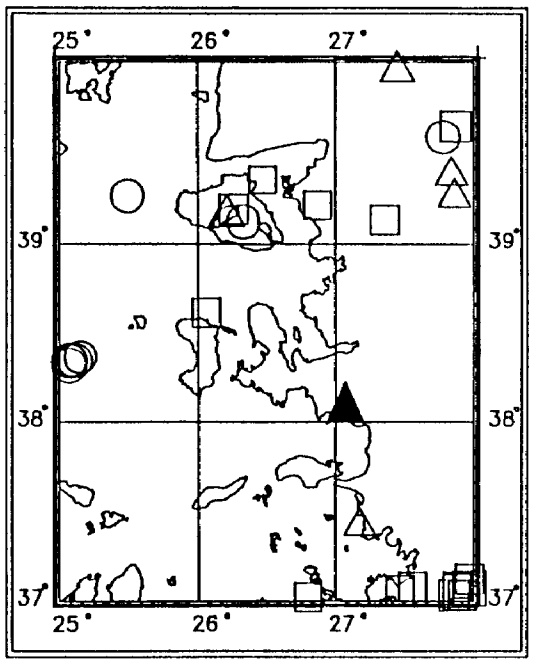

28 Events
Scale 1: 6000000

Depth(km)
□ < 10
○ 10 <and< 30
△ 30 <

M= 6.0
M= 5.0
M= 4.0
M= 3.0
0 100
Km

Fig. 16

INTERMEDIATE EARTHQUAKE PREDICTION IN CENTRAL GREECE

by

J. LATOUSSAKIS and G.N. STAVRAKAKIS

The method described in the previous paper has been applied to the area of Central Greece (Thessalia) in order to diagnose current TIPs or not.

For that purpose, the earthquake catalog of the Geodynamic Institute of the National Observatory of Athens was used for the time period 1972 - 1993. The catalogue includes 15.934 events of magnitude Ms in the range 3.5 to 7.6, that occurred in the area 23^0-42^0 N and 19^0-29^0 E. For this range of magnitute the catalogue is complete, especially for the investigated area of central Greece, as indicated in the figures 1 to 3.

For the compilation of the catalogue of the main shocks we remove the aftershocks using the spatial and the magnitude limits as summarized in the table 1.

TABLE 1: Criteria for removing aftershocks from the NOA-catalogue

M	3.5-3.99	3.99-4.4.49	4.99-4.99	4.99-5.49	5.49-5.99	5.99-6.50	6.50-7.60
r(M) KM	10	15	20	30	40	50	80
t(M) DAYS	5	10	20	46	91	183	365

As mentioned above, the algorithm M8 was applied to the area with a centre 39.20-23.20^0 E and radius 2R (Mo) = [exp(Mo-5.6)+1] where Mo equal to 5.5 and 6.0 , and for the time period July 1972 till June 1993.

The obtained results are summarized in Tables 2 and 3. As can be seen in these tables the algorithm indicates posterior TIP for all events occurred in the past in the region of interest. It also shows in both cases current TIPs (cTIP). Figure 4 and 5 illustrate the functions computed by the algorithm M8.

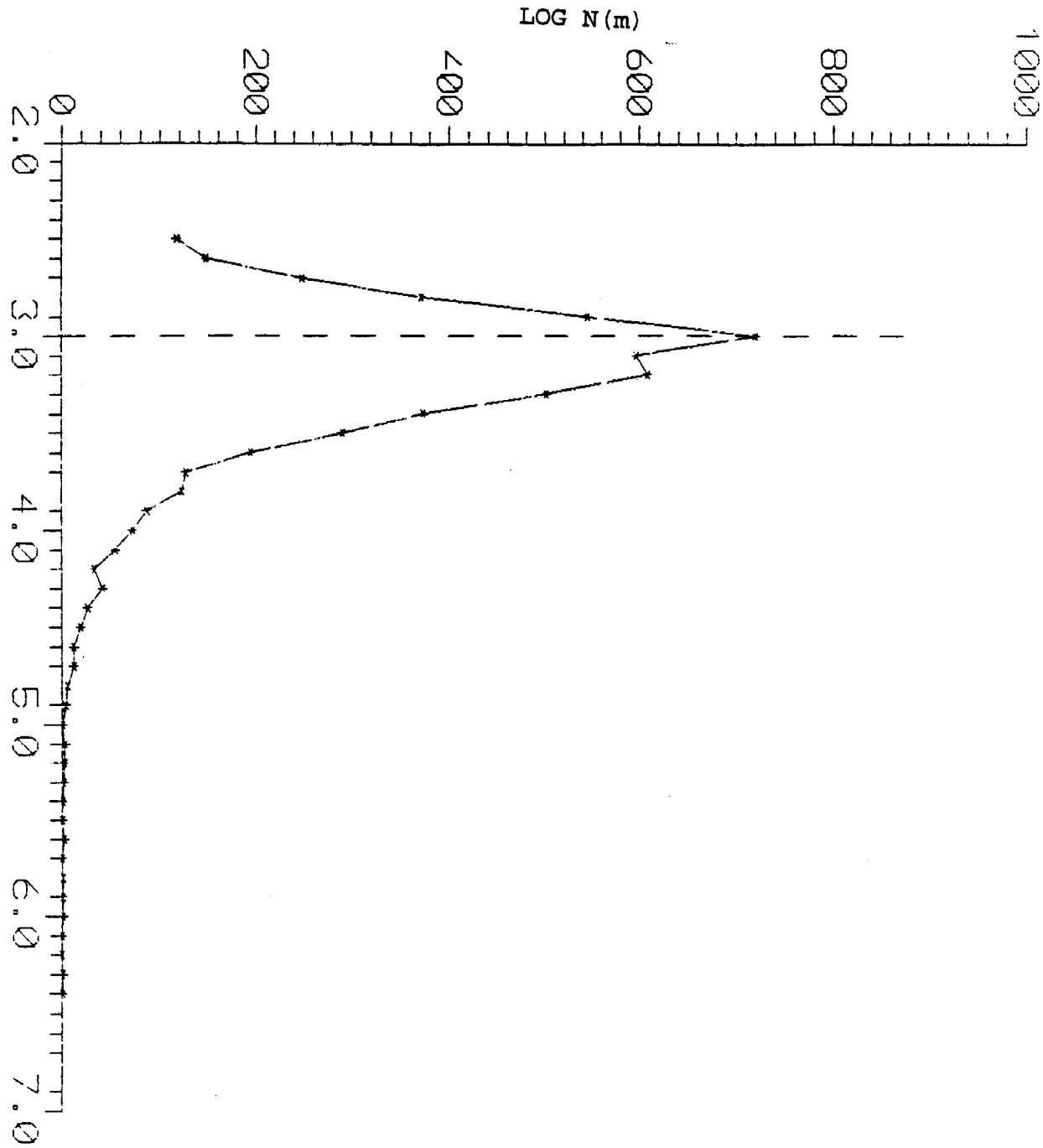

Fig.1: Test of completeness of the NOA's catalogue

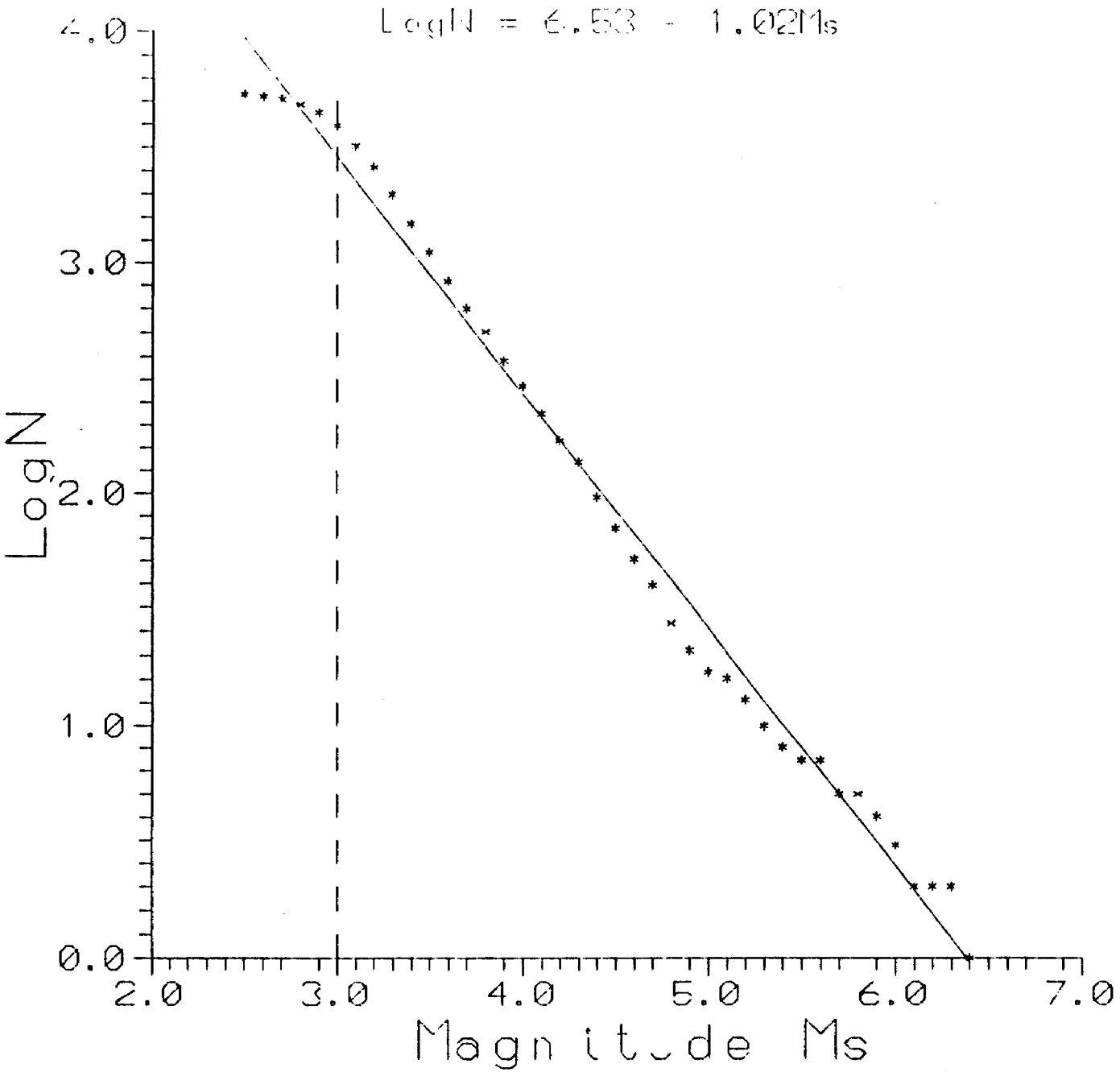

Fig.2: Test of completeness of the NOA's catalogue

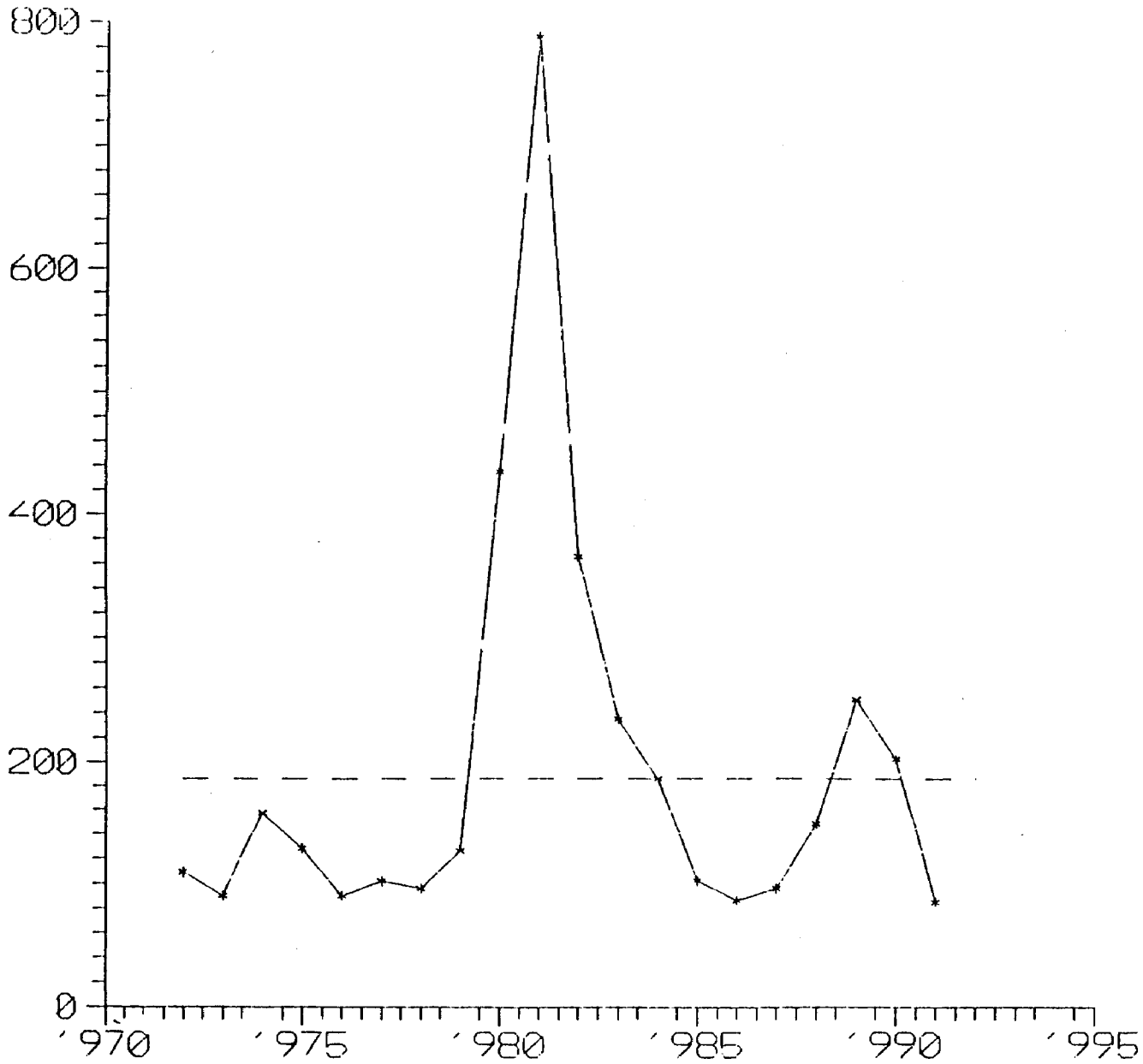

Fig.3: Test of c pleteness of the NOA's catalog

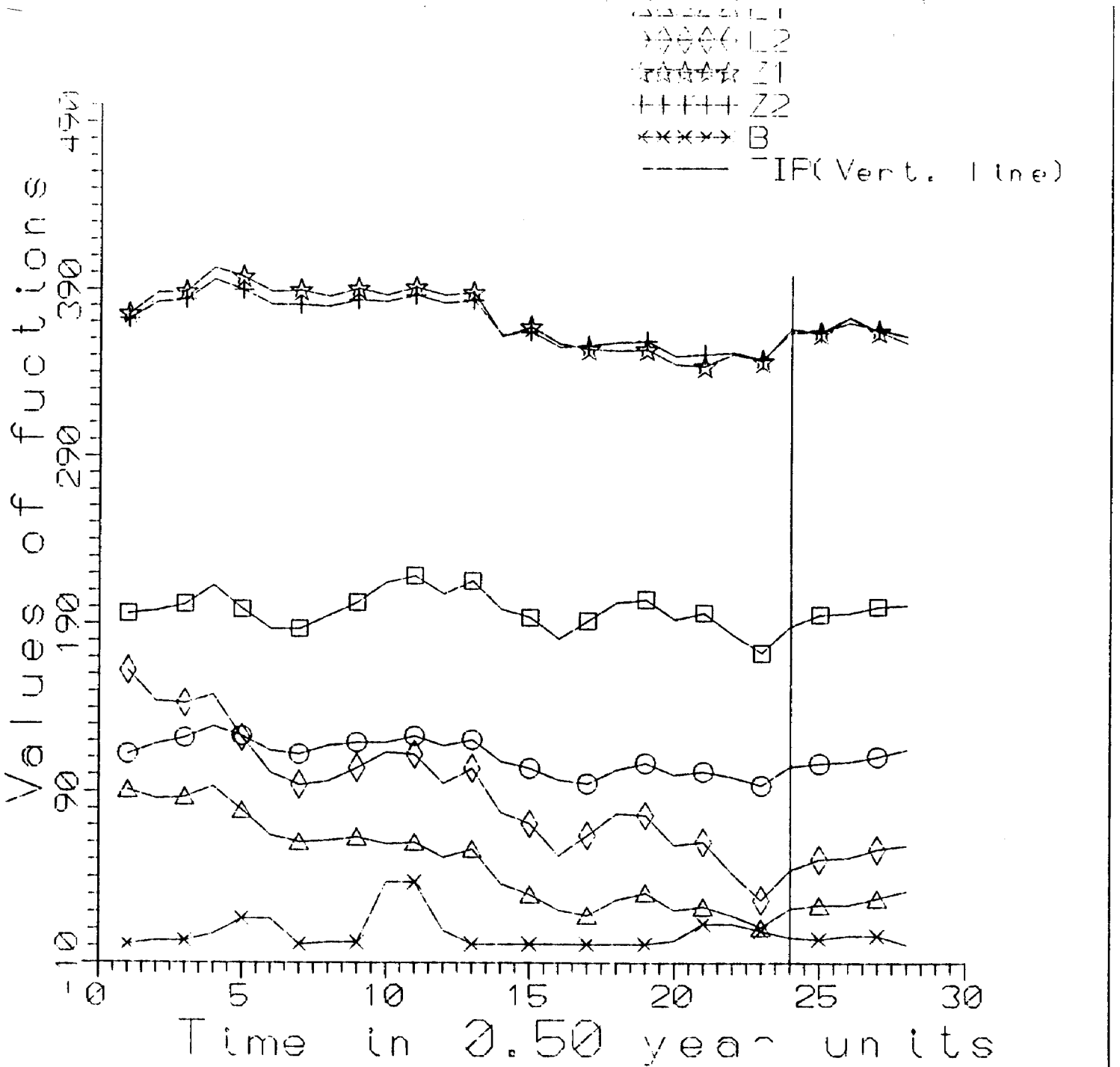

Fig.4: F ctions computed by the algorit M8 for central Greece and

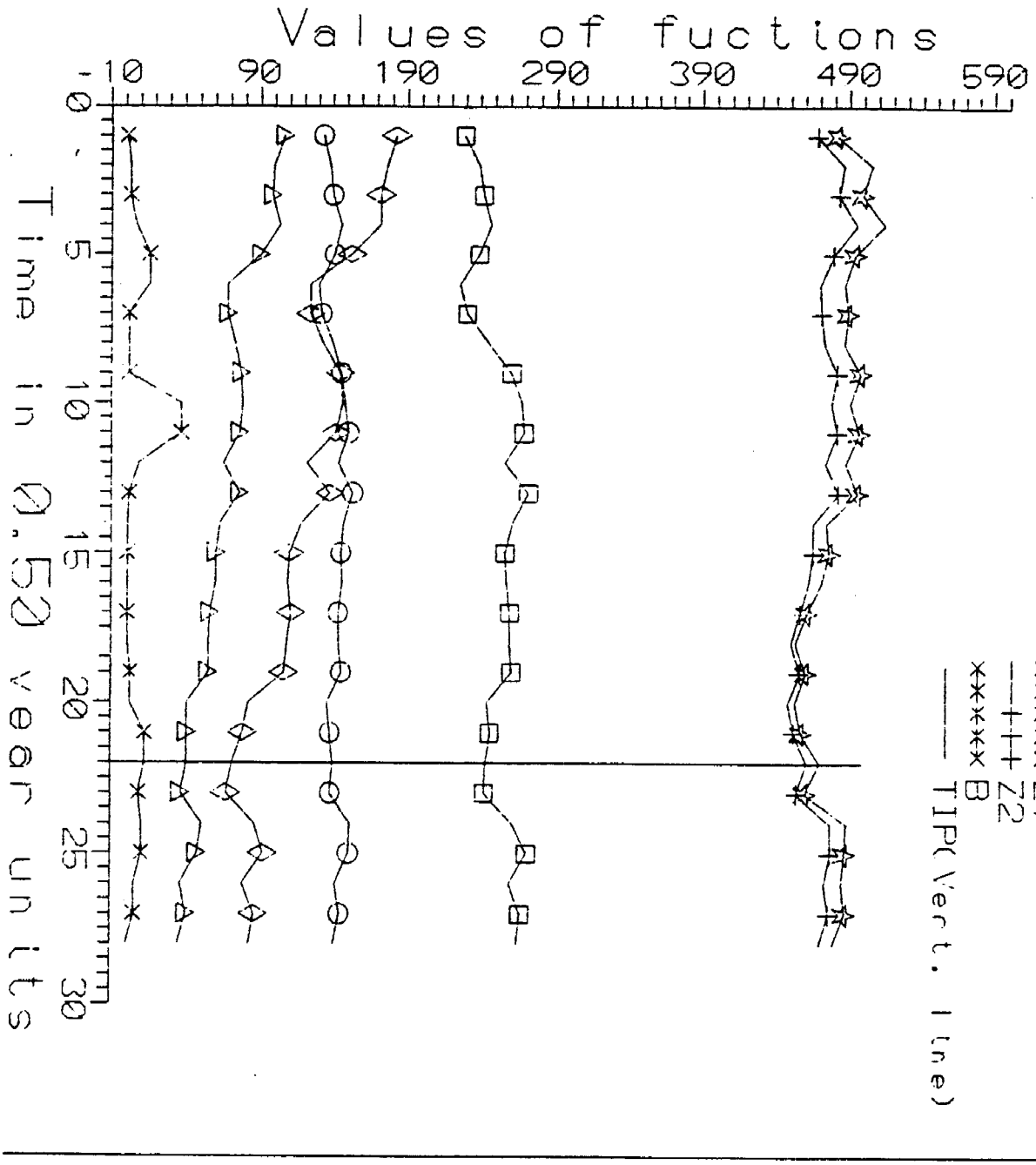

Fig.5: Functions comput) by the algorithm M8 for centr) Greece abd for Mo = 6.0

TABLE 2: Results of the algorithm M8 for the area of central ...
and for Mo = 5.5

```
1. Catalog of main shocks : mawcr.dat          Mo = 5.50
2. Time interval (Tb,Te) = (1972 1992);
    Step in time  dt =  .50000 years
    Activity is estimated in a period from Tb up to Te
    Constants Ma, e are fixed in catalog; alfa = 0
    2*R(Mo) = (exp(Mo-5.6)+1)°
3.   1  circles    R =R(mo) km
No.  lat     lon    T*: ye mo da ; No.  lat     lon    T*: ye mo da :
 1) 39.20    23.20    1972  7  1;
4.  7 functions in the TIP diagnosis
No. func  m    mm     a    aa    s/dt  u/dt  To    beta    d
 1)   n  act          15          12
 2)   n  act          30          12
 3)   l  act          15          12          1972
 4)   l  act          30          12          1972
 5)   s  act  shf     15 0.50     12                  0.46  0.67
 6)   s  act  shf     30 0.50     12                  0.46  0.67
 7)   b  shf  shf   2.00 0.20      2
5. Constants of diagnostics:
  Quantile p = (for b, for others) = ( .25   .10)
  Time window for "simultaneous" extrema lex =  6*dt
  Thresholds (G and H) = (  4    6)
  Alarm duration Tau = 10*dt
Radius of  circles       105 km
Magnitude thresholds in Region No. 1   ( 47 quakes per year )
 1: 3.8010.00;  2: 3.6010.00;  3: 3.8010.00;  4: 3.6010.00;  5: 3.80 5.00;
 6: 3.60 5.00;  7: 3.50 5.29;
    Strong quake: 1980  7  9  2 10 3920  2390   0 570   0 in Region No.  1
    Strong quake: 1980  7  9  2 11 3920  2390   0 650  29 in Region No.  1
    Strong quake: 1980  7  9  2 35 3920  2270   0 610  18 in Region No.  1
    Strong quake: 1985  4 30 18 14 3924  2289  13 580  12 in Region No.  1
    Strong quake: 1989  3 19  5 37 3929  2357  13 580  46 in Region No.  1
stip  1 ( 39.20:  23.20)*(1979  7  1 : 1984  7  1)  4  7  4  7
stip  1 ( 39.20:  23.20)*(1980  7  1 : 1985  7  1)  4  7  4  7
stip  1 ( 39.20:  23.20)*(1982  7  1 : 1987  7  1)  4  7  4  7
stip  1 ( 39.20:  23.20)*(1983  7  1 : 1988  7  1)  4  7  4  7
stip  1 ( 39.20:  23.20)*(1984  7  1 : 1989  7  1)  4  7  4  7
stip  1 ( 39.20:  23.20)*(1986  7  1 : 1991  7  1)  4  7  4  7
stip  1 ( 39.20:  23.20)*(1987  7  1 : 1992  7  1)  4  7  4  7
stip  1 ( 39.20:  23.20)*(1988  7  1 : 1993  7  1)  4  7  4  7
ctip  1 ( 39.20:  23.20)*(1990  7  1 : 1995  7  1)  4  7  4  7
ctip  1 ( 39.20:  23.20)*(1991  7  1 : 1996  7  1)  4  7  4  7
ctip  1 ( 39.20:  23.20)*(1992  7  1 : 1997  7  1)  4  7  4  7
```

Region No. 1	1972	39.20	23.20				
	1	2	3	4	5	6	7
3: 5 4.2 1972 7 1	9*	19*	-	-	128*	144*	1*
3: 5 4.9 1972 12 30	22*	36*	-	-	219*	219*	2*
3: 5 4.7 1973 7 1	37*	63*	-	-	266*	263*	2*
3: 5 5.4 1973 12 30	43*	73*	-	-	276*	274*	2*
3: 5 4.4 1974 7 1	48*	86*	-	-	285*	283*	2*
3: 5 5.3 1974 12 31	61*	108*	-	-	304*	302*	8*
3: 5 4.6 1975 7 1	74*	128*	-	-	327*	324*	8*
3: 5 4.3 1975 12 31	82*	146*	-	-	335*	334*	2*
3: 5 5.1 1976 7 1	92*	164*	-	-	352*	350*	3*
3: 5 4.6 1976 12 30	98*	172*	-	-	360*	357*	3*
3: 5 5.1 1977 7 1	110*	187*	-	-	374*	370*	5*
3: 5 4.4 1977 12 30	119*	204*	-	-	381*	378*	5*
3: 5 4.6 1978 7 1	122*	206*	-	-	388*	384*	2*
4: 7 4.9 1978 12 31	112*	196*	91*	162*	375*	372*	1*
4: 7 5.3 1979 7 1	118*	198*	86*	144*	388*	382*	3*
4: 7 4.5 1979 12 31	122*	202*	87*	143*	389*	384*	3*
4: 7 4.8 1980 7 1	129*	213*	93*	148*	403*	396*	7*
4: 7 6.5 1980 12 30	123*	199*	79*	122*	398*	390*	16*
4: 7 4.9 1981 7 1	114*	187*	64*	101*	389*	381*	16*

4:	7	4.5	1982	7	1	117*	195*	61*	96*	386*	380*	2*
4:	7	4.8	1982	12	31	119*	203*	63*	104*	391*	384*	2*
4:	7	4.3	1983	7	1	119*	215*	59*	113*	387*	383*	37*
4:	7	5.1	1983	12	31	123*	219*	60*	112*	392*	387*	37*
4:	7	4.4	1984	7	1	117*	208*	51*	95*	387*	382*	9*
4:	7	4.9	1984	12	30	121*	216*	56*	104*	389*	384*	1*
4:	7	5.8	1985	7	1	108*	199*	36*	78*	362*	363*	1*
4:	7	4.9	1985	12	30	104*	194*	30*	71*	368*	365*	1*
4:	7	4.9	1986	7	1	97*	181*	21*	52*	358*	356*	1*
4:	7	4.5	1986	12	31	95*	192*	18*	64*	355*	357*	1*
4:	7	4.2	1987	7	1	103*	203*	27*	77*	354*	359*	1*
4:	7	5.3	1987	12	31	107*	205*	31*	76*	355*	360*	1*
4:	7	5.1	1988	7	1	100*	193*	21*	58*	346*	351*	3*
4:	7	5.0	1988	12	30	102*	197*	23*	60*	345*	352*	13*
4:	7	5.8	1989	7	1	99*	184*	18*	42*	352*	353*	13*
4:	7	5.0	1989	12	30	94*	173*	11*	27*	348*	349*	9*
4:	7	4.8	1990	7	1	105*	189*	22*	44*	367*	365*	5*
4:	7	4.6	1990	12	31	107*	196*	24*	50*	365*	365*	4*
4:	7	4.7	1991	7	1	108*	197*	24*	51*	374*	371*	6*
4:	7	4.6	1991	12	31	111*	201*	28*	56*	366*	367*	6*
4:	7	4.0	1992	7	1	115*	202*	32*	58*	359*	363*	1*

Number of stnp s = 8; ttnp s = 0; ctip s = 8; ftnp s = 0; e.c. s =

TABLE 3: Results of the algorithm M8 for the area of central Greece and for Mo=6.6

```
1. Catalog of main shocks : mawcr.dat          Mo = 6.00
2. Time interval (Tb,Te) = (1972 1992);
     Step in time  dt =  .50000 years
     Activity is estimated in a period from Tb up to Te
     Constants Ma, e are fixed in catalog; alfa = 0
     2*R(Mo) = (exp(Mo-5.6)+1)*
3.    1  circles      R =R(Mo) km
No.   lat      lon    T*: ye mo da : No.  lat      lon    T*: ye mo da .
 1) 39.20    23.20    1972  7  1:
4.   7 functions in the TIP diagnosis
No. func  m     mm      a    aa    s/dt  d/dt   To    beta    d
 1)    n  act           20          12
 2)    n  act           40          12
 3)    1  act           20          12          1972
 4)    1  act           40          12          1972
 5)    s  act  shf      20 0.50     12                  0.46  0.67
 6)    s  act  shf      40 0.50     12                  0.46  0.67
 7)    b  shf  shf   2.00 0.20      2
5. Constants of diagnostics:
   Quantile p = (for b, for others) = ( .25   .10)
   Time window for "simultaneous" extrema Tex =  5*dt
   Thresholds (G and H) = (  4    5)
   Alarm duration Tau = 10*dt
Radius of  circles       138 km
Magnitude thresholds in Region No. 1    ( 77 quakes per year )
 1: 3.9010.00;  2: 3.7010.00;  3. 3.9010.00;  4: 3.7010.00;  5: 3.90 5.50.
 6. 3.70 5.50;  7: 4.00 5.79;
     Strong quake: 1980  7  9  2 11 3920  2390    0 650  29 in Region No.  1
     Strong quake: 1980  7  9  2 35 3920  2270    0 610  18 in Region No.  1
     Strong quake: 1981  2 24 20 53 3814  2300    0 680 158 in Region No.  1
     Strong quake: 1982  1 18 19 27 3950  2450    0 690  88 in Region No   1
stip  1 ( 39.20: 23.20)*(1979  7  1 : 1984  7  1)  4  7  4  7
stip  1 ( 39.20: 23.20)*(1980  7  1 : 1985  7  1)  4  7  4  7
ttip  1 ( 39.20: 23.20)*(1983  7  1 : 1988  7  1)  4  7  4  7
ttip  1 ( 39.20: 23.20)*(1984  7  1 : 1989  7  1)  4  7  4  7
ttip  1 ( 39.20: 23.20)*(1985  7  1 : 1990  7  1)  4  7  4  7
ttip  1 ( 39.20: 23.20)*(1986  7  1 : 1991  7  1)  4  7  4  7
ttip  1 ( 39.20: 23.20)*(1987  7  1 : 1992  7  1)  4  7  4  7
ttip  1 ( 39.20: 23.20)*(1988  7  1 : 1993  7  1)  4  7  4  7
ctip  1 ( 39.20: 23.20)*(1989  7  1 : 1994  7  1)  4  7  4  7
 tip  1 ( 39.20: 23.20)*(1990  7  1 : 1995  7  1)  4  7  4  7
ctip  1 ( 39.20: 23.20)*(1991  7  1 : 1996  7  1)  4  7  4  7
ctip  1 ( 39.20: 23.20)*(1992  7  1 : 1997  7  1)  4  7  4  7
```

Region No. 1	1972	39.20			23.20		
	1	2	3	4	5	6	7
3: 5 4.3 1972 7 1	9*	20*	-	-	148*	165*	0*
3: 5 4.9 1972 12 30	29*	50*	-	-	259*	259*	2*
3: 5 4.7 1973 7 1	45*	73*	-	-	298*	298*	2*
3: 5 5.4 1973 12 30	52*	87*	-	-	325*	322*	2*
3: 5 4.4 1974 7 1	57*	100*	-	-	332*	331*	1*
3. 5 5.3 1974 12 31	71*	121*	-	-	390*	378*	12*
3: 5 5.2 1975 7 1	92*	152*	-	-	419*	408*	12*
3. 5 4.3 1975 12 31	101*	168*	-	-	424*	415*	3*
3: 5 5.1 1976 7 1	111*	188*	-	-	443*	432*	3*
3: 5 4.6 1976 12 30	120*	203*	-	-	451*	442*	3*
3: 5 5.1 1977 7 1	130*	221*	-	-	467*	456*	5*
3: 5 5.2 1977 12 30	142*	242*	-	-	480*	469*	5*
3: 5 5.2 1978 7 1	148*	250*	-	-	495*	481*	1*
4: 7 4.9 1978 12 31	133*	229*	106*	182*	482*	468*	1*
4: 7 5.3 1979 7 1	138*	239*	99*	176*	505*	486*	3*
4. 7 4.5 1979 12 31	140*	242*	98*	172*	499*	483*	3*
4: 7 4.8 1980 7 1	146*	247*	103*	172*	514*	495*	7*
4: 7 6.5 1980 12 30	141*	239*	90*	153*	494*	479*	16*
4: 7 6.8 1981 7 1	**130***	**226***	**68***	**124***	**487***	**470***	**16***
4. 7 4.6 1981 12 30	132*	231*	68*	124*	480*	471*	2*

4:	7	6.9	1982	7	1	140*	246*	73*	133*	487*	473*	2*	
4:	7	4.8	1982	12	31	146*	261*	77*	145*	498*	482*	2*	
4:	7	4.4	1983	7	1	149*	268*	78*	147*	491*	478*	37*	
4:	7	5.1	1983	12	31	151*	269*	76*	142*	497*	482*	37*	
4:	7	4.8	1984	7	1	144*	257*	65*	122*	488*	474*	9*	
4:	7	4.9	1984	12	30	154*	272*	76*	138*	496*	483*	2*	
4:	7	5.8	1985	7	1	148*	262*	63*	118*	475*	466*	1*	
4:	7	4.9	1985	12	30	146*	257*	60*	110*	477*	466*	1*	
4:	7	4.9	1986	7	1	147*	258*	60*	109*	472*	463*	1*	
4:	7	4.5	1986	12	31	144*	260*	56*	111*	462*	457*	1*	
4:	7	4.5	1987	7	1	144*	260*	55*	108*	454*	451*	1*	
4:	7	5.3	1987	12	31	146*	261*	55*	106*	461*	457*	3*	
4:	7	5.1	1988	7	1	136*	245*	41*	82*	454*	449*	3*	
4:	7	5.0	1988	12	30	138*	247*	41*	78*	458*	453*	13*	
4:	7	5.8	1989	7	1	140*	244*	41*	71*	471*	462*	13*	
4:	7	5.0	1989	12	30	138*	243*	37*	67*	461*	455*	9*	
4:	7	5.0	1990	7	1	152*	262*	51*	86*	489*	478*	11*	
4:	7	5.0	1990	12	31	151*	271*	48*	92*	488*	478*	11*	
4:	7	4.7	1991	7	1	142*	260*	37*	78*	486*	474*	6*	
4:	7	5.0	1991	12	31	145*	267*	41*	86*	488*	477*	6*	
4:	7	4.8	1992	7	1	141*	265*	36*	83*	480*	471*	1*	

Number of strip's = 2, ttip's = 0, ctip's = 4, ftip's = 0, e.c. s =

FINAL REPORT OF THE GEOPHYSICAL AND GEOTHERMY DIVISION, UNIVERSITY OF ATHENS ON THE "E.C.P.F.E" PROJECT (No 122/1/11/91)

E. LAGIOS, *Scientific Responsible*

PRELIMINARY ACCOUNTS OF A TECTONOMAGNETIC EXPERIMENT IN EAST - CENTRAL GREECE

By

E. Lagios, P. Sotiropoulos
Department of Geophysics & Geothermy, University of Athens, panepistimiopolis, Ilissia, Athens 157 84, Greece.

G. Tsokas, G. Variemezis & K. Papazachos
Department of Geophysics, University of Thessaloniki, Thessaloniki 540 06, Greece.

ABSTRACT

This paper presents the preliminary results of a tectonomagnetic experiment in the broader area of Aghialos (Eastern-Central Greece) as part of a multi-disciplinary earthquake prediction program. The applicability of the tectonomagnetic phenomenon related to earthquake energy release is the main target of this experiment at this initial phase. A network of 10 total field magnetic stations, distributed along the almost E-W trending fault system, was established in the area and remeasured few time since 1992. Simultaneous data recording was performed at the base and at the other stations of the network, and magnetic differences were then possibe to be established. A pattern of significant amplitude of magnetic differences was observed at the western part of the network, ranging between 20-180 nT, decreasing gradually to the east, where the magnetic differences attain negative values of about -15 nT. The strong amplitude of the observed magnetic change at the western distribution of the stations should rather be attributed to the abundant ophiolite outcrops, which are expected to be connected at depth. It is difficult to interpret these magnetic field changes in terms of the seismomagnetic effect and make any other assessment related to earthquake prediction phenomena, without longer period observations and detailed consideration of the local seismicity pattern, which is at a very low level in the present stage.

INTRODUCTION

A possible relationship between a large magnitude earthquake and a local geomagnetic change in the epicentral area of a seismogenic zone has long been one of the important problems in solid geophysics (Nagata, 1972). Recently interesting accounts on this subject were outlined: In Japan, the detection of a 5 nT precursory and coseismic event was reported (Rikitake, 1980). In California, several magnetic anomalies, which may be related to precursory seismic events have been observed (Mueller et al., 1980). A possible interpretation of these observations is that perturbations of the stress field in the epicentral region may produce detectable variations in the magnetization of rocks prior

to and during the seismic event. In fact, existing laboratory data show that magnetic susceptibility and remanent magnetization exhibit a pronounced stress dependence.

In our study area, it seems appropriate to apply the experimental procedures for the detection of magnetic field changes related to precursory seismic phenomena in a region where active tectonics exist and produce large magnitude earthquakes. Besides the existence of ophiolitic exposures, which usually exhibit strong intensity of magnetization, is favorable for detailed study and application of seismomagnetic experiments.

BRIEF GEOTECTONIC ACCOUNT

Most of the study area is covered by Holocene alluvial deposits and clays of Pleistocene age. However, the most interesting feature is the ophiolithic exposures (Fig. 1), the presence of which play an important role in the applied experiment, enhancing the signal of the seismomagnetic effect. Two theories have been outlined related to the origin of the ophiolites. One theory considers the ophiolitic mass of the Pelagonian zone as autochthonous (Brunn, 1961). However, more recent aspects adopt the idea that the Pelagonic ophiolites are allochthonous; they have been trasported from the east, from the Axios Zone (Mercier, 1975; Vergely, 1976), and have been deposited over the pre-Cretaceous basement of the Pelagonic or even the "sub-Pelagonic" Zone more to the west. The overthrusting of the ophiolites took place during the Upper Jurassic.

The ophiolitic mass is subsequently covered by the Middle-Upper Cretaceous sediments. The schist-chert formations (radiolarites, sandstones, pelites with white limestone lences and enclosed ophiolitic bodies) of Lower Cretaceous, take the form of tectonic melange and underlie the ophiolitic cover. Finally, the flysch of the Pelagonic Zone occurs at a few places (Mountrakis, 1983).

Three main tectonic phases characterize the study area (Caputo & Pavlides, 1991): (i) A compressional one with ENE-WSW directional stress, which was active during the Middle Miocene, (ii) A Late Miocene - Pliocene tensional one, acting in a NE-SW direction, which reactivated the latest Alpine structures of a NW-SE direction, and (iii) An active Middle Pleistocene - Holocene tensional one, having an almost N-S direction, which created recent faults of almost E-W direction. These E-W directional active faults seem to attract the interest of the present research.

DATA AQUISITION

A network of 10 permanent total field magnetometric stations was installed in the broader area of Aghialos, in August 1992. The distribution of the stations, together with the main fau lting features, can be seen in figure 1. The main seismogenic faults have approximately an E-W direction. The stations have been distributed on both sides of the fault system, covering thus the whole of the study area.

An aluminium pole of about two meter length inserted vertically in a permanent concret construction into ground. The sensor of the magnetometer was firmly placed in a wooden base on top of the pole. In this manner the sensor is always at a standard height and orientation for the recording of the magnetic field values during all periods of the remeasurement of the network. The station at Neochoraki was permanenty chosen to be the base station, to which all other station values are referred to, mainly because it is a few kilometers away from the study faults, and it seems to be characterized by low anthropogenic noise.

The recording of the geomagnetic field was taking place simultaneously at the base-station and at two or three other stations of the network, depending on the available number of magnetometers of each remeasurement, preferably during the night period to avoid the strong day-time variations of the geomagnetic field and the probable industrial interferences. The type of the instruments used is the total field magnetometer manufactured by GEOMETRICS, model G-856 with digital memory and storage. They were usually set to record at 30 or 60 seconds time interval. The remeasurement of the network was planned to take place every 3-4 months, approximately .

DATA ANALYSIS

The geomagnetic field at any point of the Earth's surface is the sum of (i) the Earth's magnetic field, (ii) the effects of the

remanent magnetization, (iii) the magnetic field arising directly from the magnetizing susceptibility of the rocks, (iv) the effects of magnetic field generated by ionospheric and magnetospheric currents, (v) the effects of magnetic fields generated by telluric currents, and (vi) anthropogenic magnetic fields arising from industrial activity. Tectonomagnetic signals are expected to be due to changes by the effects of remanent magnetization and by the magnetic susceptibility of the rocks. All the other effects should be considered as not being related to the seismomagnetic effect and therefore should be removed.

The most straightforward method to remove these non-related effects is to make differential measurements of the geomagnetic field between two locations on the surface separated by a few kilometers. The base must be few kilometrs away from the fault in order to avoid magnetic influence due to the crustal stress changes. The differential measurements of the geomagnetic field is calculated (Lagios et al., 1989) as:

$$\delta B_{bs}(t) = B_b(t) - B_s(t),$$

where $B_b(t)$ and $B_s(t)$ are the total field magnetic measurements at sites b (base-station) and s (station), respectively. Then the detection of any possible seismomagnetic effect is based on the evolution of B_{bs} with time. The method of simple differences of total geomagnetic field between base and station reduce the magnetic disturbances about 95% (Davis et al., 1981). The remaining 5% of the natural magnetic disturbance is due to electromagnetic induction which, being dependent on the subsurface

conductivity distribution, is generally dissimilar between any two locations and, therefore, out of phace. Moreover, total field magnetometers used in such studies suffer the limitation that they measure only one component of the geomagnetic field, while effective elimination of the magnetic disturbances requires the knowledge of all three components (Davis et al., 1981).

We can introduce a further degree of improvement to our results by minimizing the random fluctuations generated by instrumental electronic noise and high localized electromagnetic induction effects by applying various smoothing techniques. Such an attempt applied here was the removal of a linear trend, and then the application of a Fast Fourier Transform to low-pass filter data. The linear trend is reinserted in the original data set of the procedure (Press et al., 1986).

Anthropogenic noise can be a serious problem because of its irregular characteristics. In order to minimize the probability of registering industrial noise we have carefully chosen the stations away from inhabited areas and industrial activity. This is the reason for recording data only during the night period.

RESULTS - DISCUSSION

The simultaneous recording at the base station and at other stations of the network resulted in magnetic differences with respect to Neochoraki (base), having estimated accuracies shown in Table 1. It can be seen that relatively low standard deviation

values of the magnetic diffrences were achieved, ranging from 1-5 nT for most of the stations. There were, however, three stations, BZI, MVR, SKP, which exhibited standard deviation values greater than 10 nT. This phenomenon, which is not generally desirable, does not systematically happen, but only once for each station.

Considerable magnetic differences, well above the standard deviation level, are observed for most of the stations. The most significant changes take place at the western part of the network. Bouzi (BZI), Skopia (SKP), Narthaki (NRK) and Thavmako (TMK) show a differential magnetic change of about 180, 110, 35 and 20 nT, respectively, for the period August 1992 to August 1993. This is a positive magnetic difference, which is an order of magnitude larger than the estimated standard deviation level.

Stations at the eastern part of the network do not show differences of such a high amplitude for the same time period. Perdika (PRD), Microthiva (MKT), Mavrolofos (MVL) and Neraida (NRD) exhibit almost a negligible change. It is also noticed that the high amplitude magnetic changes observed at the western part of the network, gradually decline eastwards attaining non-significant values at the eastern part.

Time variation diagrams of the observed magnetic differences, to show the actual change between 1992 and 1993, were made, presented in figures 2, 3 and 4. The two stations Skopia (SKP) and Bouzi (BZI), which show the largest amplitude of magnetic change,

present a steady positive increase, while Narthaki (NRK) and Thavmako (TMK) show a step-like positive change. The rest of the stations present a picture, which approximately flactuates around the same level.

It is rather difficult to interpret these magnetic field changes registered by the network. Longer time period observations are required in order to establish a clearer picture of longer term variations of the magnetic field, associated with the seismic energy released in the area. The seismic activity was at a very low level during the first and last measurement of the network. No large magnitude earthquakes took place in the area. As a consequence, taking into account the low level of the seismicity picture and the relatively short time of observing the local magnetic field (approximately one year), it is not possible to confidently express views about the observed magnetic differences of large amplitude particularly at the western part of the network.

It is very much interesting though to continue the remeasurements of the network, closely examine the local seismic events, and correlate their epicenters and time of occurence with distinct patterns of observed magnetic differences probably registered by the magnetic network.

REFERENCES

Caputo R. & Pavlides (1991). Neotectonic structure and evolution of Thessaly. Bull. Hellen. Geol. Soc., XXV/3, 119-133 (in greek).

Davis, P.M., Jackson, D.D., Searls, C.A. & McPherron R.L. (1981). Detection of tectonomagnetic events using multi-channel predictive filtering. J. Geophys. Res.,86, 1731-1737, (1981).

Lagios E., Tzanis A., Chailas S. & Wyss M. (1989). Surveillance of Thera volcano, Greece : Monitoring of the geomagnetic field. Proc. "Thera and the Aegean World III", Volume 2, 207-215.

Mercier J. (1966). Etude geologique les zones internes des Helleniques en Macedoine centrale. Contribution a l' etude d' metamorphisme et de l' evolution magmatique de zones intern des Hellenides. Ann. Geol. des pays Hell., (20), 1968B.

Mountrakis D. (1983). Lectures in the Geology of Greece. Public. Aristoteles University of Thessaloniki, 140 p. (in greek).

Mueller R.J., Johnston M.J.S., Smith S.E. & Keller V. (1980). U.S. Geological survey magnetometer network and measurement techniques in western U.S.A. Open-file report No. 81-1346, Menlo Park, California.

Press H.W., Flanner B.P., Teukolsky S.A. & Vetterling W.T. (1986). Numerical recipes: The art of scientific computing. Cambridge University Press, ***** p.

Rikitake, T. (1968). Geomagnetism and earthquake prediction. Tectonophysics, 6, 59.

Vergely P. (1976). Chevachement vers l' Ouest et retrocharriag vers l' Est des Ophiolites: deux phases tectoniques au cours d Jurassique superieur - Eocretace dans les Hellenides internes. Bull. Soc. geol. France (7) XVIII, No 2. p. 231.

FIGURE CAPTIONS

Figure 1. Distribution of the total field magnetometric stations in the broader area of Aghialos, together with the main faults and outcrops of ophiolites.

Figure 2. Variation of the total field magnetic differences at stations Skopia (SKP), Bouzi (BZI) and Thavmako (TMK).

Figure 3. Variation of the total field magnetic differences at stations Petroto (PTR), Neraida (NRD) and Narthaki (NRK).

Figure 4. Variation of the total field magnetic differences at stations Perdika (PRD), Mavrolofos (MVR) and Mikrothiva (MKT).

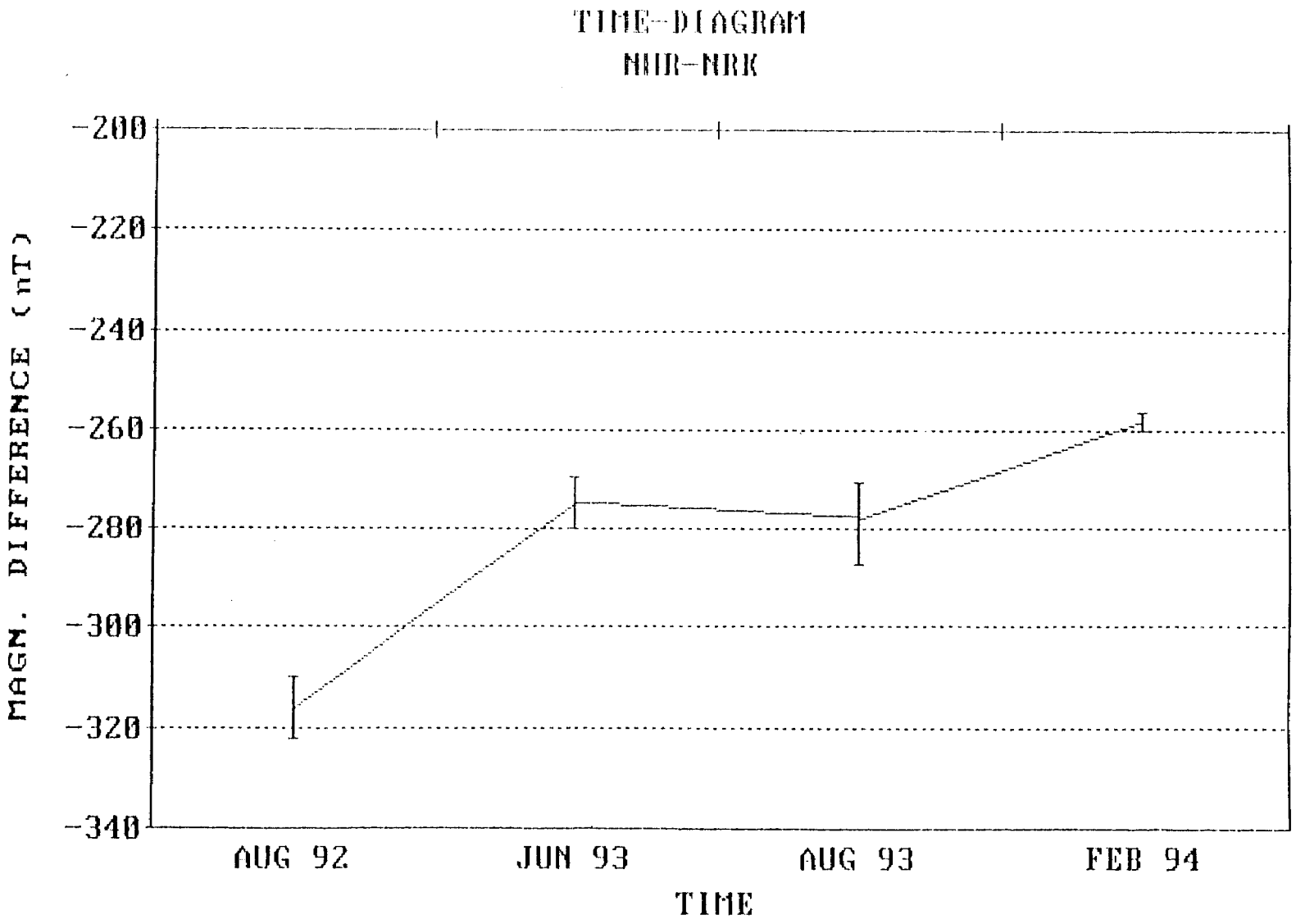
TIME-DIAGRAM
NHR-NRK
MAGN. DIFFERENCE (nT)
-200
-220
-240
-260
-280
-300
-320
-340
AUG 92
JUN 93
AUG 93
FEB 94
TIME

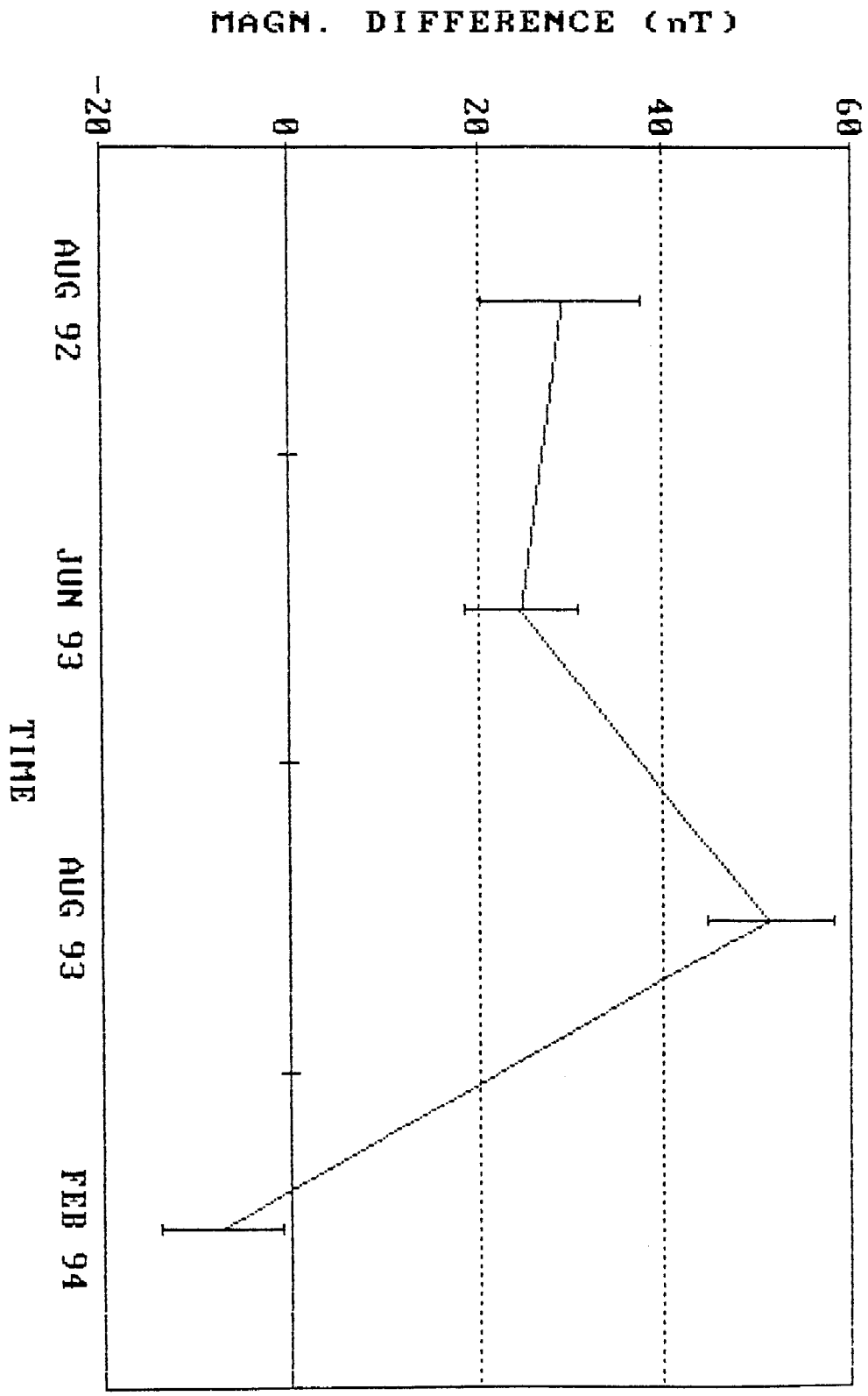

TIME-DIAGRAM
NHR-TRK

STATION		1992	1993		1994
CODE	NAME	AUG	JUN	AUG	FEB
TMK	THAVMAKO	28.90 ± 8.7	24.6 ± 6.2	51.5 ± 6.7	-7.5 ± 6.6
BZI	BOUZI	64.69 ± 7.3	123.3 ± 5.5	242.6 ± 10.4	151.7 ± 6.7
PTR	PETROTO	-	47.2 ± 0.5	28.9 ± 4.2	40.1 ± 4.4
SKP	SKOPIA	54.30 ± 6.1	104.5 ± 4.9	167.2 ± 14.6	113.3 ± 1.9
NRK	NARTHAKI	-316.20 ± 6.3	-274.7 ± 5.0	-278.0 ± 7.3	-258.26 ± 1.7
NRD	NERAIDA	-200.10 ± 2.7	-189.1 ± 1.9	-192.6 ± 1.0	-195.70 ± 1.7
PRD	PERDIKA	-135.00 ± 2.4	-119.8 ± 1.0	-151.4 ± 3.2	-121.70 ± 2.3
MKT	MIKROTHIVA	-101.86 ± 4.0	- 98.4 ± 4.8	-106.9 ± 3.3	- 75.40 ± 4.15
MVR	MAVROLOFOS	- 75.30 ± 26.9	- 77.6 ± 4.9	- 77.6 ± 3.1	- 65.80 ± 3.1

TABLE 1

MAGNETIC DIFFERENCES (nT)
BETWEEN BASE (NEOCHORAKI)
AND STATIONS.

TIME-DIAGRAM
NIR-FTIR

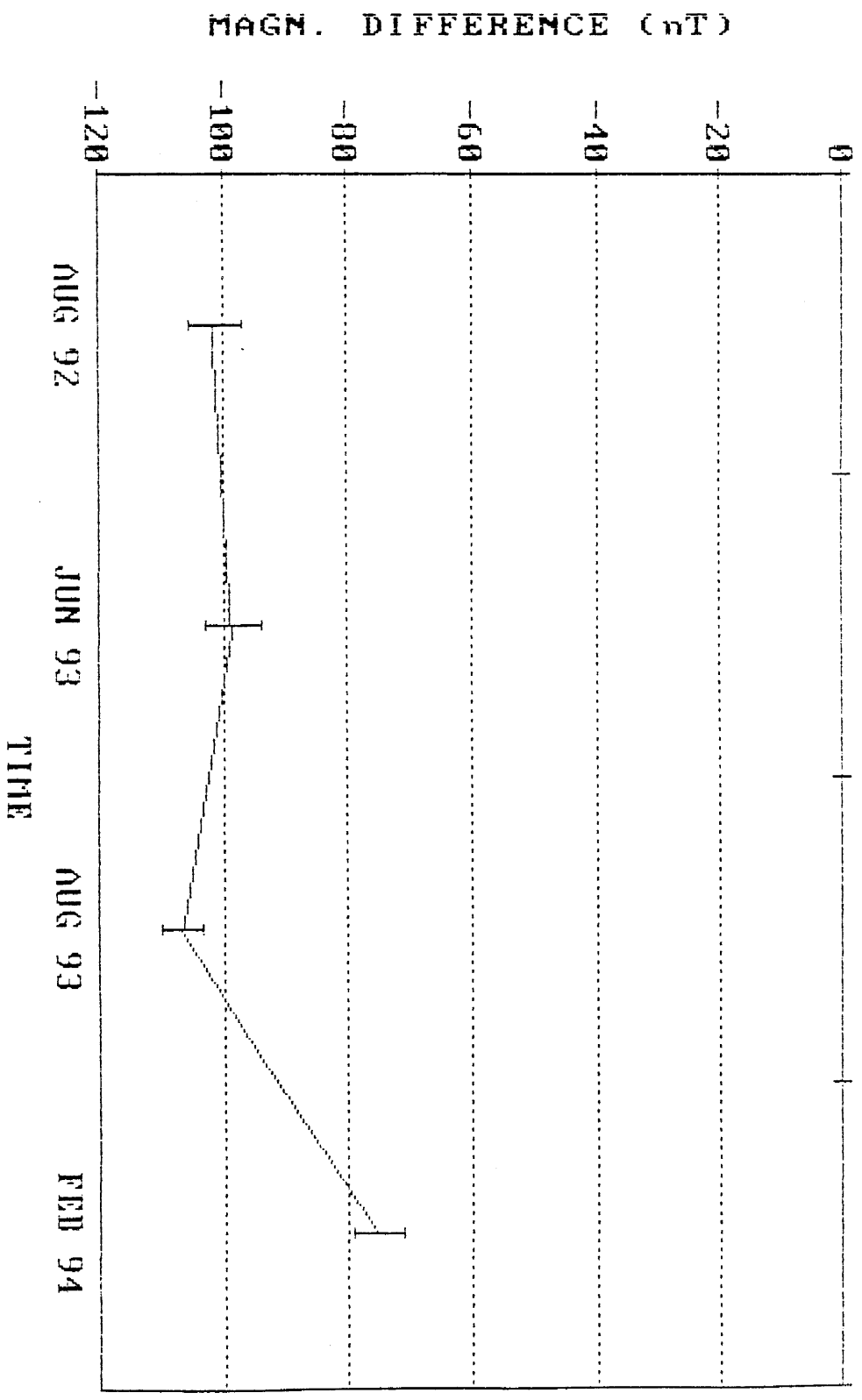

TIME DIAGRAM
MHR-MRT

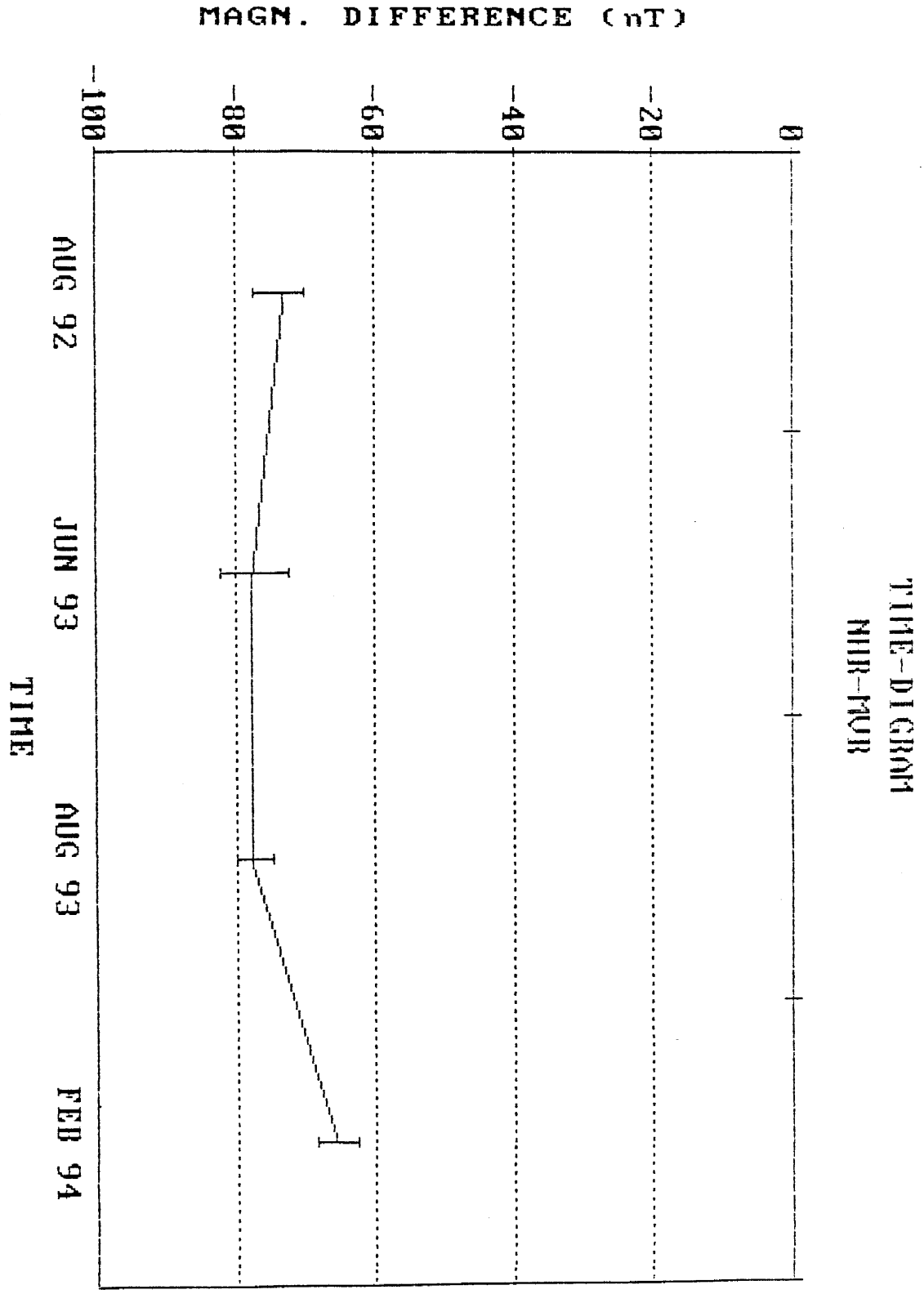
MAGN. DIFFERENCE (nT)
-100
-80
-60
-40
-20
0
TIME
FEB 94
AUG 93
JUN 93
AUG 92
TIME-DIGRAM
NHR-MUR

TIME DIAGRAM
MAIN-MAID

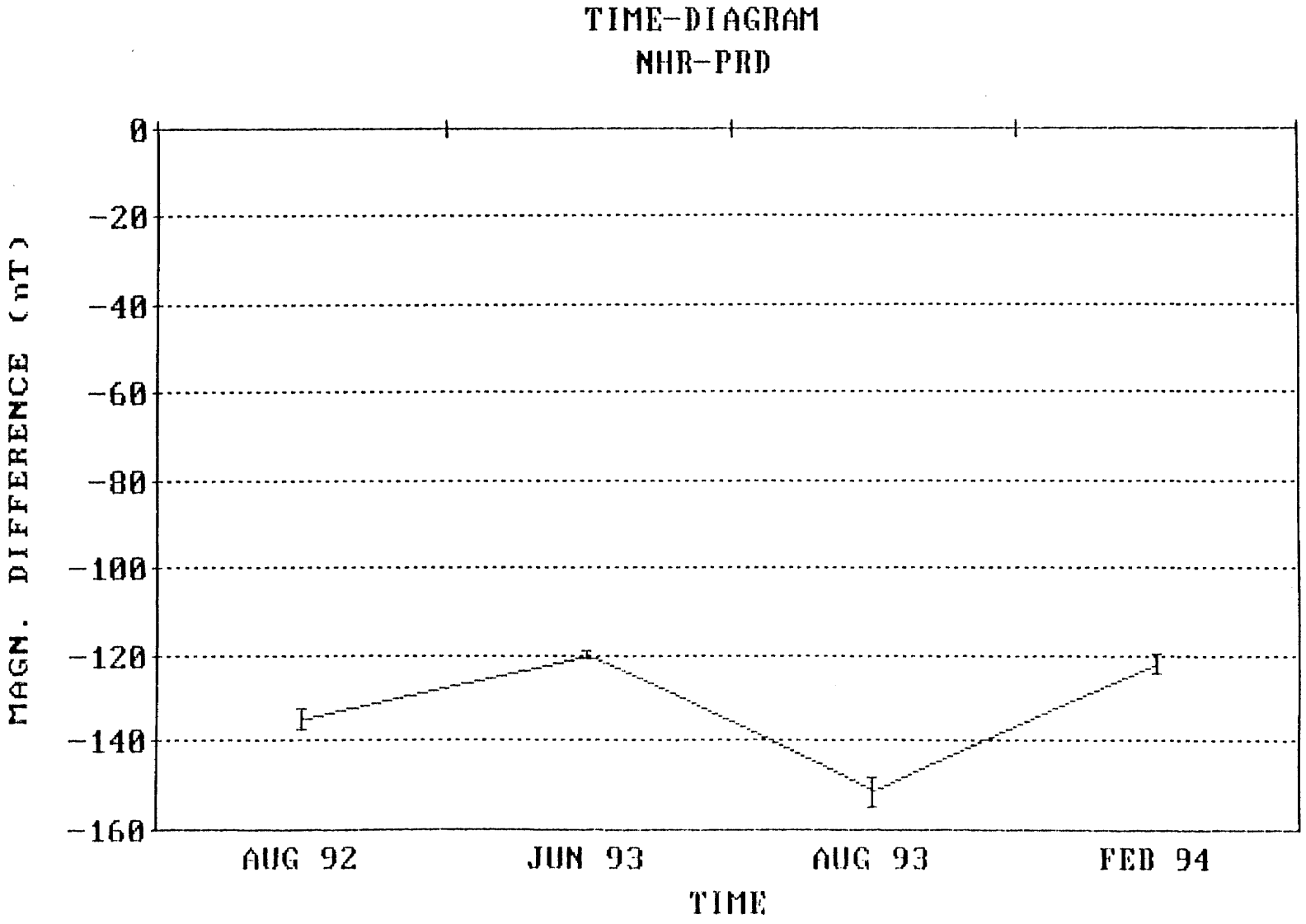
TIME-DIAGRAM
NHR-PRD
MAGN. DIFFERENCE (nT)
0
-20
-40
-60
-80
-100
-120
-140
-160
AUG 92
JUN 93
AUG 93
FEB 94
TIME

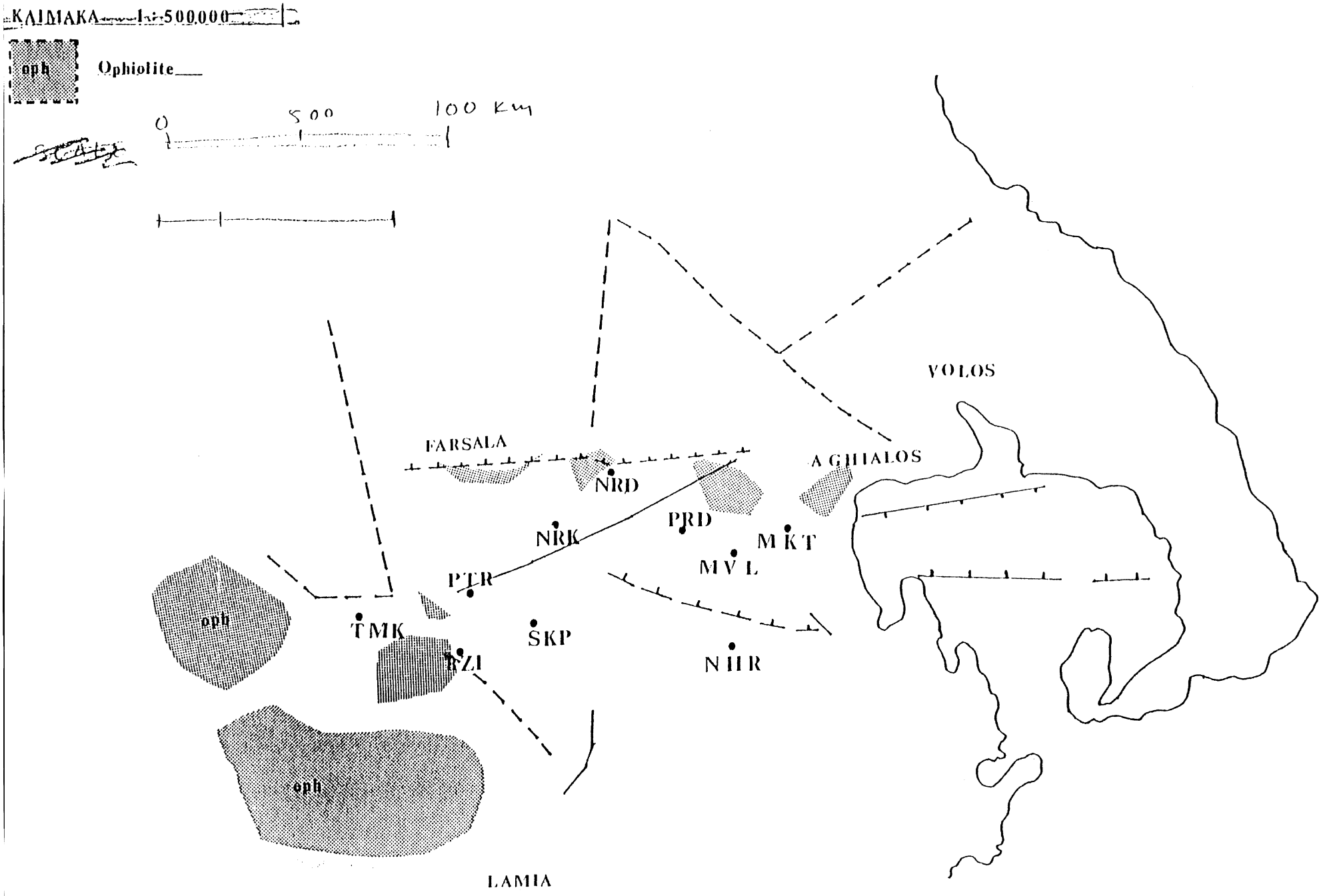
KALIMAKA 1:500000
oph
Ophiolite
0
500
100 Km
VOLOS
FARSALA
AGHIALOS
NRD
PRD
NRK
MKT
MVL
PTR
TMK
SKP
TZI
NHR
oph
oph
LAMIA

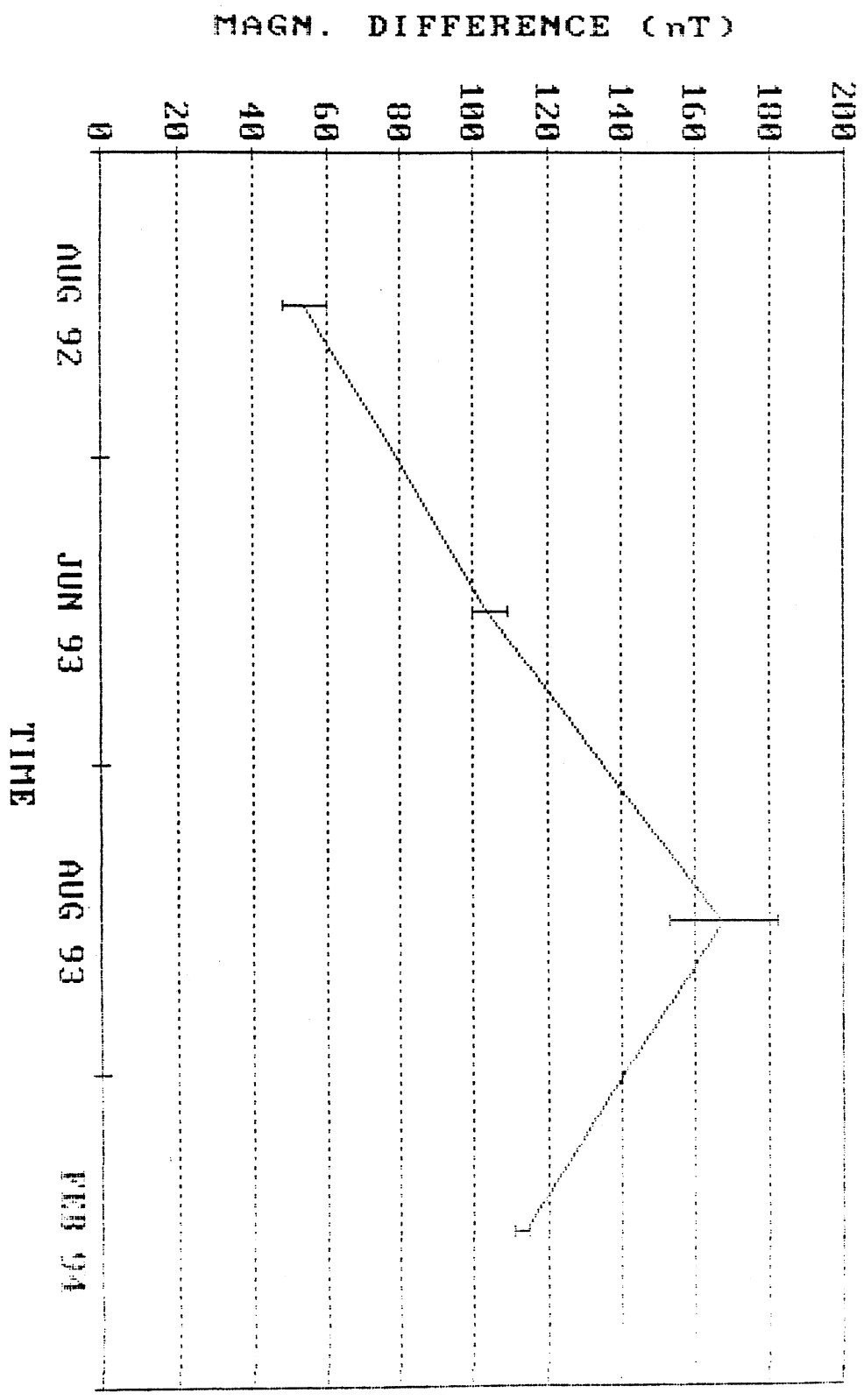

TIME-DIAGRAM
MUR-SAP

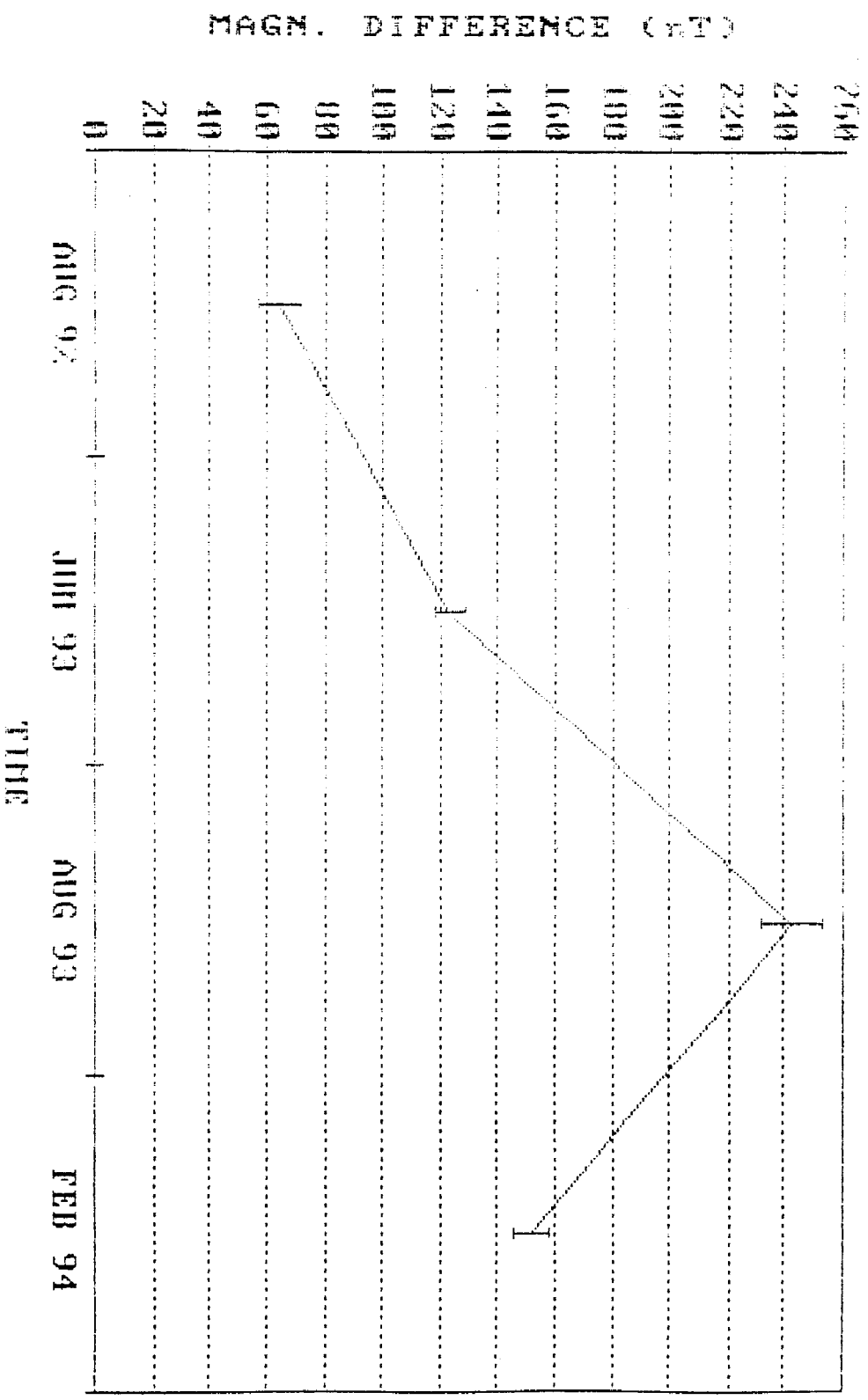
MAGN. DIFFERENCE (nT)
0
20
40
60
80
100
120
140
160
180
200
220
240
260
TIME
FEB 94
AUG 93
JAN 93
26 JUN